



저작자표시-비영리 2.0 대한민국

이용자는 아래의 조건을 따르는 경우에 한하여 자유롭게

- 이 저작물을 복제, 배포, 전송, 전시, 공연 및 방송할 수 있습니다.
- 이차적 저작물을 작성할 수 있습니다.

다음과 같은 조건을 따라야 합니다:



저작자표시. 귀하는 원저작자를 표시하여야 합니다.



비영리. 귀하는 이 저작물을 영리 목적으로 이용할 수 없습니다.

- 귀하는, 이 저작물의 재이용이나 배포의 경우, 이 저작물에 적용된 이용허락조건을 명확하게 나타내어야 합니다.
- 저작권자로부터 별도의 허가를 받으면 이러한 조건들은 적용되지 않습니다.

저작권법에 따른 이용자의 권리는 위의 내용에 의하여 영향을 받지 않습니다.

이것은 [이용허락규약\(Legal Code\)](#)을 이해하기 쉽게 요약한 것입니다.

[Disclaimer](#)



Ph.D. Dissertation of Hyunwoong Ko

Essays on Genetics of Brain Aging

뇌 연령에 대한 유전학적 연구

July 2022

Seoul National University

Interdisciplinary Program in Cognitive Science

Hyunwoong Ko

Essays on Genetics of Brain Aging

뇌 연령에 대한 유전학적 연구

지도교수 임 정 준

이 논문을 공학박사 학위논문으로 제출함

2022년 07월

**서울대학교 대학원
협동과정 인지과학전공
고현웅**

고현웅의 공학박사 학위논문을 인준함

2022년 07월

위원장 류현모 (인)

부위원장 임정준 (인)

위원 원홍희 (인)

위원 명우재 (인)

위원 곽세열 (인)

Abstract

Ko, Hyunwoong

Interdisciplinary Program in Cognitive Science

Seoul National University

Numerous definitions of aging have been proposed as a result of the rising interest in aging. Recent technological advancements have led to the development of a novel method for estimating aging, known as brain age estimation. Brain magnetic resonance imaging (MRI) scans are typically used as representative brain image data for estimating brain age. It has been evident over the past decade that brain age can be utilized as a clinical indicator and as a tool for assessing the brain aging of an individual. However, the method for estimating brain age has still not converged, and the biological validity of the proxy indicator of brain aging has not been clearly identified. Therefore, to establish the robustness of brain age as an indicator of brain aging, it is essential to improve and compare estimation methods and ensure the corresponding biological validity.

This thesis consists of two studies on brain age. The first study compared the performance of seven different methods for estimating brain age and offers a multimodality-based brain age estimation method based on diffusion- and T1-weighted images. The study included 34,430 UK Biobank

participants for whom both T1-weighted and diffusion-weighted images were available. After calculating the brain age of 4,560 healthy individuals without a disease, it was also applied to the remaining 29,870 non-healthy participants. A total of 225 diffuse-weighted images and 154 T1-weighted images were used to estimate age of the brain. The study revealed that XGBoost performed the best (MAE = 3.50). It has been demonstrated that brain age, as assessed by XGBoost, is related to several health indices.

The second study provides genetic results for an estimated brain age based on XGBoost. Among 34,430 UK Biobank participants with estimated brain ages, genetic analyses were conducted on 29,909 European ancestries with genotype data. A genome-wide association study (GWAS) was conducted first, and a post-GWAS on the genetic variation was subsequently conducted. The BOLT-LMM was performed to explore genetic variants related to brain age, and seven independent lead single nucleotide polymorphisms (SNPs) were secured at a threshold of $P < 5 \times 10^{-8}$. Two out of seven SNPs were considered potential causal variants related to brain age: rs35771878 and rs2316768. These SNPs were linked to the *TLR1* gene and *MAPT-ASI*, respectively, which were shown to be genes related to neurodegeneration. Then, using LDSC analysis, it was determined that 21% of heredity was based on SNPs; it was established that the SNPs were expressed in the tissue of the central nervous system. Finally, genetic correlation analysis demonstrated a hereditary link between brain age and type 2 diabetes.

Keywords: Aging, Brain Aging, BrainAGE, GWAS

Student Number: 2017-32891

Table of Contents

Chapter 1. Introduction	01
1.1. An overview of aging	01
1.2. The concept of brain aging.....	03
1.3. The literature review of brain age.....	06
1.4. Motivation.....	08
1.5. Thesis structure	09
Chapter 2. Estimation of BrainAGE.....	10
2.1. Introduction.....	10
2.2. Methods	10
2.2.1. Participants	10
2.2.2. Data acquisition and processing	12
2.2.3. Predictive modeling	13
2.2.4. Calculating BrainAGE and age bias correction.....	16
2.3. Results	17
2.3.1. Demographics of participants by training and test set	17
2.3.2. Model comparisons	18

2.3.3. BrainAGE and other health-related factors	20
2.4. Discussions	23
Chapter 3. Genetics of BrainAGE	25
3.1. Introduction.....	25
3.2. Methods	25
3.2.1. Participants	25
3.2.2. Genotyping and quality control	26
3.2.3. Genome-wide association analysis	27
3.2.4. Gene mapping and functional annotation.....	28
3.2.5. Pathway analysis.....	28
3.2.6. GWAS Atlas PheWAS and GWAS Catalog	29
3.2.7. Heritability and cell type-specific analysis.....	29
3.2.8. Genetic correlation.....	30
3.3. Results	30
3.3.1. Genome-wide significant association signals	30
3.3.2. Functional annotation of the identified loci and biological pathway.....	36
3.3.3. PheWAS of genetic risk loci associated with BrainAGE ...	39

3.3.4. SNP heritability and partitioned heritability results	43
3.3.5. LDSC-SEG heritability partitioning results	45
3.3.6. Genetic correlation results.....	46
3.4. Discussions	47
Chapter 4. Conclusion	51
4.1. Thesis results	52
4.2. Thesis contributions.....	53
4.3. Recommendations for future research	54
Bibliography	56
Appendix.....	62
Abstract in Korean	167
Acknowledgment	169

List of Tables

Table 1. Participants' characteristics by data set.....	18
Table 2. Performance metrics for BrainAGE prediction models	19
Table 3. The lead SNPs in the 7 loci related with BrainAGE	35
Table A1. UK Biobank neuroimaging phenotypes used in data analysis	62
Table A2. Feature importance (XGBoost)	89
Table A3. Results of correlational analysis for BrainAGE and health-related outcomes.....	101
Table A4. eQTL results of the BrainGWAS	102
Table A5. Enrichment for heritability partitioned based on 53 functional genomic annotation	119
Table A6. Results from the Multiple-tissue of gene expression analysis ..	122
Table A7. Results from the Multiple-tissue analysis of chromatin data (validation).....	129

Table A8. Results from the central nervous system (Cahoy) type of gene expression 152

Table A9. Results from the ImmGen dataset 153

List of Figures

Figure 1. A conceptual figure of brain aging	05
Figure 2. Comparisons of relationship between brain-predicted and chronological age according to age bias correction (total sample)	20
Figure 3. Correlation analysis of BrainAGE and health-related outcomes..	22
Figure 4. A Manhattan plot for the GWAS of BrainAGE.....	31
Figure 5. The quantile-quantile (Q-Q) plot of expected P values versus observed P values in BrainAGE GWAS	32
Figure 6. Regional plot for the rs35771878	33
Figure 7. Regional plot for the rs2316768.....	34
Figure 8. Tissues mapped onto the lead SNPs in eQTL analysis	37
Figure 9. Frequencies of mapped genes in eQTL analysis	38
Figure 10. PheWAS plot (rs4141740)	39
Figure 11. PheWAS plot (rs12693975).....	40

Figure 12. PheWAS plot (rs35771878).....	40
Figure 13. PheWAS plot (rs76647546).....	41
Figure 14. PheWAS plot (rs2316768)	42
Figure 15. Partitioned heritability of BrainAGE GWAS	44
Figure 16. LDSC-SEG heritability.....	46

Chapter 1

Introduction

1.1. An overview of aging

Globally, people are living longer than they did a century ago. Because of advances in science, most people may anticipate to live into their 60s and beyond. However, aging is still inevitable for every people in the world. Every country is experiencing an increase in the number of older people and their proportion of the population. Given that aging contributes to a number of socioeconomic issues, interest in methods to overcome or delay aging has been steadily increasing.

Aging is defined by a progressive loss of physiological integrity, which compromises function and increases mortality risk.¹ Essentially, the term “aging” refers to a series of functional decreases that are connected with increasing age and generally start after sexual maturation.² Biological hallmarks of aging include characteristic

functional changes at the molecular and cellular levels, diminishing physiological homeostasis at the organism level, and a decline in one's ability to perform routine physical and mental tasks.^{1,2}

Chronological age is the most well-established risk factor for functional impairment, degenerative disease, and mortality. Regardless of chronological age, some individuals appear frail and seem to age fast, whereas others do not seem to undergo significant physiological degeneration until a certain age/until they are quite old. The heterogeneity in the context of chronological age has led researchers to study aging mechanisms more accurately. In an effort to identify age, a biomarker of aging has been defined as follows: A biomarker of aging is a biological characteristic of an organism that, either by itself or as part of a multivariate composite, can more accurately predict functional ability at a later age in the absence of disease than can chronological age.³ A 2006 study defined the concept and computation of biological age.⁴ This is a method that is still commonly used, and several biological age estimation methods have also been developed: DNA methylation, telomere length, and composite biomarkers of various protein measurements are used to quantify biological age.⁵⁻⁷

1.2. The concept of brain aging

The brain structure changes during the course of lifetime of an individual.⁸ Brain aging can also be measured, which builds on well-established prediction methods using neuroimaging-derived phenotypes and brain magnetic resonance imaging (MRI).⁹ T1-weighted MRI shows age-related declines in gray and white matter volume, cortical thinning, and structural alterations in subcortical nuclei.^{10,11} The microstructure of white matter varies with age, as demonstrated by diffusion-weighted MRI; typical changes to indicators of microstructure, such as reduced fractional anisotropy (FA) and increased mean diffusivity (MD), are assumed to reflect demyelination or axonal degeneration.¹²

Once the brain age prediction learned in healthy controls becomes a normative model, it is then implemented to a new participant to measure the extent to which their neural states deviate from the norm and the kinds of abnormalities estimated. The “brain-age gap” or “brain-predicted age difference”—the discrepancy between a predicted individual age and their chronological age—is the primary outcome metric in brain age prediction. Positive brain-age gaps indicate “accelerated” or “premature” aging, which occurs when an anticipated brain age of individual is greater than their chronological age. In contrast, a negative brain-age gap is referred to

as “delayed” aging (Figure 1). In this way, brain age estimations can offer crucial clinical information about a person’s state of health and illness risk.¹³ According to a recent study, brain age is a better predictor of mortality than DNA methylation age and leukocyte telomere length.¹⁴ Thus, it is anticipated that the study of brain age will contribute to our understanding of the biology of aging.

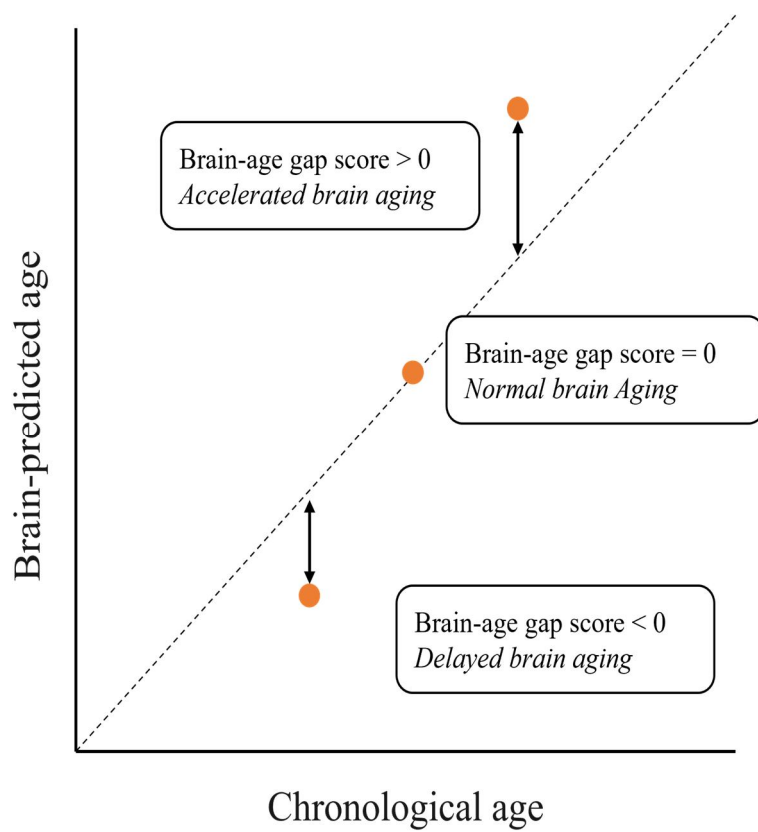


Figure 1. A conceptual figure of brain aging.

1.3. The literature review of brain age

The brain deteriorates with time, which also has an impact on physical health. In order to assess the aging of the brain, neuroscientists have developed a method to create specific *in vivo* biomarkers. In 2010, a neuroimaging study demonstrated that a T1-weighted MRI-based age estimation framework could help recognize brain changes before the onset of clinical symptoms, aiding early diagnosis of neurodegenerative diseases, such as Alzheimer's disease (AD).¹⁵ There has been a considerable increase in the number of studies increase in the number of studies on brain age over the past decade.¹⁶ Owing to the complex dimensional nature of the human brain, various techniques have been used to predict brain age, and comparisons among the techniques have also been performed. The type of neuroimage data (*i.e.*, voxel-based or surface-based) and number of samples were also of interest for selecting a predictive model.¹⁷ From the statistical method, partial least squares (PLS), to machine learning (ML) algorithms, such as Gaussian process regression, relevance vector regression (RVR), and extreme gradient boost (XGBoost), and recently, deep neural network model using convolutional neural network (CNN) are also used to estimate brain age.¹⁸⁻²² Mean absolute error (MAE), the cost function for the predictive model, is characterized by a consistent correlation with chronological

age.¹⁵ In general, CNN techniques are excellent for raw images, and models, such as (*i.e.*, cortical volume or thickness), whereas XGBoost shows relatively good performance for region-based features.^{23,24}

Brain modalities have also been a subject of interest in the context of research on brain age. A series of neuroimaging techniques may correspond to the interest of researchers. Most studies used T1-weighted structural MRI images to estimate brain age. Additional information about brain connectivity, iron deposition, hyperintensities of white matter, and functional activity of specific tasks and rest could potentially increase accuracy, given that aging affects not only aspects of structure of brain but also function and that both can be accessed using different types of neuroimaging techniques.²⁵ T1-weighted MRI and diffusion-weighted MRI imaging data were found to be more relevant than other neuroimaging modalities in estimating brain age.²⁵ To accurately determine brain aging, some studies have also used high-dimensional data called image-derived phenotypes (IDPs).²⁶⁻²⁸ IDPs are derived from calculations that integrate several types of neuroimages to produce a scalar quantity from the processed neuroimaging data, which include both functional and structural images.²⁹

Brain age is known to be associated with diverse clinical phenotypes. Typically, it is associated with a neurological disorder and

psychometric disorder, where the former includes AD, Parkinson's disorder, mild cognitive imposition, epilepsy, stroke, traumatic brain injury, and multiple sclerosis, and the latter includes schizophrenia, bipolar disorder, and major depressive disorder.³⁰ Age of the brain has also been linked to health, physical, biological, and lifestyle factors, and even mortality.^{14 30}

Researchers are now focusing on the molecular level of approaches due to accumulated evidence on brain age. At the genome-wide level, independent lead single nucleotide polymorphisms (SNPs) were identified in three studies using T1-weighted MRI. These SNPs were mainly related to neurological phenotypes or genes.^{23,24,31} In another research, IDPs were redefined in several ways and divided into mode and cluster levels, and distinct SNPs were identified.²⁷ Further genetic research on brain age may contribute to an expanding map of biological background for brain age.

1.4. Motivation

More robust evidence, especially biological background, should be required to develop brain age marker as a biomarker for aging. The biological implications of brain age have not been adequately studied in the past. It is likely that more biological annotation for brain age was not

discovered because the data used to estimate the brain age model was only available for a single modality or the traits were too high dimensional. In the current thesis, brain age is defined as multimodality, followed by a genetic study for brain age estimates. This thesis has three main objectives: (a) screening the best model to estimate brain age; (b) identifying genetic variants related to brain age; (c) discovering biological annotations for brain age.

1.5. Thesis structure

The conceptual review of aging and brain aging that has been completed thus far in Chapter 1 also explains the necessity of the thesis. The remaining part of the thesis can be divided into two folds: Chapters 2 and 3. Chapter 2 defines brain age using multimodal neuroimaging traits and contrasts the results of brain age estimation according to different ML algorithms for optimizing the results. In Chapter 3, a GWAS is first used to identify the genetic variations that affect brain aging, and a post-GWAS approach is then used to produce biological annotation for the genetic variables. In Chapter 4, the conclusions of the thesis are suggested.

Chapter 2

Estimation of BrainAGE

2.1. Introduction

The gap between a participant's expected brain age and their chronological age was employed to estimate the predictions of the models at an individual level. This measure is also known as brain-age gap estimation, or BrainAGE.¹⁵ According to a recent study, T1-weighted MRI and diffusion MRI data are most useful in estimating BrainAGE.²⁵ Additionally, the performance of the algorithm can fluctuate depending on the cohort and the characteristics of input data.¹⁷ Therefore, the purpose of this chapter is to compare various predictive models and identify the one that is best for BrainAGE prediction.

2.2. Methods

2.2.1. Participants

42,032 individuals from UK Biobank were selected for the current

study. Of these, 34,678 individuals underwent the brain imaging visit without missing one or more neuroimaging modalities; 248 participants were excluded because they did not have decent or excellent self-reported health rating. A total of 34,430 participants were examined for further analysis (aged 45–82 years, n = 18,261 females). Two subsample dataset were established: a training set for the predictive model and a test set for the trained model. Only individuals who satisfied the requirements for being healthy at the imaging visit were included in the training data. ICD-10 coded diagnosis; a self-reported long-term illness, infirmity or disability; self-reported diabetes; and stroke history were all grounds for exclusion. This resulted in n = 4,560 (mean age = 62.19 ± 7.2 years, 2,332 females) participants. The test set constituted the remaining n = 29,870 individuals (age_{mean} = 63.98 ± 7.7 , 15,929 females).

Each participants provided their informed consent about the participant of the study. The North West Multi-Centre Research Ethics Committee has granted UK Biobank ethical approval. The UK Biobank data access protocols provide access to the UK Biobank data (<https://www.ukbiobank.ac.uk/researchers>).

2.2.2. Data acquisition and processing

Details on the UK Biobank neuroimaging data are available at: https://biobank.ctsu.ox.ac.uk/crystal/crystal/docs/brain_mri.pdf. Briefly, T1-weighted MRI used an MPRAGE sequence with 1-mm isotropic resolution. With a multiband acceleration factor of 3, 2-mm isotropic resolution, 2 b-values ($b = 1,000, 2000 \text{ s/mm}^2$), and diffusion MRI data were collected. 50 diffusion-encoding directions were collected for diffusion-weighted shells (covering 100 distinct directions over the 2 b-values).²⁵

The imaging-derived phenotypes developed centrally by researchers involved in UK Biobank²⁹ and distributed through the data showcase served as the data implemented in the current study (<http://biobank.ctsu.ox.ac.uk/crystal/index.cgi>). The data included the T1-weighted (regional volume) and diffusion-weighted MRI summary metrics that were available. The following numbers identify the last batch of neuroimaging data: T1-weighted = 165, diffusion-weighted MRI = 675. This resulted in a total of 840 neuroimaging phenotypes (see Table A1 in Appendix).

2.2.3. Predictive modeling

All experiments were carried out using R version 4.0.4.³² For the modeling, a system with an Intel Core-i9-10980XE 3.0-GHz processors and 128GB of RAM was used.

To prevent overfitting, overlapping regions of brain volume explaining age were chosen prior to BrainAGE prediction. Of the 165 phenotypes, the following 11 were excluded: “volumetric scaling from T1 head image to standard space,” “volume of peripheral cortical gray matter normalized for head size,” “volume of peripheral cortical gray matter,” “volume of ventricular cerebrospinal fluid normalized for head size,” “volume of ventricular cerebrospinal fluid,” “volume of gray matter normalized for head size,” “volume of gray matter,” “volume of white matter normalized for head size,” “volume of white matter,” “volume of brain gray + white matter normalized for head size,” “volume of brain gray + white matter” (from data field 25000 to 25010, see Table A1). For diffusion MRI, to reduce data complexity and overfitting, only three characteristics found to be related to aging were included in the analysis. Of the 675 phenotypes, 225 were included: FA, the directional coherence of water molecule diffusion; MD, the magnitude of water molecule diffusion; isotropic volume fraction, the measure of extracellular water diffusion; and so on.³³ Of the 840

neuroimaging phenotypes, only 393 traits were used for further analysis.

The healthy data were randomly divided into training ($n = 3,696$, 80%) and validation sets ($n = 864$, 20%) to develop a multimodality healthy aging model, ensuring that model accuracy could be assessed without biases. To consider the various measuring scales employed by the multiple imaging modalities, all neuroimaging phenotypes were standardized.

To predict age from neuroimage data, five regression algorithms were used to determine age from neuroimaging traits. The five base models are presented below, one of which has a nonlinear kernelized function and makes use of polynomial and radial basis function (RBF) kernels; together, they amount to seven different algorithms. R-squared (R^2), root mean square error (RMSE), and MAE were calculated for each predictive model using 10-fold cross-validation (CV) with 10 repetitions in order to evaluate the significance of the general model performances. These results were then compared to null distributions calculated from 1,000 iterations.

Ordinary least squares (OLS): This is a standard regression method that minimizes the sum of squared errors between the true

values and predicted outcomes.

Partial least squares (PLS)¹⁸: PLS construct components using the correlations between input X and output Y, projects input X and output Y into a new space, minimizes the sum of squares of errors, and finally provides a linear regression model that derives the elements of the input and the output that can account the most common variance between the X and the Y.

Relevance vector regression (RVR)²⁰: RVR is an extension of support vector regression³⁴ based on Bayesian approaches. A vector of independent hyperparameters that lower the size of the data set is produced as a result of the explicit zero-mean Gaussian prior that is explicitly imposed on the model parameters. The type of kernel that must be given determines the behavior of the RVR, whereas all other parameters are automatically determined by the learning process itself. Here a linear, polynomial, or RBF kernel was used, where the latter two kernels need to be adjusted for scale, degree, and sigma.

Least absolute shrinkage and selection operator (LASSO)³⁵: LASSO algorithm enforces an L1 penalty, where the objective is to reduce the absolute estimates of regression coefficients of the model. Beta values automatically decrease to zero when they shrink below a

predetermined limit (lambda). As a result, the model's variance is reduced, producing a sparse solution (*i.e.*, regularization), which in turn works to choose useful features and eliminate uninformative ones.

Extreme gradient boosting (XGBoost)²²: XGBoost is the exertion of a gradient-boosted tree method which employs a regularized gradient-boosting technique to precisely predict the outcome Y, which includes advanced regularization to reduce overfitting. It incorporates weaker models with stronger models to improve the global performance. A randomized grid search can be carried out for each model during training to optimize hyperparameters. For the brain age model, the optimized parameters were maximum depth = 4, number of estimators = 220, and learning rate = 0.05.

2.2.4. Calculating BrainAGE and age bias correction

Each person's BrainAGE was calculated by deducting their chronological age from the brain-predicted age by the best performing predictive algorithm. A recent study that revealed a proportional bias in brain-age estimation—whereby the gap between chronological (actual) age and brain-predicted age is inversely connected with chronological (actual) age—led to the implementation of an age bias correcting

approach.^{26,36} Regarding, the regression line between age (the input X) and brain-predicted age (the output Y) in the training set was computed. The brain-predicted age values in the testing set were then adjusted using the slope and intercept of that line by removing the intercept and dividing by the slope. The bias correction was applied to obtain the BrainAGE score, which is the result of deducting chronological age from predicted age.²⁵

2.3. Results

2.3.1. Demographics of participants by training and test set

The total sample was divided into a test set and training set, and the two groups were contrasted (Table 1). Age was marginally lower in the training set compared to the test set. The proportion of females was also higher in the test set. As mentioned earlier, the test set had higher proportions of stroke history and a diagnosis of diabetes because the training set had these characteristics as exclusion (Section 2.2.1).

Table 1. Participants' characteristics by data set

Characteristics	Training set	Test set
N	4,560	29,870
Age, mean ± SD	62.19 ± 7.21	63.98 ± 7.67
Female, % (n)	51.1% (2,332)	53.3% (15,929)
ICD-10 diagnosis, % (n) [*]	0% (0)	97.0% (28,986)
Diabetes, % (n)	0% (0)	5.8% (1,733)
Stroke, % (n)	0% (0)	1.4 % (425)

* Having at least one diagnosis from the ICD-10

2.3.2. Model comparisons

The results from the 10-fold CV of each model on BrainAGE are summarized in Table 2. XGBoost showed lower MAE and RMSE, and OLS showed the highest R^2 . XGBoost—which showed the lowest MAE—the most important metric of BrainAGE estimation—was selected as the final model. In addition, the relative importance of phenotypes obtained through the XGBoost algorithm is presented in Table A2.

Table 2. Performance metrics for BrainAGE prediction models

Method	MAE	RMSE	R^2
OLS	3.51	4.509	0.603
PLS	3.93	4.986	0.511
RVR _{linear}	62.07	62.321	0.385
RVR _{poly}	3.53	4.511	0.600
RVR _{radial}	4.57	6.634	0.333
LASSO	3.56	4.539	0.590
XGBoost	3.50	4.499	0.602

Note. 10-fold cross-validation was applied.

Abbreviations. LASSO, least absolute shrinkage and selection operator; MAE, mean absolute error; OLS, ordinary least squares; PLS, partial least squares; RMSE, root mean squared error; RVR, relevance vector regression; XGBoost, extreme gradient boosting.

2.3.3. BrainAGE and other health-related factors

When applying the XGBoost-BrainAGE model to the total sample, The performance was comparable to that in the healthy sample: MAE = 3.80, $R^2 = 0.64$, RMSE = 4.794. Before and after the age bias correction, age predicted by the brain and chronological age were consistently correlated. (Figure 2A and B); however, it was confirmed that the relationship between BrainAGE and chronological age altered (Figure 2C and 2D). As a result, the age-dependency effect has been eliminated.

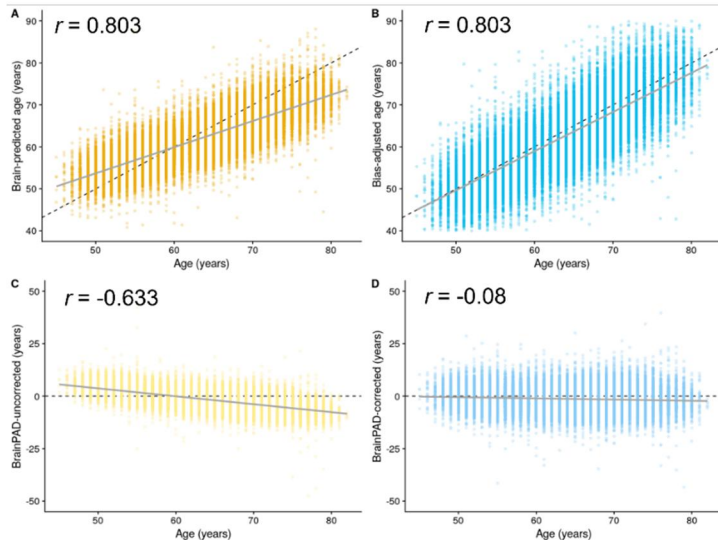


Figure 2. Comparisons of relationship between brain-predicted and chronological age according to age bias correction (total sample).

The association between the bias-adjusted BrainAGE values and the 21 selected health-related outcomes was investigated. (Figure 3). P values were calculated and false discovery rate (FDR) corrected. After adjustment, increasing BrainAGE was related with higher duration to complete trail making tasks (both numeric and alphanumeric path); hip circumference; weight; long-standing illness reports, disability, or infirmity; systolic/diastolic blood pressure; body mass index; overall health rating; lower fluid intelligence score; number of puzzles correctly solved; number of puzzles correct; height; and hand grip strength.

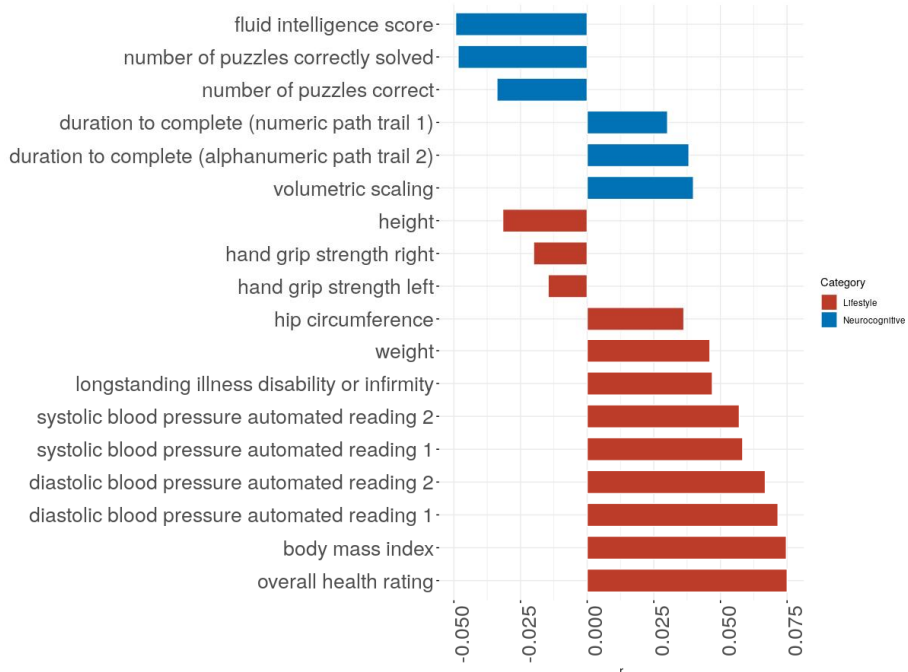


Figure 3. Correlation analysis of BrainAGE and health-related outcomes. Red indicates lifestyle factor and blue indicates neurocognitive factor.

2.4. Discussions

In this chapter, experiments with algorithms for estimating BrainAGE were conducted, and the performance of the models was investigated. In summary, XGBoost of seven predictive models demonstrated the best metrics in terms of MAE and RMSE, which were used in subsequent analysis. BrainAGE value obtained after age bias correction tended to positively correlate with risk factors for diseases and negatively correlate with health outcomes.

The MAE metric derived from the XGBoost model was 3.5, similar to the results of previous studies implementing XGBoost for estimating BrainAGE.^{37,38} Because it has the advantage of minimizing potential overfitting and flexibility, XGBoost is expected to be used to predict BrainAGE.²² Unexpectedly, it has been confirmed that the reference model OLS performs well, similar to XGBoost. However, the OLS model seemed to be underfitted within the training set (*i.e.*, MAE in the training set > MAE in the validation set). In terms of R^2 , there are several input traits; hence, the value is bound to be high according to the basic characteristics of the OLS model. More comparisons and exploration of linear models and ML algorithms will be required in future research.

Considering the relationship with health-related markers in the correlation analysis, BrainAGE can serve as a proxy for aging for overall physical health, not only for brain aging. This is almost similar to the outcome of the previous study using the LASSO algorithm.²⁵ This is consistent with the study that used BrainAGE to predict mortality, indicating that the brain aging marker could be used comprehensibly even in environments such as public health settings to convey complex information to individuals.¹⁴ These findings naturally lead to further research on the biological background of BrainAGE and its relationship with other aging markers.

Taken together, the utility of multimodal-based brain aging marker is confirmed, and its validity for health outcomes is also identified. Therefore, it may be essential to solidify the concept of BrainAGE into a more robust index of aging by securing a biological background. The results in this chapter will be used in the phenotype for genome-wide association later in Chapter 3.

Chapter 3

Genetics of BrainAGE

3.1. Introduction

Genetic studies showed the genetic variants of BrainAGE.^{23,24,27,31} These findings were expected to clarify the genetic architecture of BrainAGE, but the results were mostly limited in explaining the biology of BrainAGE. Therefore, in this chapter, for BrainAGE obtained from multimodal neuroimaging data (*i.e.*, T1-weighted MRI and diffusion MRI), genetic variants were first identified, and then biological annotations of BrainAGE were explored through the defined genetic variants. To this end, the GWAS and the post-GWAS were conducted.

3.2. Methods

3.2.1 Participants

The equivalent participants who were utilized in Chapter 2 were included (see Section 2.1.1).

3.2.2 Genotyping and quality control

The Affymetrix UK Biobank Axiom or Affymetrix UK BiLEVE Axiom arrays (Santa Clara, CA, USA), both of which have more than 800,000 variants and have above 95% coverage, were used to genotype 487,409 samples of UK Biobank (version 3, March 2018). Imputation based on a combined UK 10K and 1,000 Genomes Project panel was done centrally by the UK Biobank; SHAPEIT3¹⁷ was used for phasing, while IMPUTE2¹⁸ was used for imputation. The imputed data from the GWAS was subjected to the following exclusion criteria for variant-level quality control (QC): Hardy–Weinberg equilibrium $P < 1 \times 10^{-6}$, call rate $< 95\%$, and minor allele frequency (MAF) $< 1 \times 10^{-4}$. Additionally, if the MAF values or imputation quality scores (INFO) were below 0.005 or 0.4, the variants were removed; A posterior call probability of less than 0.90 was used to define missing genotypes. The number of 9,575,249 SNPs satisfied the QC criteria. The sample-level QC exclusion measures applied to the imputed GWAS data were as follows: non-Europeans, samples with mismatched sex, putative sex chromosome aneuploidy or no sex information, and individuals who withdrew from the UK Biobank study. Finally, 29,909 participants those who were European ancestry were included in the analysis of the 34,430 who had BrainAGE score.

3.2.3 Genome-wide association analysis

A linear mixed model was implemented in BOLT-LMM^{39,40} to test the association between genetic variants and BrainAGE. Compared with standard linear regression, the mixed model has the advantage of correcting the relatedness as well as residual population stratification within the study sample. Instead, population substructure or related individuals in the GWAS result in power reduction or an excess of false-positive association signals.⁴¹ It has been previously demonstrated that the genome-wide significant association signals can be stronger than the signals obtained in a standard linear regression model due to the larger sample size analyzed by BOLT-LMM. Age, sex, educational qualification, total MRI volume, head motion, imaging center, genotyping array, and 10 principal components from genetic ancestry analysis are used to protect against potential confounding.

Using FUMA platform, independent significant loci with $P < 5 \times 10^{-8}$ and $r^2 \geq 0.1$ were discovered from the results of the genome-wide association study.⁴² The maximum distance between LD (linkage disequilibrium) blocks to combine within a risk locus was 3,000 kb. In the phase 3 of the 1000 Genomes Project, European population genetic data were used as a reference panel for LD analyses. ANNOVAR⁴³ in FUMA⁴⁴ was utilized to map genetic variants to genes and detect the function of the

SNPs. Regional plots of candidate variants were visualized using the FUMA platform.

3.2.4 Gene mapping and functional annotation

For the independent risk loci found by LD clumping, the FUMA platform was used to inspect expression quantitative trait loci (eQTL) and evidence of functional annotation. eQTL mapping maps variants to genes with a significant eQTL association using Genotype-Tissue Expression (GTEx) version 8.⁴⁵ Based on results of eQTL SNP-gene pairs in FUMA, eQTL associations at an FDR <0.05 were regarded as significant.

3.2.5 Pathway analysis

Pathway of biological annotation analysis was conducted on findings from gene-based analysis by MAGMA implemented in FUMA platform.⁴⁶ With the usage of the Gene Ontology (GO) Consortium database, the enriched gene set was investigated.⁴⁷

3.2.6 GWAS Atlas PheWAS and GWAS Catalog

Whether the loci reported associations in issued GWAS archived

in the NHGRI-EBI database overlapped with the genetic risk loci found in the current GWAS was examined using the FUMA platform.⁴⁸ Using the GWAS Atlas database, lists of connected phenotypes were displayed using a genome-wide association study (PheWAS) of the seven lead SNPs.⁴⁹

3.2.7 Heritability and cell type-specific analysis

Using the GWAS summary results, the SNP-based heritability for BrainAGE was determined using LD score regression (LDSC).⁵⁰ The precomputed European LD scores of the 1000 Genomes Project phase3 were obtained from website (<https://github.com/bulik/ldsc>). SNPs in the MHC region were excluded, and common autosomal variants with a MAF > 1 % in the European population were included.

For prioritizing tissues or cell types related with phenotype, cell type-specific analyses were conducted, and tissue-specific level of significant enrichment was explored based on gene expression data with the GWAS summary.⁵¹ Several gene sets were used: Finucane *et al.*,⁵¹ Cahoy *et al.*,⁵² multitissue gene expression (includes both GTEx data⁵³ and Franke lab data^{54,55}), multitissue chromatin (includes Roadmap Epigenomics⁵⁶ and ENCODE data⁵⁷), and ImmGen data.⁵⁸

3.2.8 Genetic correlation

In order to discover the underpinning shared genetic architecture and obtain biological insights, the level of trait-wide genetic correlation (r_g) between BrainAGE and 107 selected traits was calculated by using LDSC software.⁵⁰ European GWAS summary statistics of 107 traits from publicly accessible data were used. All GWAS summary statistics used in genetic correlational analysis passed quality control process; MAF was $> 0.5\%$, and imputation quality score was > 0.8 . The FDR correction was also used.

3.3. Results

3.3.1 Genome-wide significant association signals

Genome-wide association analysis of BrainAGE was performed for European-descent samples using linear mixed model estimation. Using a clumping method, seven genomic loci reaching the genome-wide significance level of $P < 5 \times 10^{-8}$, with the most significant variants in each of the loci being considered the lead SNPs, were identified (Figures 4 and 5). The quantile–quantile (Q–Q) plot of the genome-wide association analysis demonstrated genomic inflation

($\lambda_{GC} = 1.096$), owing to expected polygenicity, which was supported by an LDSC intercept of 1.0034 and standard error of 0.0068. Lead SNPs of BrainAGE are listed in Table 3. The highest significance of the associations was observed at rs2316768, which maps to chromosome 17. Given the two risk loci located in chromosomes 4 and 17 were most likely to be considered the potential causal variants for BrainAGE (Figure 4), the regional plots for the variants were visualized (Figures 6 and 7).

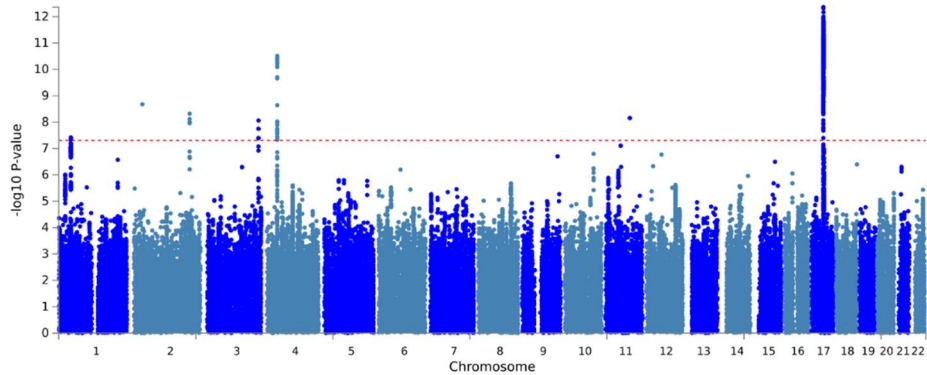


Figure 4. A Manhattan plot for BrainAGE. The x-axis demonstrates genomic positions, and the y-axis represents statistical significance transformed as $-\log_{10}(P)$ values.

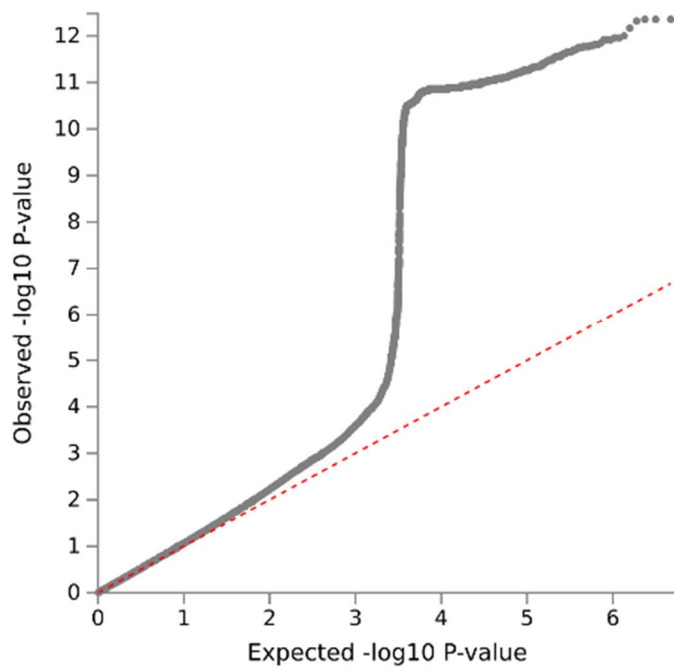


Figure 5. The quantile-quantile (Q-Q) plot of expected P values versus observed P values in BrainAGE GWAS. The red dashed line demonstrates the distribution under the null hypothesis.

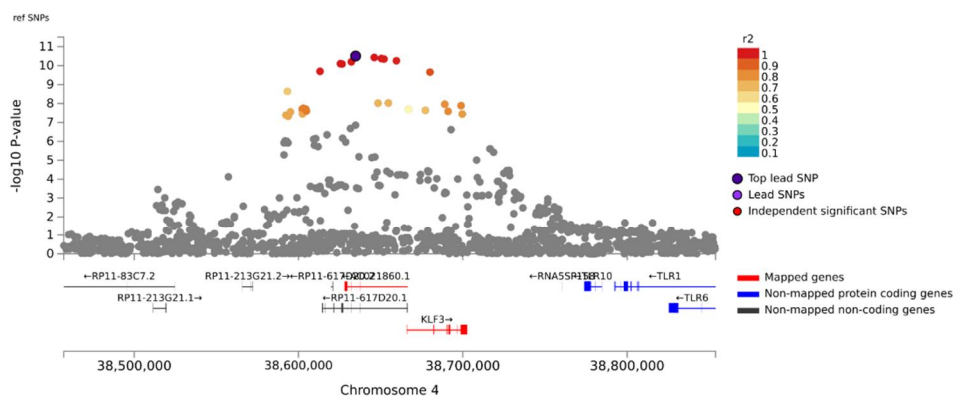


Figure 6. Regional plot for the rs35771878

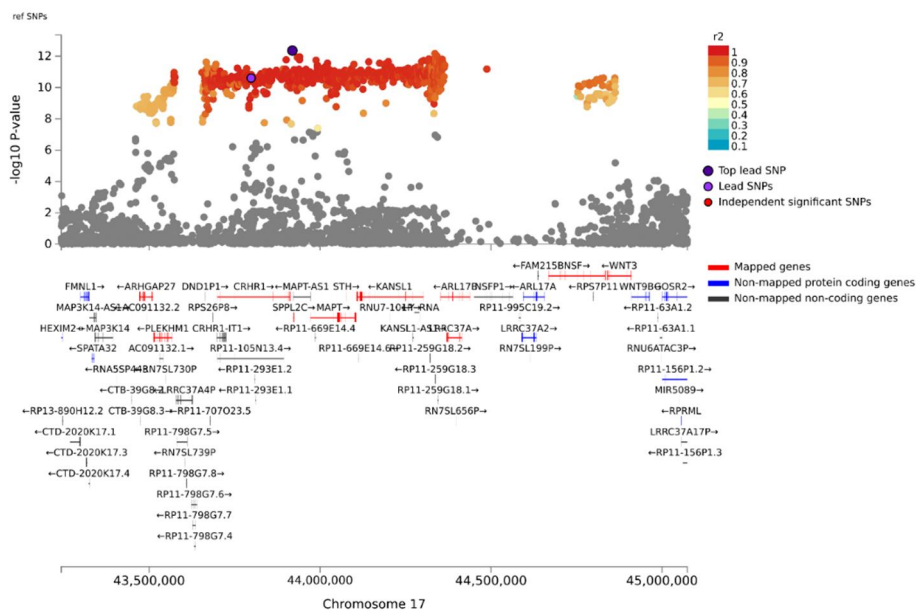


Figure 7. Regional plot for the rs2316768

Table 3. The lead SNPs in the seven loci related with BrainAGE

SNP ID	CHR	BP	A1/A2	EAF	β	SE	P value	Nearest genes
rs4141740	1	43842827	A/T	0.373	0.24	0.045	3.8×10^{-8}	<i>MED8</i>
rs6748456	2	30835496	G/C	0.001	9.99	1.649	2.1×10^{-9}	<i>LCLAT1</i>
rs12693975	2	203720745	G/A	0.180	-0.32	0.055	4.8×10^{-9}	<i>ICAIL</i>
rs76925501	3	187621684	G/A	0.001	7.00	1.166	8.7×10^{-9}	<i>RP11-44H4.1</i>
rs35771878	4	38634757	G/A	0.285	0.30	0.046	3.1×10^{-11}	<i>RP11-617D20.1:AC021860.1</i>
rs76647546	11	88929531	G/A	0.003	10.64	1.740	7.0×10^{-9}	<i>TYR</i>
rs2316768	17	43919073	T/G	0.238	0.39	0.054	4.4×10^{-13}	<i>MAPT-AS1</i>

A1 = effect allele; A2 = noneffect allele; β = beta coefficient; BP = base position; CHR = chromosome; EAF = effect allele frequency.

3.3.2 Functional annotation of the identified loci and biological pathway

The GTEx database implemented the FUMA platform was used to carry out the functional annotation of genome-wide association results, connecting the linked variations with pertinent genes. Based on eQTL analysis, the GWAS SNPs mapping to eQTL genes was found (Table A4). Four of seven SNPs were identified for 28 genes in 54 different tissues; rs4141740 (*CDC20*, *MED8*, *MPL*, *PTPRF*, *SZT2*, *TIE1*), rs12693975 (*CARF*, *FAM117B*, *ICA1L*, *NBEAL1*, *WDR12*), rs35771878 (*TLR1*), rs2316768 (*ACBD4*, *ARHGAP27*, *ARL17A*, *ARL17B*, *CRHR1*, *DCAKD*, *FMNL1*, *KANSL1*, *LRRC37A*, *LRRC37A2*, *MAPT*, *NMT1*, *NSF*, *PLEKHM1*, *SPPL2C*, and *WNT3*). The rs2316768 was mapped to the largest number of tissues and genes. Figure 8 shows the frequencies of the enriched results for each tissue. A total of 49 tissues were enriched, indicating four variants are associated with tissues throughout the whole human body. The frequencies of 28 genes are plotted in Figure 9. The top 10 genes were found to be related to brain measures (mainly MRI), cardiovascular traits, blood pressure, and educational attainment in the GWAS Catalog database. The detailed result of eQTL analysis is presented in Table A4.

MAGMA tissue specificity analysis identified only vagina tissue enriched in the 30 GTEx tissue database. After Bonferroni multiple

correction, MAGMA gene set analysis identified 152 gene ontology biological processes: *GO_bp:go regulation_of_muscle_contraction* ($P_{\text{Bonferroni}} < 0.05$).

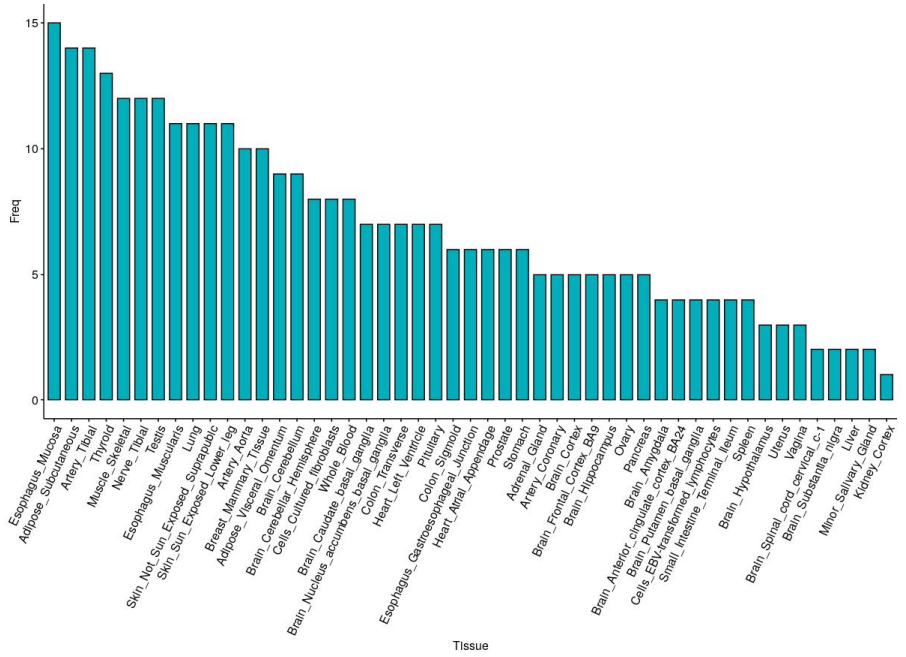


Figure 8. Tissues mapped onto the lead SNPs in eQTL analysis.

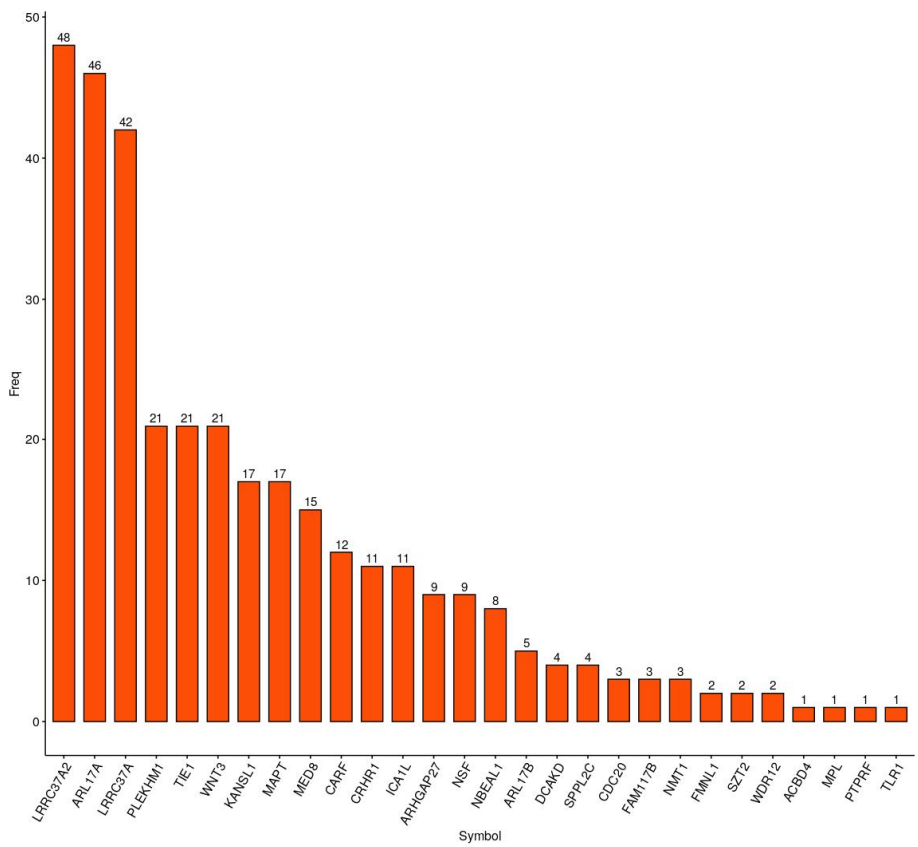


Figure 9. Frequencies of mapped genes in eQTL analysis.

3.3.3 PheWAS of genetic risk loci associated with BrainAGE

To identify the types of phenotypes sharing genetic etiologies with BrainAGE, PheWAS of seven lead SNPs were conducted. Five of seven SNPs showed an association passing the Bonferroni threshold and were further explored: rs4141740, rs12693975, rs35771878, rs76647546, and rs2316768 (Figures 10, 11, 12, 13, and 14). The variants were mainly related to neurological phenotypes as well as immunological and metabolic phenotypes.

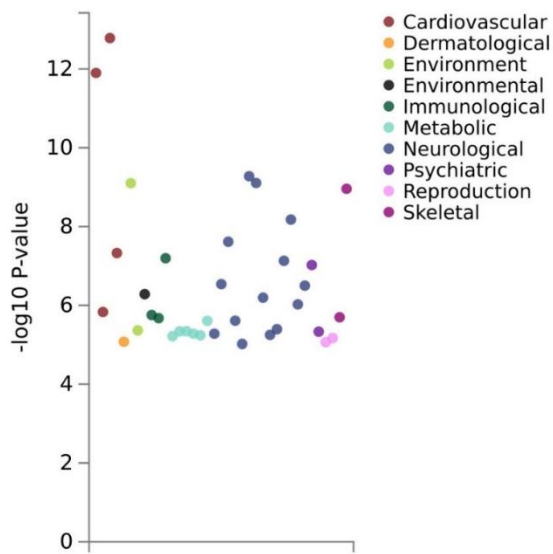


Figure 10. PheWAS plot (rs4141740)

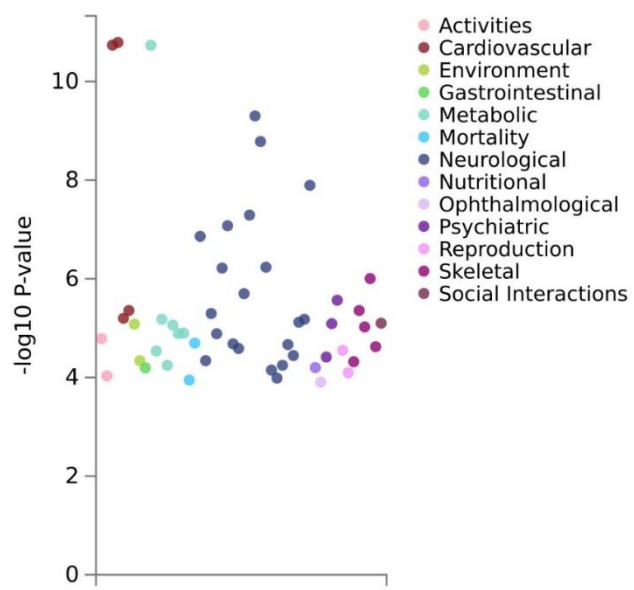


Figure 11. PheWAS plot (rs12693975)

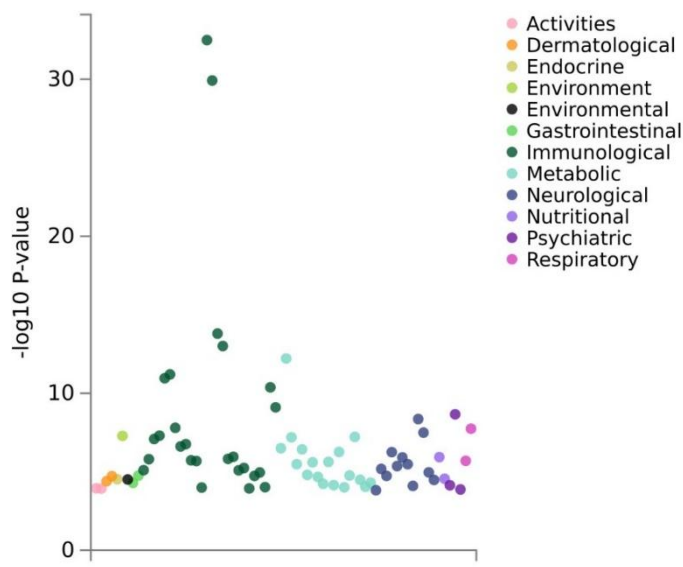


Figure 12. PheWAS plot (rs35771878)

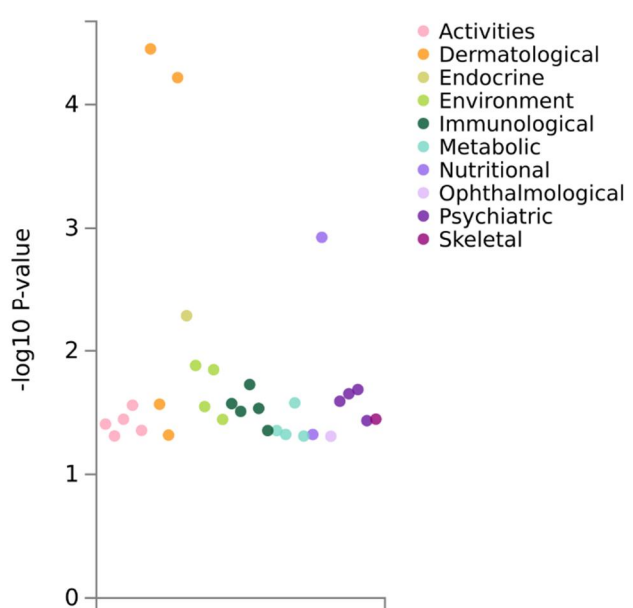


Figure 13. PheWAS plot (rs76647546)

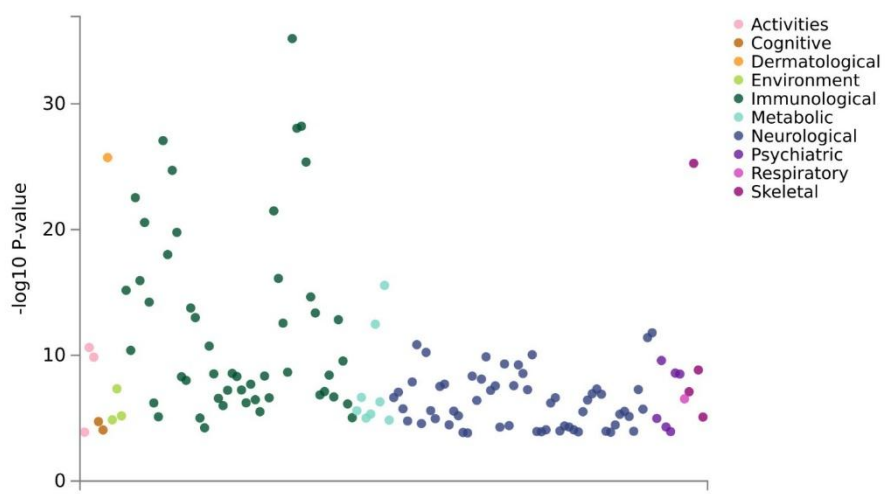


Figure 14. PheWAS plot (rs2316768)

3.3.4 SNP heritability and partitioned heritability results

LDSC was used to calculate both SNP-based heritability and cell-type stratified heritability. SNP heritability of BrainAGE was estimated to be 21% for 53 genomic functions based on the full baseline model, which was consistent with the prior study using T1-weighted MRI only.²³ Figure 15 and Table A5 show the result of functional enrichment for 53 annotations. Only the “Conserved Lindblad Toh” passed the FDR correction, which provides evidence for the biological importance of evolutionarily conserved in mammals.⁵⁹ The rate of variants for the conserved region was 2.6 percent, as well as the enrichment estimates represented 15.1 ($P = 5.04 \times 10^{-13}$).

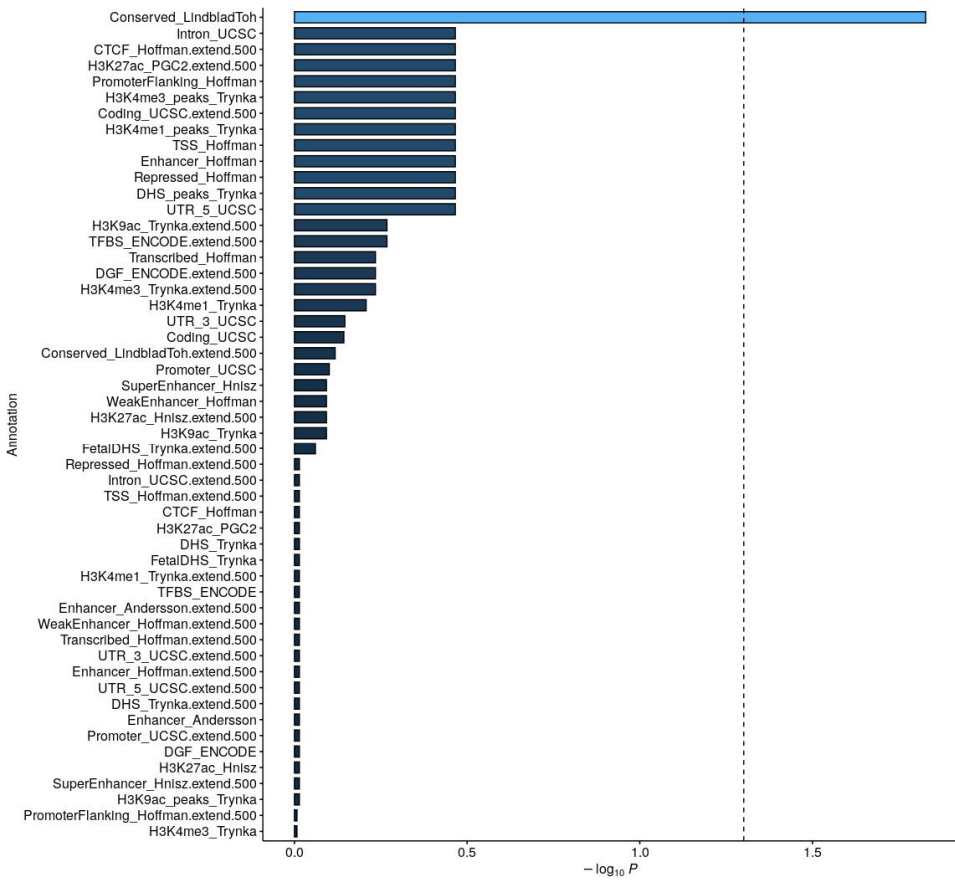


Figure 15. Partitioned heritability of BrainAGE. The line shows the threshold ($P < 0.05$).

3.3.5 LDSC-SEG heritability partitioning results

LDSC to specifically expressed genes (LDSC-SEG) was performed using the 205 tissues and cell types.⁵¹ The 205 specifically expressed gene annotations divided into BrainAGE were obtained from two gene expression data sets (GTEx and Franke lab database).⁵¹ According to an analysis of BrainAGE across multiple tissues, the central nervous system (CNS) tissues, such as the amygdala, substantia nigra, corpus striatum, and spinal cord, were enriched at an FDR of < 0.05 (Table A6). However, these findings were not validated in multi-chromatin data set; 13 in the CNS tissues of 483 tissues were marginally enriched at an FDR of 0.06 (Table A7). Figure 16 shows the LDSC-SEG results. No other significant results were found in Cahoy and ImmGen database (Tables A8 and A9).

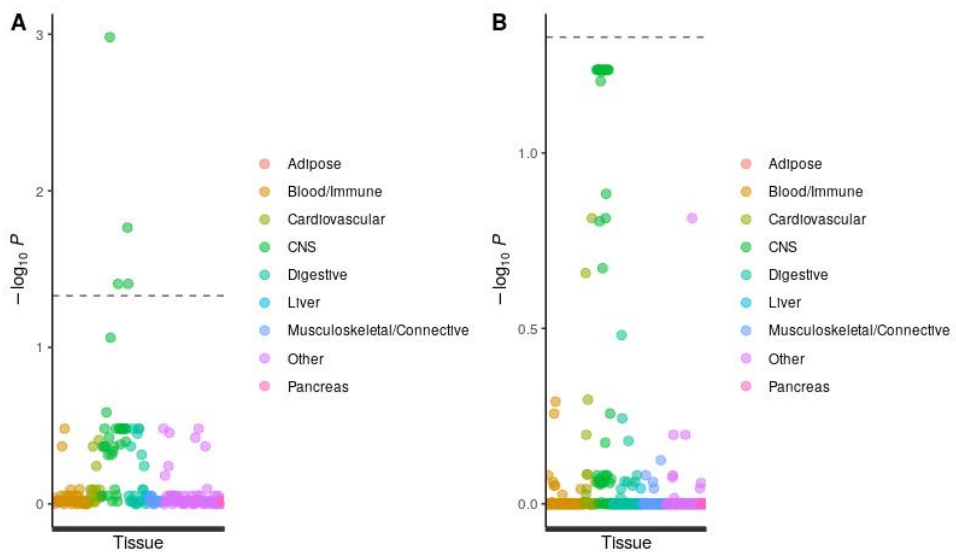


Figure 16. LDSC-SEG heritability. (A) Results of multiple-tissue enrichment using gene expression database. (b) Results of multiple-tissue enrichment using chromatin database. The dashed line indicates the threshold of $FDR < 0.05$.

3.3.6 Genetic correlation results

LDSC was used to determine whether SNPs related with health-associated phenotypes shared genetic background with SNPs for BrainAGE. A significant correlation was observed between BrainAGE and type 2 diabetes ($r_g = 0.17$) after FDR correction. No other traits were significant in the analysis.

3.4. Discussions

In this chapter, the genomic variants associated with BrainAGE were identified, and the genetic architecture for mutations was explored at the genome-wide association level. To this end, the linear mixed model implemented in BOLT-LMM was employed, and secondary web-based platforms, such as the FUMA and GWAS atlas, were used. LDSC analysis, SNP-based heritability, partitioned heritability using cell-/tissue-type database, and genetic correlation were explored.

First, the GWAS result identified seven lead SNPs. Upon visualization of regional plots, it is confirmed that the two lead SNPs had a relatively higher LD than the other SNPs: rs35771878 and rs2316768. This suggests that these two variants are likely to be potential causal variants affecting BrainAGE.

In the case of rs2316768, the position of the variants is adjacent to the position reported in the previous GWAS finding,²³ suggesting that the results are replicated even when using different algorithms from previous studies and multimodal-based neuroimaging data as input. With regard to gene mapping, the result includes *MAPT* and *MAPT-ASI*, suggesting a neurodegenerative process. *MAPT* encodes the tau protein, which has been identified in a variety of neurodegenerative diseases such

as dementia.⁶⁰ In the human genome, *MAPT-ASI* overlaps its 5' untranslated region (UTR) and extends 52 kb upstream of MAPT, contributing to the tauopathies.⁶¹ Given these genes are essential in neurodegeneration,⁶² ⁶³ the results suggest that the variants related to BrainAGE can be markers to capture brain aging in humans. However, the results of the eQTL analysis show this variant is mapped into varied genes and tissues, representing a pleiotropic feature of the variants. Further studies are needed to investigate the shared etiology between BrainAGE and other health-related traits.

The variant rs35771878 only mapped *TLR1*, expressed in the esophagus mucosa. Toll-like receptors (TRLs) are involved in the activation and regulation of the immune response via recognizing specific pathogens.⁶⁴ It has been demonstrated that TLRs are activated by both endogenous ligands, such as heat-shock proteins and DNA, and microbial components, which are expressed in the normal esophagus.⁶⁵ Age-associated alterations in TLR function can contribute to inflammatory dysregulation and impaired adaptive immunity, resulting in reduced function of humans.⁶⁶ ⁶⁷

The gene set analysis shows that 152 genes are involved in the regulation of muscle contraction. Additionally, the PheWAS results

showed genetic overlap with neurological disease, immunological traits, metabolic traits, and other health-related traits across a range of human phenotypes. These results indicate that BrainAGE is related not only to brain aging but also to overall health, which is consistent with the results of Chapter 2.

Across the data, the SNP-based heritability of BrainAGE is estimated to be 21% (SE = 0.02). Partitioned heritability analysis supports a role for BrainAGE in regions conserved in mammals. Cell/tissue-type specific analysis shows that BrainAGE is enriched in CNS tissues in multiple gene expression, suggesting that BrainAGE is involved in the neurobiological process. However, BrainAGE is not enriched for the neural cell, Cahoy mice for brain database. In contrast to eQTL and geneset analysis results, partitioning heritability analyses exclusively represent CNS-specific results. It might be assumed that CNS-related variations would play a role in the heritable factors for BrainAGE. On the other hand, such results may not have been explained by only CNS-related features. Given that brain aging is affected by abundant events across the life span, future research should be investigated more carefully on the discrepancies.

Only type 2 diabetes exhibited significant genetic overlap with BrainAGE, concordant with reported phenotypic correlations.⁶⁸⁻⁷⁰ It may

support the potential clinical relevance of BrainAGE related to an abnormal level of metabolic syndromes. Increased fasting glucose is a hyperglycemic status that predisposes individuals to a high risk of developing type 2 diabetes.⁷¹ Additionally, changes in glucose levels are recognized to increase neurodegeneration.⁷² The significance of glucose uptake in brain aging has been reaffirmed by recent research of BrainAGE estimation utilizing fluorodeoxyglucose positron emission tomography, which revealed that cerebral hypometabolic signals have greater validity compared to structural MRI markers.⁷³ Thus, the shared etiology between diabetes and brain aging may be related to blood glucose. Evidence that the brain is involved in glucose homeostatic regulation suggests that more research is needed on the relationship between metabolic impairment and BrainAGE.⁷⁴⁻⁷⁶

Together, BrainAGE is a trait with heritable characteristics and is related to a wide range of phenotypes. At tissue level, it is confirmed that variants of BrainAGE are mainly involved in CNS. Finally, the link with diabetes suggests that further clinical study is needed to discover the shared etiology between the two traits.

Chapter 4

Conclusion

The current thesis presents a new approach for BrainAGE, in which estimation of BrainAGE is based on multimodal neuroimage data, and reveals genetic architecture through the GWAS and the post-GWAS methods. Seven predictive models are used to estimate BrainAGE, and model comparisons are used to choose the model that performs the best metrics. In the GWAS, the linear mixed model implemented in the BOLT-LMM is employed to identify genetic variants with regard to BrainAGE. Subsequently, functional annotations are mapped for the variants. In the post-GWAS, the LDSC analysis is conducted to estimate SNP-based heritability, specific heritability enrichment by cell/tissue types, and genetic correlations.

4.1 Thesis results

In Chapter 1, the overall concept of aging and the concept of brain aging are introduced. Brain aging, which is introduced relatively recently, is mainly estimated using neuroimage data, and the ML method is mainly used for estimation. This estimated brain aging index is referred to as BrainAGE, which is associated with health-related outcomes. Recent studies have argued that BrainAGE is responsible for certain aspects of biological aging.^{13,77}

In Chapter 2, XGBoost shows the best metrics, in which MAE is 3.5 years and RMSE is 4.499. Further, recent research have shown that XGBoost is the most popular algorithm with good performance.⁷⁸⁻⁸⁰ After age bias correction, BrainAGE value has positive relationships with risk factors for disease and negative relationships with health outcomes. These results were similar to previous studies, suggesting that estimated BrainAGE is valid.

Seven genetic variants for BrainAGE are identified by GWAS in Chapter 3, two of which are probably possible causal variants responsible for BrainAGE: rs35771878 and rs2316768. With regard to the variants, the role of *TLR1* and *MAPT-ASI* genes is accounted for the aging of the brain. Partitioned heritability of 21% is almost equivalent

to the previous finding,²⁴ suggesting that BrainAGE is enriched in the conserved region in mammals. Specific cell-/tissue-type enrichment analysis shows that variants of BrainAGE GWAS play a role in CNS tissues. Finally, the link between type 2 diabetes is discovered using genetic correlation analysis.

4.2. Thesis contribution

Despite its informative features and benefits in describing aging and disease, the study of brain aging based on neuroimaging data has been less popular. With regard to the basic mechanistic of BrainAGE, fewer studies have followed to uncover the molecular and cellular processes driving these phenotypic changes. To this end, the current thesis provides three objectives mentioned in the early section: (a) screening the best model to estimate brain age; (b) identifying genetic variants related to brain age; and (c) discovering biological annotations for brain age. Based on all findings, BrainAGE can be considered to be a biologically valid concept.

Findings from an estimation of BrainAGE based on 35,000 individuals and a genetic study involving about 30,000 people can be highly credible. Clinical and fundamental research findings that support

this result provide additional biological support for the study's finding. BrainAGE will be able to solidify its position as a method to evaluate biological age in more areas by gaining the biological validity of the notion determined by the ML technique.

4.3. Recommendations for future research

There are several issues with the thesis. Given that the concept of BrainAGE essentially involves estimating age, the complete elimination of the age-dependence effect from BrainAGE score is unclear. Although many additional changes have been made to address this problem, the age bias correction still requires caution.⁸¹ In terms of neuroimage data, multimodal-based data still contain only structural features. Given that vascular variables are linked to anatomical changes in the brain,⁸² biological annotations may have produced relatively few findings in this thesis. Additional details on the biological background of BrainAGE can be identified if the functional measures of the brain is taken into account, such as functional MRI markers. The application of the experimental design of GWAS requires a larger sample size compared to phenotypic studies. For height, 100,000 individuals are the bare minimum needed for SNPs to be necessary in order to explain

50% of SNP heritability.⁸³ Therefore, to provide more reliable estimates, future studies must ensure a larger sample size of over 100,000. Other biological age markers are not taken into account in the current findings. Further research on BrainAGE is required, given the genetic overlap with other biological aging that has been discovered. Given that alteration of the brain occurs over a life span,⁸⁴ a longitudinal study design or research on the relationship with other variables of internal individual characteristics or environmental factors that cause a change of BrainAGE should also be added.

Bibliography

- 1 López-Otín, C., Blasco, M. A., Partridge, L., Serrano, M. & Kroemer, G. The hallmarks of aging. *Cell* **153**, 1194-1217 (2013).
- 2 Melzer, D., Pilling, L. C. & Ferrucci, L. The genetics of human ageing. *Nature Reviews Genetics* **21**, 88-101 (2020).
- 3 Baker III, G. T. & Sprott, R. L. Biomarkers of aging. *Experimental gerontology* **23**, 223-239 (1988).
- 4 Klemara, P. & Doubal, S. A new approach to the concept and computation of biological age. *Mechanisms of ageing and development* **127**, 240-248 (2006).
- 5 Blackburn, E. H., Greider, C. W. & Szostak, J. W. Telomeres and telomerase: the path from maize, Tetrahymena and yeast to human cancer and aging. *Nature medicine* **12**, 1133-1138 (2006).
- 6 Horvath, S. DNA methylation age of human tissues and cell types. *Genome biology* **14**, 1-20 (2013).
- 7 Sebastiani, P. *et al.* Biomarker signatures of aging. *Aging cell* **16**, 329-338 (2017).
- 8 Brouwer, R. M. *et al.* Genetic variants associated with longitudinal changes in brain structure across the lifespan. *Nature neuroscience* **25**, 421-432 (2022).
- 9 Cole, J. H., Franke, K. & Cherbuin, N. in *Biomarkers of human aging* 293-328 (Springer, 2019).
- 10 Raz, N. *et al.* Regional brain changes in aging healthy adults: general trends, individual differences and modifiers. *Cerebral cortex* **15**, 1676-1689 (2005).
- 11 Wardlaw, J. M. *et al.* Neuroimaging standards for research into small vessel disease and its contribution to ageing and neurodegeneration. *The Lancet Neurology* **12**, 822-838 (2013).
- 12 Song, S.-K. *et al.* Demyelination increases radial diffusivity in corpus callosum of mouse brain. *Neuroimage* **26**, 132-140 (2005).
- 13 Cole, J. H., Marioni, R. E., Harris, S. E. & Deary, I. J. Brain age and other bodily ‘ages’: implications for neuropsychiatry. *Molecular psychiatry* **24**, 266-281 (2019).
- 14 Cole, J. H. *et al.* Brain age predicts mortality. *Molecular psychiatry* **23**, 1385-1392 (2018).
- 15 Franke, K., Ziegler, G., Klöppel, S., Gaser, C. & Initiative, A. s. D. N.

- Estimating the age of healthy subjects from T1-weighted MRI scans using kernel methods: exploring the influence of various parameters. *Neuroimage* **50**, 883-892 (2010).
- 16 Baecker, L., Garcia-Dias, R., Vieira, S., Scarpazza, C. & Mechelli, A. Machine learning for brain age prediction: Introduction to methods and clinical applications. *EBioMedicine* **72**, 103600 (2021).
- 17 Baecker, L. *et al.* Brain age prediction: A comparison between machine learning models using region-and voxel-based morphometric data. *Human brain mapping* **42**, 2332-2346 (2021).
- 18 Garthwaite, P. H. An interpretation of partial least squares. *Journal of the American Statistical Association* **89**, 122-127 (1994).
- 19 LeCun, Y., Bottou, L., Bengio, Y. & Haffner, P. Gradient-based learning applied to document recognition. *Proceedings of the IEEE* **86**, 2278-2324 (1998).
- 20 Tipping, M. E. Sparse Bayesian learning and the relevance vector machine. *Journal of machine learning research* **1**, 211-244 (2001).
- 21 Rasmussen, C. E. in *Summer school on machine learning*. 63-71 (Springer).
- 22 Chen, T. & Guestrin, C. in *Proceedings of the 22nd ACM SIGKDD international conference on knowledge discovery and data mining*. 785-794.
- 23 Jónsson, B. A. *et al.* Brain age prediction using deep learning uncovers associated sequence variants. *Nature communications* **10**, 1-10 (2019).
- 24 Kaufmann, T. *et al.* Common brain disorders are associated with heritable patterns of apparent aging of the brain. *Nature neuroscience* **22**, 1617-1623 (2019).
- 25 Cole, J. H. Multimodality neuroimaging brain-age in UK Biobank: relationship to biomedical, lifestyle, and cognitive factors. *Neurobiology of aging* **92**, 34-42 (2020).
- 26 Smith, S. M., Vidaurre, D., Alfaro-Almagro, F., Nichols, T. E. & Miller, K. L. Estimation of brain age delta from brain imaging. *Neuroimage* **200**, 528-539 (2019).
- 27 Smith, S. M. *et al.* Brain aging comprises many modes of structural and functional change with distinct genetic and biophysical associations. *Elife* **9**, e52677 (2020).
- 28 Ramduny, J., Bastiani, M., Huedepohl, R., Sotiropoulos, S. N. & Chechlacz, M. The association between inadequate sleep and accelerated brain ageing. *Neurobiology of Aging* **114**, 1-14 (2022).

- 29 Miller, K. L. *et al.* Multimodal population brain imaging in the UK Biobank prospective epidemiological study. *Nature neuroscience* **19**, 1523-1536 (2016).
- 30 Wrigglesworth, J. *et al.* Factors associated with brain ageing-a systematic review. *BMC neurology* **21**, 1-23 (2021).
- 31 Ning, K. *et al.* Improving brain age estimates with deep learning leads to identification of novel genetic factors associated with brain aging. *Neurobiology of Aging* **105**, 199-204 (2021).
- 32 Team, R. C. R: A language and environment for statistical computing. (2013).
- 33 Cox, S. R. *et al.* Ageing and brain white matter structure in 3,513 UK Biobank participants. *Nature communications* **7**, 1-13 (2016).
- 34 Cortes, C. & Vapnik, V. Support vector machine. *Machine learning* **20**, 273-297 (1995).
- 35 Tibshirani, R. Regression shrinkage and selection via the lasso. *Journal of the Royal Statistical Society: Series B (Methodological)* **58**, 267-288 (1996).
- 36 Liang, H., Zhang, F. & Niu, X. Investigating systematic bias in brain age estimation with application to post-traumatic stress disorders. Report No. 1065-9471, (Wiley Online Library, 2019).
- 37 De Lange, A.-M. G. *et al.* Multimodal brain-age prediction and cardiovascular risk: The Whitehall II MRI sub-study. *NeuroImage* **222**, 117292 (2020).
- 38 Anatürk, M. *et al.* Prediction of brain age and cognitive age: Quantifying brain and cognitive maintenance in aging. *Human brain mapping* **42**, 1626-1640 (2021).
- 39 Loh, P.-R. *et al.* Efficient Bayesian mixed-model analysis increases association power in large cohorts. *Nature genetics* **47**, 284 (2015).
- 40 Loh, P.-R., Kichaev, G., Gazal, S., Schoech, A. P. & Price, A. L. Mixed-model association for biobank-scale datasets. *Nature genetics* **50**, 906-908 (2018).
- 41 Yang, J., Zaitlen, N. A., Goddard, M. E., Visscher, P. M. & Price, A. L. Advantages and pitfalls in the application of mixed-model association methods. *Nature genetics* **46**, 100-106 (2014).
- 42 Watanabe, K., Taskesen, E., Van Bochoven, A. & Posthuma, D. Functional mapping and annotation of genetic associations with FUMA. *Nature communications* **8**, 1-11 (2017).
- 43 Wang, K., Li, M. & Hakonarson, H. ANNOVAR: functional annotation of genetic variants from high-throughput sequencing data.

- Nucleic acids research* **38**, e164-e164 (2010).
- 44 Watanabe, K., Umićević Mirkov, M., de Leeuw, C. A., van den Heuvel, M. P. & Posthuma, D. Genetic mapping of cell type specificity for complex traits. *Nature communications* **10**, 1-13 (2019).
- 45 Consortium, G. The GTEx Consortium atlas of genetic regulatory effects across human tissues. *Science* **369**, 1318-1330 (2020).
- 46 de Leeuw, C. A., Mooij, J. M., Heskes, T. & Posthuma, D. MAGMA: generalized gene-set analysis of GWAS data. *PLoS computational biology* **11**, e1004219 (2015).
- 47 Consortium, G. O. Expansion of the Gene Ontology knowledgebase and resources. *Nucleic acids research* **45**, D331-D338 (2017).
- 48 Buniello, A. *et al.* The NHGRI-EBI GWAS Catalog of published genome-wide association studies, targeted arrays and summary statistics 2019. *Nucleic acids research* **47**, D1005-D1012 (2019).
- 49 Watanabe, K. *et al.* A global overview of pleiotropy and genetic architecture in complex traits. *Nature genetics* **51**, 1339-1348 (2019).
- 50 Bulik-Sullivan, B. *et al.* An atlas of genetic correlations across human diseases and traits. *Nature genetics* **47**, 1236-1241 (2015).
- 51 Finucane, H. K. *et al.* Heritability enrichment of specifically expressed genes identifies disease-relevant tissues and cell types. *Nature genetics* **50**, 621-629 (2018).
- 52 Cahoy, J. D. *et al.* A transcriptome database for astrocytes, neurons, and oligodendrocytes: a new resource for understanding brain development and function. *Journal of Neuroscience* **28**, 264-278 (2008).
- 53 Consortium, G. *et al.* The Genotype-Tissue Expression (GTEx) pilot analysis: multitissue gene regulation in humans. *Science* **348**, 648-660 (2015).
- 54 Fehrman, R. S. *et al.* Gene expression analysis identifies global gene dosage sensitivity in cancer. *Nature genetics* **47**, 115-125 (2015).
- 55 Pers, T. *et al.* Genetic Investigation of ANthropometric Traits (GIANT) Consortium Biological interpretation of genome-wide association studies using predicted gene functions. *Nat. Commun* **6**, 5890 (2015).
- 56 Kundaje, A. *et al.* Integrative analysis of 111 reference human epigenomes. *Nature* **518**, 317-330 (2015).
- 57 Consortium, E. P. An integrated encyclopedia of DNA elements in the human genome. *Nature* **489**, 57 (2012).

- 58 Heng, T. S. *et al.* The Immunological Genome Project: networks of gene expression in immune cells. *Nature immunology* **9**, 1091-1094 (2008).
- 59 Finucane, H. K. *et al.* Partitioning heritability by functional annotation using genome-wide association summary statistics. *Nature genetics* **47**, 1228-1235 (2015).
- 60 Allen, M. *et al.* Association of MAPT haplotypes with Alzheimer's disease risk and MAPT brain gene expression levels. *Alzheimer's research & therapy* **6**, 1-14 (2014).
- 61 Simone, R. *et al.* MIR-NATs repress MAPT translation and aid proteostasis in neurodegeneration. *Nature* **594**, 117-123 (2021).
- 62 Kovacs, G. G. Tauopathies. *Handbook of clinical neurology* **145**, 355-368 (2018).
- 63 Wegmann, S. *et al.* Experimental evidence for the age dependence of tau protein spread in the brain. *Science advances* **5**, eaaw6404 (2019).
- 64 Ozinsky, A. *et al.* The repertoire for pattern recognition of pathogens by the innate immune system is defined by cooperation between toll-like receptors. *Proceedings of the National Academy of Sciences* **97**, 13766-13771 (2000).
- 65 Kauppila, J. H. & Selander, K. S. Toll-like receptors in esophageal cancer. *Frontiers in immunology* **5**, 200 (2014).
- 66 Shaw, A. C., Joshi, S., Greenwood, H., Panda, A. & Lord, J. M. Aging of the innate immune system. *Current opinion in immunology* **22**, 507-513 (2010).
- 67 Fulop, T., Franceschi, C., Hirokawa, K. & Pawelec, G. *Handbook of Immunosenescence*. (Springer, 2019).
- 68 Franke, K., Gaser, C., Manor, B. & Novak, V. Advanced BrainAGE in older adults with type 2 diabetes mellitus. *Frontiers in aging neuroscience* **5**, 90 (2013).
- 69 Hwang, I. *et al.* Prediction of brain age from routine T2-weighted spin-echo brain magnetic resonance images with a deep convolutional neural network. *Neurobiology of Aging* **105**, 78-85 (2021).
- 70 Sone, D. *et al.* Neuroimaging-derived brain age is associated with life satisfaction in cognitively unimpaired elderly: A community-based study. *Translational psychiatry* **12**, 1-6 (2022).
- 71 Levitzky, Y. S. *et al.* Impact of impaired fasting glucose on cardiovascular disease: the Framingham Heart Study. *Journal of the American College of Cardiology* **51**, 264-270 (2008).
- 72 Cherbuin, N. & Walsh, E. I. Sugar in mind: untangling a sweet and

- sour relationship beyond type 2 diabetes. *Frontiers in neuroendocrinology* **54**, 100769 (2019).
- 73 Lee, J. *et al.* Deep learning-based brain age prediction in normal aging and dementia. *Nature Aging* **2**, 412-424 (2022).
- 74 Schwartz, M. W. *et al.* Cooperation between brain and islet in glucose homeostasis and diabetes. *Nature* **503**, 59-66 (2013).
- 75 Roh, E., Song, D. K. & Kim, M.-S. Emerging role of the brain in the homeostatic regulation of energy and glucose metabolism. *Experimental & molecular medicine* **48**, e216-e216 (2016).
- 76 Camandola, S. & Mattson, M. P. Brain metabolism in health, aging, and neurodegeneration. *The EMBO journal* **36**, 1474-1492 (2017).
- 77 Cole, J. H. Neuroimaging-derived brain-age: an ageing biomarker? *Aging (Albany NY)* **9**, 1861 (2017).
- 78 Beck, D. *et al.* White matter microstructure across the adult lifespan: A mixed longitudinal and cross-sectional study using advanced diffusion models and brain-age prediction. *NeuroImage* **224**, 117441 (2021).
- 79 de Lange, A.-M. G. *et al.* Prominent health problems, socioeconomic deprivation, and higher brain age in lonely and isolated individuals: A population-based study. *Behavioural Brain Research* **414**, 113510 (2021).
- 80 de Lange, A. M. G. *et al.* Mind the gap: Performance metric evaluation in brain-age prediction. *Human Brain Mapping* (2022).
- 81 Butler, E. R. *et al.* Pitfalls in brain age analyses. Report No. 1065-9471, (Wiley Online Library, 2021).
- 82 Iadecola, C. The overlap between neurodegenerative and vascular factors in the pathogenesis of dementia. *Acta neuropathologica* **120**, 287-296 (2010).
- 83 O'Connor, L. J. The distribution of common-variant effect sizes. *Nature genetics* **53**, 1243-1249 (2021).
- 84 Bethlehem, R. A. *et al.* Brain charts for the human lifespan. *Nature* **604**, 525-533 (2022).

Appendix

Table A1. UK Biobank neuroimaging phenotypes used in data analysis

Neuroimaging phenotype	Data field
Volumetric scaling from T1 head image to standard space	25000
Volume of peripheral cortical grey matter normalised for head size	25001
Volume of peripheral cortical grey matter	25002
Volume of ventricular cerebrospinal fluid normalised for head size	25003
Volume of ventricular cerebrospinal fluid	25004
Volume of grey matter normalised for head size	25005
Volume of grey matter	25006
Volume of white matter normalised for head size	25007
Volume of white matter	25008
Volume of brain grey + white matter normalised for head size	25009
Volume of brain grey + white matter	25010
Volume of thalamus left	25011
Volume of thalamus right	25012
Volume of caudate left	25013
Volume of caudate right	25014
Volume of putamen left	25015
Volume of putamen right	25016
Volume of pallidum left	25017
Volume of pallidum right	25018
Volume of hippocampus left	25019
Volume of hippocampus right	25020
Volume of amygdala left	25021
Volume of amygdala right	25022
Volume of accumbens left	25023
Volume of accumbens right	25024
Volume of brain stem 4th ventricle	25025
Volume of grey matter in frontal pole left	25782
Volume of grey matter in frontal pole right	25783

Volume of grey matter in insular cortex left	25784
Volume of grey matter in insular cortex right	25785
Volume of grey matter in superior frontal gyrus left	25786
Volume of grey matter in superior frontal gyrus right	25787
Volume of grey matter in middle frontal gyrus left	25788
Volume of grey matter in middle frontal gyrus right	25789
Volume of grey matter in inferior frontal gyrus pars triangularis left	25790
Volume of grey matter in inferior frontal gyrus pars triangularis right	25791
Volume of grey matter in inferior frontal gyrus pars opercularis left	25792
Volume of grey matter in inferior frontal gyrus pars opercularis right	25793
Volume of grey matter in precentral gyrus left	25794
Volume of grey matter in precentral gyrus right	25795
Volume of grey matter in temporal pole left	25796
Volume of grey matter in temporal pole right	25797
Volume of grey matter in superior temporal gyrus anterior division left	25798
Volume of grey matter in superior temporal gyrus anterior division right	25799
Volume of grey matter in superior temporal gyrus posterior division left	25800
Volume of grey matter in superior temporal gyrus posterior division right	25801
Volume of grey matter in middle temporal gyrus anterior division left	25802
Volume of grey matter in middle temporal gyrus anterior division right	25803
Volume of grey matter in middle temporal gyrus posterior division left	25804
Volume of grey matter in middle temporal gyrus posterior division right	25805
Volume of grey matter in middle temporal gyrus temporooccipital part left	25806
Volume of grey matter in middle temporal gyrus temporooccipital part right	25807
Volume of grey matter in inferior temporal gyrus anterior division	25808

left	
Volume of grey matter in inferior temporal gyrus anterior division	
right	25809
Volume of grey matter in inferior temporal gyrus posterior division	
left	25810
Volume of grey matter in inferior temporal gyrus posterior division	
right	25811
Volume of grey matter in inferior temporal gyrus temporooccipital	
part left	25812
Volume of grey matter in inferior temporal gyrus temporooccipital	
part right	25813
Volume of grey matter in postcentral gyrus left	25814
Volume of grey matter in postcentral gyrus right	25815
Volume of grey matter in superior parietal lobule left	25816
Volume of grey matter in superior parietal lobule right	25817
Volume of grey matter in supramarginal gyrus anterior division left	25818
Volume of grey matter in supramarginal gyrus anterior division right	25819
Volume of grey matter in supramarginal gyrus posterior division left	25820
Volume of grey matter in supramarginal gyrus posterior division right	25821
Volume of grey matter in angular gyrus left	25822
Volume of grey matter in angular gyrus right	25823
Volume of grey matter in lateral occipital cortex superior division left	25824
Volume of grey matter in lateral occipital cortex superior division right	25825
Volume of grey matter in lateral occipital cortex inferior division left	25826
Volume of grey matter in lateral occipital cortex inferior division right	25827
Volume of grey matter in intracalcarine cortex left	25828
Volume of grey matter in intracalcarine cortex right	25829
Volume of grey matter in frontal medial cortex left	25830
Volume of grey matter in frontal medial cortex right	25831
Volume of grey matter in juxtapositional lobule cortex formerly	
supplementary motor cortex left	25832
Volume of grey matter in juxtapositional lobule cortex formerly	
supplementary motor cortex right	25833
Volume of grey matter in subcallosal cortex left	25834

Volume of grey matter in subcallosal cortex right	25835
Volume of grey matter in paracingulate gyrus left	25836
Volume of grey matter in paracingulate gyrus right	25837
Volume of grey matter in cingulate gyrus anterior division left	25838
Volume of grey matter in cingulate gyrus anterior division right	25839
Volume of grey matter in cingulate gyrus posterior division left	25840
Volume of grey matter in cingulate gyrus posterior division right	25841
Volume of grey matter in precuneous cortex left	25842
Volume of grey matter in precuneous cortex right	25843
Volume of grey matter in cuneal cortex left	25844
Volume of grey matter in cuneal cortex right	25845
Volume of grey matter in frontal orbital cortex left	25846
Volume of grey matter in frontal orbital cortex right	25847
Volume of grey matter in parahippocampal gyrus anterior division left	25848
Volume of grey matter in parahippocampal gyrus anterior division right	25849
Volume of grey matter in parahippocampal gyrus posterior division left	25850
Volume of grey matter in parahippocampal gyrus posterior division right	25851
Volume of grey matter in lingual gyrus left	25852
Volume of grey matter in lingual gyrus right	25853
Volume of grey matter in temporal fusiform cortex anterior division left	25854
Volume of grey matter in temporal fusiform cortex anterior division right	25855
Volume of grey matter in temporal fusiform cortex posterior division left	25856
Volume of grey matter in temporal fusiform cortex posterior division right	25857
Volume of grey matter in temporal occipital fusiform cortex left	25858
Volume of grey matter in temporal occipital fusiform cortex right	25859
Volume of grey matter in occipital fusiform gyrus left	25860

Volume of grey matter in occipital fusiform gyrus right	25861
Volume of grey matter in frontal operculum cortex left	25862
Volume of grey matter in frontal operculum cortex right	25863
Volume of grey matter in central opercular cortex left	25864
Volume of grey matter in central opercular cortex right	25865
Volume of grey matter in parietal operculum cortex left	25866
Volume of grey matter in parietal operculum cortex right	25867
Volume of grey matter in planum polare left	25868
Volume of grey matter in planum polare right	25869
Volume of grey matter in heschls gyrus includes h1 and h2 left	25870
Volume of grey matter in heschls gyrus includes h1 and h2 right	25871
Volume of grey matter in planum temporale left	25872
Volume of grey matter in planum temporale right	25873
Volume of grey matter in supracalcarine cortex left	25874
Volume of grey matter in supracalcarine cortex right	25875
Volume of grey matter in occipital pole left	25876
Volume of grey matter in occipital pole right	25877
Volume of grey matter in thalamus left	25878
Volume of grey matter in thalamus right	25879
Volume of grey matter in caudate left	25880
Volume of grey matter in caudate right	25881
Volume of grey matter in putamen left	25882
Volume of grey matter in putamen right	25883
Volume of grey matter in pallidum left	25884
Volume of grey matter in pallidum right	25885
Volume of grey matter in hippocampus left	25886
Volume of grey matter in hippocampus right	25887
Volume of grey matter in amygdala left	25888
Volume of grey matter in amygdala right	25889
Volume of grey matter in ventral striatum left	25890
Volume of grey matter in ventral striatum right	25891
Volume of grey matter in brainstem	25892
Volume of grey matter in iiv cerebellum left	25893
Volume of grey matter in iiv cerebellum right	25894

Volume of grey matter in v cerebellum left	25895
Volume of grey matter in v cerebellum right	25896
Volume of grey matter in vi cerebellum left	25897
Volume of grey matter in vermis vi cerebellum	25898
Volume of grey matter in vi cerebellum right	25899
Volume of grey matter in crus i cerebellum left	25900
Volume of grey matter in vermis crus i cerebellum	25901
Volume of grey matter in crus i cerebellum right	25902
Volume of grey matter in crus ii cerebellum left	25903
Volume of grey matter in vermis crus ii cerebellum	25904
Volume of grey matter in crus ii cerebellum right	25905
Volume of grey matter in viib cerebellum left	25906
Volume of grey matter in vermis viib cerebellum	25907
Volume of grey matter in viib cerebellum right	25908
Volume of grey matter in viia cerebellum left	25909
Volume of grey matter in vermis viia cerebellum	25910
Volume of grey matter in viia cerebellum right	25911
Volume of grey matter in viib cerebellum left	25912
Volume of grey matter in vermis viib cerebellum	25913
Volume of grey matter in viib cerebellum right	25914
Volume of grey matter in ix cerebellum left	25915
Volume of grey matter in vermis ix cerebellum	25916
Volume of grey matter in ix cerebellum right	25917
Volume of grey matter in x cerebellum left	25918
Volume of grey matter in vermis x cerebellum	25919
Volume of grey matter in x cerebellum right	25920
Mean FA in middle cerebellar peduncle on FA skeleton	25056
Mean FA in pontine crossing tract on FA skeleton	25057
Mean FA in genu of corpus callosum on FA skeleton	25058
Mean FA in body of corpus callosum on FA skeleton	25059
Mean FA in splenium of corpus callosum on FA skeleton	25060
Mean FA in fornix on FA skeleton	25061
Mean FA in corticospinal tract on FA skeleton right	25062
Mean FA in corticospinal tract on FA skeleton left	25063

Mean FA in medial lemniscus on FA skeleton right	25064
Mean FA in medial lemniscus on FA skeleton left	25065
Mean FA in inferior cerebellar peduncle on FA skeleton right	25066
Mean FA in inferior cerebellar peduncle on FA skeleton left	25067
Mean FA in superior cerebellar peduncle on FA skeleton right	25068
Mean FA in superior cerebellar peduncle on FA skeleton left	25069
Mean FA in cerebral peduncle on FA skeleton right	25070
Mean FA in cerebral peduncle on FA skeleton left	25071
Mean FA in anterior limb of internal capsule on FA skeleton right	25072
Mean FA in anterior limb of internal capsule on FA skeleton left	25073
Mean FA in posterior limb of internal capsule on FA skeleton right	25074
Mean FA in posterior limb of internal capsule on FA skeleton left	25075
Mean FA in retrolenticular part of internal capsule on FA skeleton right	25076
Mean FA in retrolenticular part of internal capsule on FA skeleton left	25077
Mean FA in anterior corona radiata on FA skeleton right	25078
Mean FA in anterior corona radiata on FA skeleton left	25079
Mean FA in superior corona radiata on FA skeleton right	25080
Mean FA in superior corona radiata on FA skeleton left	25081
Mean FA in posterior corona radiata on FA skeleton right	25082
Mean FA in posterior corona radiata on FA skeleton left	25083
Mean FA in posterior thalamic radiation on FA skeleton right	25084
Mean FA in posterior thalamic radiation on FA skeleton left	25085
Mean FA in sagittal stratum on FA skeleton right	25086
Mean FA in sagittal stratum on FA skeleton left	25087
Mean FA in external capsule on FA skeleton right	25088
Mean FA in external capsule on FA skeleton left	25089
Mean FA in cingulum cingulate gyrus on FA skeleton right	25090
Mean FA in cingulum cingulate gyrus on FA skeleton left	25091
Mean FA in cingulum hippocampus on FA skeleton right	25092
Mean FA in cingulum hippocampus on FA skeleton left	25093
Mean FA in fornix cres/stria terminalis on FA skeleton right	25094
Mean FA in fornix cres/stria terminalis on FA skeleton left	25095
Mean FA in superior longitudinal fasciculus on FA skeleton right	25096
Mean FA in superior longitudinal fasciculus on FA skeleton left	25097

Mean FA in superior frontooccipital fasciculus on FA skeleton right	25098
Mean FA in superior frontooccipital fasciculus on FA skeleton left	25099
Mean FA in uncinate fasciculus on FA skeleton right	25100
Mean FA in uncinate fasciculus on FA skeleton left	25101
Mean FA in tapetum on FA skeleton right	25102
Mean FA in tapetum on FA skeleton left	25103
Mean MD in middle cerebellar peduncle on FA skeleton	25104
Mean MD in pontine crossing tract on FA skeleton	25105
Mean MD in genu of corpus callosum on FA skeleton	25106
Mean MD in body of corpus callosum on FA skeleton	25107
Mean MD in splenium of corpus callosum on FA skeleton	25108
Mean MD in fornix on FA skeleton	25109
Mean MD in corticospinal tract on FA skeleton right	25110
Mean MD in corticospinal tract on FA skeleton left	25111
Mean MD in medial lemniscus on FA skeleton right	25112
Mean MD in medial lemniscus on FA skeleton left	25113
Mean MD in inferior cerebellar peduncle on FA skeleton right	25114
Mean MD in inferior cerebellar peduncle on FA skeleton left	25115
Mean MD in superior cerebellar peduncle on FA skeleton right	25116
Mean MD in superior cerebellar peduncle on FA skeleton left	25117
Mean MD in cerebral peduncle on FA skeleton right	25118
Mean MD in cerebral peduncle on FA skeleton left	25119
Mean MD in anterior limb of internal capsule on FA skeleton right	25120
Mean MD in anterior limb of internal capsule on FA skeleton left	25121
Mean MD in posterior limb of internal capsule on FA skeleton right	25122
Mean MD in posterior limb of internal capsule on FA skeleton left	25123
Mean MD in retrolenticular part of internal capsule on FA skeleton right	25124
Mean MD in retrolenticular part of internal capsule on FA skeleton left	25125
Mean MD in anterior corona radiata on FA skeleton right	25126
Mean MD in anterior corona radiata on FA skeleton left	25127
Mean MD in superior corona radiata on FA skeleton right	25128
Mean MD in superior corona radiata on FA skeleton left	25129

Mean MD in posterior corona radiata on FA skeleton right	25130
Mean MD in posterior corona radiata on FA skeleton left	25131
Mean MD in posterior thalamic radiation on FA skeleton right	25132
Mean MD in posterior thalamic radiation on FA skeleton left	25133
Mean MD in sagittal stratum on FA skeleton right	25134
Mean MD in sagittal stratum on FA skeleton left	25135
Mean MD in external capsule on FA skeleton right	25136
Mean MD in external capsule on FA skeleton left	25137
Mean MD in cingulum cingulate gyrus on FA skeleton right	25138
Mean MD in cingulum cingulate gyrus on FA skeleton left	25139
Mean MD in cingulum hippocampus on FA skeleton right	25140
Mean MD in cingulum hippocampus on FA skeleton left	25141
Mean MD in fornix cres/stria terminalis on FA skeleton right	25142
Mean MD in fornix cres/stria terminalis on FA skeleton left	25143
Mean MD in superior longitudinal fasciculus on FA skeleton right	25144
Mean MD in superior longitudinal fasciculus on FA skeleton left	25145
Mean MD in superior frontooccipital fasciculus on FA skeleton right	25146
Mean MD in superior frontooccipital fasciculus on FA skeleton left	25147
Mean MD in uncinate fasciculus on FA skeleton right	25148
Mean MD in uncinate fasciculus on FA skeleton left	25149
Mean MD in tapetum on FA skeleton right	25150
Mean MD in tapetum on FA skeleton left	25151
Mean MO in middle cerebellar peduncle on FA skeleton	25152
Mean MO in pontine crossing tract on FA skeleton	25153
Mean MO in genu of corpus callosum on FA skeleton	25154
Mean MO in body of corpus callosum on FA skeleton	25155
Mean MO in splenium of corpus callosum on FA skeleton	25156
Mean MO in fornix on FA skeleton	25157
Mean MO in corticospinal tract on FA skeleton right	25158
Mean MO in corticospinal tract on FA skeleton left	25159
Mean MO in medial lemniscus on FA skeleton right	25160
Mean MO in medial lemniscus on FA skeleton left	25161
Mean MO in inferior cerebellar peduncle on FA skeleton right	25162
Mean MO in inferior cerebellar peduncle on FA skeleton left	25163

Mean MO in superior cerebellar peduncle on FA skeleton right	25164
Mean MO in superior cerebellar peduncle on FA skeleton left	25165
Mean MO in cerebral peduncle on FA skeleton right	25166
Mean MO in cerebral peduncle on FA skeleton left	25167
Mean MO in anterior limb of internal capsule on FA skeleton right	25168
Mean MO in anterior limb of internal capsule on FA skeleton left	25169
Mean MO in posterior limb of internal capsule on FA skeleton right	25170
Mean MO in posterior limb of internal capsule on FA skeleton left	25171
Mean MO in retrolenticular part of internal capsule on FA skeleton right	25172
Mean MO in retrolenticular part of internal capsule on FA skeleton left	25173
Mean MO in anterior corona radiata on FA skeleton right	25174
Mean MO in anterior corona radiata on FA skeleton left	25175
Mean MO in superior corona radiata on FA skeleton right	25176
Mean MO in superior corona radiata on FA skeleton left	25177
Mean MO in posterior corona radiata on FA skeleton right	25178
Mean MO in posterior corona radiata on FA skeleton left	25179
Mean MO in posterior thalamic radiation on FA skeleton right	25180
Mean MO in posterior thalamic radiation on FA skeleton left	25181
Mean MO in sagittal stratum on FA skeleton right	25182
Mean MO in sagittal stratum on FA skeleton left	25183
Mean MO in external capsule on FA skeleton right	25184
Mean MO in external capsule on FA skeleton left	25185
Mean MO in cingulum cingulate gyrus on FA skeleton right	25186
Mean MO in cingulum cingulate gyrus on FA skeleton left	25187
Mean MO in cingulum hippocampus on FA skeleton right	25188
Mean MO in cingulum hippocampus on FA skeleton left	25189
Mean MO in fornix cres/stria terminalis on FA skeleton right	25190
Mean MO in fornix cres/stria terminalis on FA skeleton left	25191
Mean MO in superior longitudinal fasciculus on FA skeleton right	25192
Mean MO in superior longitudinal fasciculus on FA skeleton left	25193
Mean MO in superior frontooccipital fasciculus on FA skeleton right	25194
Mean MO in superior frontooccipital fasciculus on FA skeleton left	25195

Mean MO in uncinate fasciculus on FA skeleton right	25196
Mean MO in uncinate fasciculus on FA skeleton left	25197
Mean MO in tapetum on FA skeleton right	25198
Mean MO in tapetum on FA skeleton left	25199
Mean L1 in middle cerebellar peduncle on FA skeleton	25200
Mean L1 in pontine crossing tract on FA skeleton	25201
Mean L1 in genu of corpus callosum on FA skeleton	25202
Mean L1 in body of corpus callosum on FA skeleton	25203
Mean L1 in splenium of corpus callosum on FA skeleton	25204
Mean L1 in fornix on FA skeleton	25205
Mean L1 in corticospinal tract on FA skeleton right	25206
Mean L1 in corticospinal tract on FA skeleton left	25207
Mean L1 in medial lemniscus on FA skeleton right	25208
Mean L1 in medial lemniscus on FA skeleton left	25209
Mean L1 in inferior cerebellar peduncle on FA skeleton right	25210
Mean L1 in inferior cerebellar peduncle on FA skeleton left	25211
Mean L1 in superior cerebellar peduncle on FA skeleton right	25212
Mean L1 in superior cerebellar peduncle on FA skeleton left	25213
Mean L1 in cerebral peduncle on FA skeleton right	25214
Mean L1 in cerebral peduncle on FA skeleton left	25215
Mean L1 in anterior limb of internal capsule on FA skeleton right	25216
Mean L1 in anterior limb of internal capsule on FA skeleton left	25217
Mean L1 in posterior limb of internal capsule on FA skeleton right	25218
Mean L1 in posterior limb of internal capsule on FA skeleton left	25219
Mean L1 in retrolenticular part of internal capsule on FA skeleton right	25220
Mean L1 in retrolenticular part of internal capsule on FA skeleton left	25221
Mean L1 in anterior corona radiata on FA skeleton right	25222
Mean L1 in anterior corona radiata on FA skeleton left	25223
Mean L1 in superior corona radiata on FA skeleton right	25224
Mean L1 in superior corona radiata on FA skeleton left	25225
Mean L1 in posterior corona radiata on FA skeleton right	25226
Mean L1 in posterior corona radiata on FA skeleton left	25227

Mean L1 in posterior thalamic radiation on FA skeleton right	25228
Mean L1 in posterior thalamic radiation on FA skeleton left	25229
Mean L1 in sagittal stratum on FA skeleton right	25230
Mean L1 in sagittal stratum on FA skeleton left	25231
Mean L1 in external capsule on FA skeleton right	25232
Mean L1 in external capsule on FA skeleton left	25233
Mean L1 in cingulum cingulate gyrus on FA skeleton right	25234
Mean L1 in cingulum cingulate gyrus on FA skeleton left	25235
Mean L1 in cingulum hippocampus on FA skeleton right	25236
Mean L1 in cingulum hippocampus on FA skeleton left	25237
Mean L1 in fornix cres/stria terminalis on FA skeleton right	25238
Mean L1 in fornix cres/stria terminalis on FA skeleton left	25239
Mean L1 in superior longitudinal fasciculus on FA skeleton right	25240
Mean L1 in superior longitudinal fasciculus on FA skeleton left	25241
Mean L1 in superior frontooccipital fasciculus on FA skeleton right	25242
Mean L1 in superior frontooccipital fasciculus on FA skeleton left	25243
Mean L1 in uncinate fasciculus on FA skeleton right	25244
Mean L1 in uncinate fasciculus on FA skeleton left	25245
Mean L1 in tapetum on FA skeleton right	25246
Mean L1 in tapetum on FA skeleton left	25247
Mean L2 in middle cerebellar peduncle on FA skeleton	25248
Mean L2 in pontine crossing tract on FA skeleton	25249
Mean L2 in genu of corpus callosum on FA skeleton	25250
Mean L2 in body of corpus callosum on FA skeleton	25251
Mean L2 in splenium of corpus callosum on FA skeleton	25252
Mean L2 in fornix on FA skeleton	25253
Mean L2 in corticospinal tract on FA skeleton right	25254
Mean L2 in corticospinal tract on FA skeleton left	25255
Mean L2 in medial lemniscus on FA skeleton right	25256
Mean L2 in medial lemniscus on FA skeleton left	25257
Mean L2 in inferior cerebellar peduncle on FA skeleton right	25258
Mean L2 in inferior cerebellar peduncle on FA skeleton left	25259
Mean L2 in superior cerebellar peduncle on FA skeleton right	25260
Mean L2 in superior cerebellar peduncle on FA skeleton left	25261

Mean L2 in cerebral peduncle on FA skeleton right	25262
Mean L2 in cerebral peduncle on FA skeleton left	25263
Mean L2 in anterior limb of internal capsule on FA skeleton right	25264
Mean L2 in anterior limb of internal capsule on FA skeleton left	25265
Mean L2 in posterior limb of internal capsule on FA skeleton right	25266
Mean L2 in posterior limb of internal capsule on FA skeleton left	25267
Mean L2 in retrolenticular part of internal capsule on FA skeleton right	25268
Mean L2 in retrolenticular part of internal capsule on FA skeleton left	25269
Mean L2 in anterior corona radiata on FA skeleton right	25270
Mean L2 in anterior corona radiata on FA skeleton left	25271
Mean L2 in superior corona radiata on FA skeleton right	25272
Mean L2 in superior corona radiata on FA skeleton left	25273
Mean L2 in posterior corona radiata on FA skeleton right	25274
Mean L2 in posterior corona radiata on FA skeleton left	25275
Mean L2 in posterior thalamic radiation on FA skeleton right	25276
Mean L2 in posterior thalamic radiation on FA skeleton left	25277
Mean L2 in sagittal stratum on FA skeleton right	25278
Mean L2 in sagittal stratum on FA skeleton left	25279
Mean L2 in external capsule on FA skeleton right	25280
Mean L2 in external capsule on FA skeleton left	25281
Mean L2 in cingulum cingulate gyrus on FA skeleton right	25282
Mean L2 in cingulum cingulate gyrus on FA skeleton left	25283
Mean L2 in cingulum hippocampus on FA skeleton right	25284
Mean L2 in cingulum hippocampus on FA skeleton left	25285
Mean L2 in fornix cres/stria terminalis on FA skeleton right	25286
Mean L2 in fornix cres/stria terminalis on FA skeleton left	25287
Mean L2 in superior longitudinal fasciculus on FA skeleton right	25288
Mean L2 in superior longitudinal fasciculus on FA skeleton left	25289
Mean L2 in superior frontooccipital fasciculus on FA skeleton right	25290
Mean L2 in superior frontooccipital fasciculus on FA skeleton left	25291
Mean L2 in uncinate fasciculus on FA skeleton right	25292
Mean L2 in uncinate fasciculus on FA skeleton left	25293

Mean L2 in tapetum on FA skeleton right	25294
Mean L2 in tapetum on FA skeleton left	25295
Mean L3 in middle cerebellar peduncle on FA skeleton	25296
Mean L3 in pontine crossing tract on FA skeleton	25297
Mean L3 in genu of corpus callosum on FA skeleton	25298
Mean L3 in body of corpus callosum on FA skeleton	25299
Mean L3 in splenium of corpus callosum on FA skeleton	25300
Mean L3 in fornix on FA skeleton	25301
Mean L3 in corticospinal tract on FA skeleton right	25302
Mean L3 in corticospinal tract on FA skeleton left	25303
Mean L3 in medial lemniscus on FA skeleton right	25304
Mean L3 in medial lemniscus on FA skeleton left	25305
Mean L3 in inferior cerebellar peduncle on FA skeleton right	25306
Mean L3 in inferior cerebellar peduncle on FA skeleton left	25307
Mean L3 in superior cerebellar peduncle on FA skeleton right	25308
Mean L3 in superior cerebellar peduncle on FA skeleton left	25309
Mean L3 in cerebral peduncle on FA skeleton right	25310
Mean L3 in cerebral peduncle on FA skeleton left	25311
Mean L3 in anterior limb of internal capsule on FA skeleton right	25312
Mean L3 in anterior limb of internal capsule on FA skeleton left	25313
Mean L3 in posterior limb of internal capsule on FA skeleton right	25314
Mean L3 in posterior limb of internal capsule on FA skeleton left	25315
Mean L3 in retrolenticular part of internal capsule on FA skeleton right	25316
Mean L3 in retrolenticular part of internal capsule on FA skeleton left	25317
Mean L3 in anterior corona radiata on FA skeleton right	25318
Mean L3 in anterior corona radiata on FA skeleton left	25319
Mean L3 in superior corona radiata on FA skeleton right	25320
Mean L3 in superior corona radiata on FA skeleton left	25321
Mean L3 in posterior corona radiata on FA skeleton right	25322
Mean L3 in posterior corona radiata on FA skeleton left	25323
Mean L3 in posterior thalamic radiation on FA skeleton right	25324
Mean L3 in posterior thalamic radiation on FA skeleton left	25325

Mean L3 in sagittal stratum on FA skeleton right	25326
Mean L3 in sagittal stratum on FA skeleton left	25327
Mean L3 in external capsule on FA skeleton right	25328
Mean L3 in external capsule on FA skeleton left	25329
Mean L3 in cingulum cingulate gyrus on FA skeleton right	25330
Mean L3 in cingulum cingulate gyrus on FA skeleton left	25331
Mean L3 in cingulum hippocampus on FA skeleton right	25332
Mean L3 in cingulum hippocampus on FA skeleton left	25333
Mean L3 in fornix cres/stria terminalis on FA skeleton right	25334
Mean L3 in fornix cres/stria terminalis on FA skeleton left	25335
Mean L3 in superior longitudinal fasciculus on FA skeleton right	25336
Mean L3 in superior longitudinal fasciculus on FA skeleton left	25337
Mean L3 in superior frontooccipital fasciculus on FA skeleton right	25338
Mean L3 in superior frontooccipital fasciculus on FA skeleton left	25339
Mean L3 in uncinate fasciculus on FA skeleton right	25340
Mean L3 in uncinate fasciculus on FA skeleton left	25341
Mean L3 in tapetum on FA skeleton right	25342
Mean L3 in tapetum on FA skeleton left	25343
Mean ICVF in middle cerebellar peduncle on FA skeleton	25344
Mean ICVF in pontine crossing tract on FA skeleton	25345
Mean ICVF in genu of corpus callosum on FA skeleton	25346
Mean ICVF in body of corpus callosum on FA skeleton	25347
Mean ICVF in splenium of corpus callosum on FA skeleton	25348
Mean ICVF in fornix on FA skeleton	25349
Mean ICVF in corticospinal tract on FA skeleton right	25350
Mean ICVF in corticospinal tract on FA skeleton left	25351
Mean ICVF in medial lemniscus on FA skeleton right	25352
Mean ICVF in medial lemniscus on FA skeleton left	25353
Mean ICVF in inferior cerebellar peduncle on FA skeleton right	25354
Mean ICVF in inferior cerebellar peduncle on FA skeleton left	25355
Mean ICVF in superior cerebellar peduncle on FA skeleton right	25356
Mean ICVF in superior cerebellar peduncle on FA skeleton left	25357
Mean ICVF in cerebral peduncle on FA skeleton right	25358
Mean ICVF in cerebral peduncle on FA skeleton left	25359

Mean ICVF in anterior limb of internal capsule on FA skeleton right	25360
Mean ICVF in anterior limb of internal capsule on FA skeleton left	25361
Mean ICVF in posterior limb of internal capsule on FA skeleton right	25362
Mean ICVF in posterior limb of internal capsule on FA skeleton left	25363
Mean ICVF in retrolenticular part of internal capsule on FA skeleton right	25364
Mean ICVF in retrolenticular part of internal capsule on FA skeleton left	25365
Mean ICVF in anterior corona radiata on FA skeleton right	25366
Mean ICVF in anterior corona radiata on FA skeleton left	25367
Mean ICVF in superior corona radiata on FA skeleton right	25368
Mean ICVF in superior corona radiata on FA skeleton left	25369
Mean ICVF in posterior corona radiata on FA skeleton right	25370
Mean ICVF in posterior corona radiata on FA skeleton left	25371
Mean ICVF in posterior thalamic radiation on FA skeleton right	25372
Mean ICVF in posterior thalamic radiation on FA skeleton left	25373
Mean ICVF in sagittal stratum on FA skeleton right	25374
Mean ICVF in sagittal stratum on FA skeleton left	25375
Mean ICVF in external capsule on FA skeleton right	25376
Mean ICVF in external capsule on FA skeleton left	25377
Mean ICVF in cingulum cingulate gyrus on FA skeleton right	25378
Mean ICVF in cingulum cingulate gyrus on FA skeleton left	25379
Mean ICVF in cingulum hippocampus on FA skeleton right	25380
Mean ICVF in cingulum hippocampus on FA skeleton left	25381
Mean ICVF in fornix cres/stria terminalis on FA skeleton right	25382
Mean ICVF in fornix cres/stria terminalis on FA skeleton left	25383
Mean ICVF in superior longitudinal fasciculus on FA skeleton right	25384
Mean ICVF in superior longitudinal fasciculus on FA skeleton left	25385
Mean ICVF in superior frontooccipital fasciculus on FA skeleton right	25386
Mean ICVF in superior frontooccipital fasciculus on FA skeleton left	25387
Mean ICVF in uncinate fasciculus on FA skeleton right	25388
Mean ICVF in uncinate fasciculus on FA skeleton left	25389
Mean ICVF in tapetum on FA skeleton right	25390
Mean ICVF in tapetum on FA skeleton left	25391

Mean OD in middle cerebellar peduncle on FA skeleton	25392
Mean OD in pontine crossing tract on FA skeleton	25393
Mean OD in genu of corpus callosum on FA skeleton	25394
Mean OD in body of corpus callosum on FA skeleton	25395
Mean OD in splenium of corpus callosum on FA skeleton	25396
Mean OD in fornix on FA skeleton	25397
Mean OD in corticospinal tract on FA skeleton right	25398
Mean OD in corticospinal tract on FA skeleton left	25399
Mean OD in medial lemniscus on FA skeleton right	25400
Mean OD in medial lemniscus on FA skeleton left	25401
Mean OD in inferior cerebellar peduncle on FA skeleton right	25402
Mean OD in inferior cerebellar peduncle on FA skeleton left	25403
Mean OD in superior cerebellar peduncle on FA skeleton right	25404
Mean OD in superior cerebellar peduncle on FA skeleton left	25405
Mean OD in cerebral peduncle on FA skeleton right	25406
Mean OD in cerebral peduncle on FA skeleton left	25407
Mean OD in anterior limb of internal capsule on FA skeleton right	25408
Mean OD in anterior limb of internal capsule on FA skeleton left	25409
Mean OD in posterior limb of internal capsule on FA skeleton right	25410
Mean OD in posterior limb of internal capsule on FA skeleton left	25411
Mean OD in retrolenticular part of internal capsule on FA skeleton right	25412
Mean OD in retrolenticular part of internal capsule on FA skeleton left	25413
Mean OD in anterior corona radiata on FA skeleton right	25414
Mean OD in anterior corona radiata on FA skeleton left	25415
Mean OD in superior corona radiata on FA skeleton right	25416
Mean OD in superior corona radiata on FA skeleton left	25417
Mean OD in posterior corona radiata on FA skeleton right	25418
Mean OD in posterior corona radiata on FA skeleton left	25419
Mean OD in posterior thalamic radiation on FA skeleton right	25420
Mean OD in posterior thalamic radiation on FA skeleton left	25421
Mean OD in sagittal stratum on FA skeleton right	25422
Mean OD in sagittal stratum on FA skeleton left	25423

Mean OD in external capsule on FA skeleton right	25424
Mean OD in external capsule on FA skeleton left	25425
Mean OD in cingulum cingulate gyrus on FA skeleton right	25426
Mean OD in cingulum cingulate gyrus on FA skeleton left	25427
Mean OD in cingulum hippocampus on FA skeleton right	25428
Mean OD in cingulum hippocampus on FA skeleton left	25429
Mean OD in fornix cres/stria terminalis on FA skeleton right	25430
Mean OD in fornix cres/stria terminalis on FA skeleton left	25431
Mean OD in superior longitudinal fasciculus on FA skeleton right	25432
Mean OD in superior longitudinal fasciculus on FA skeleton left	25433
Mean OD in superior frontooccipital fasciculus on FA skeleton right	25434
Mean OD in superior frontooccipital fasciculus on FA skeleton left	25435
Mean OD in uncinate fasciculus on FA skeleton right	25436
Mean OD in uncinate fasciculus on FA skeleton left	25437
Mean OD in tapetum on FA skeleton right	25438
Mean OD in tapetum on FA skeleton left	25439
Mean ISOVF in middle cerebellar peduncle on FA skeleton	25440
Mean ISOVF in pontine crossing tract on FA skeleton	25441
Mean ISOVF in genu of corpus callosum on FA skeleton	25442
Mean ISOVF in body of corpus callosum on FA skeleton	25443
Mean ISOVF in splenium of corpus callosum on FA skeleton	25444
Mean ISOVF in fornix on FA skeleton	25445
Mean ISOVF in corticospinal tract on FA skeleton right	25446
Mean ISOVF in corticospinal tract on FA skeleton left	25447
Mean ISOVF in medial lemniscus on FA skeleton right	25448
Mean ISOVF in medial lemniscus on FA skeleton left	25449
Mean ISOVF in inferior cerebellar peduncle on FA skeleton right	25450
Mean ISOVF in inferior cerebellar peduncle on FA skeleton left	25451
Mean ISOVF in superior cerebellar peduncle on FA skeleton right	25452
Mean ISOVF in superior cerebellar peduncle on FA skeleton left	25453
Mean ISOVF in cerebral peduncle on FA skeleton right	25454
Mean ISOVF in cerebral peduncle on FA skeleton left	25455
Mean ISOVF in anterior limb of internal capsule on FA skeleton right	25456
Mean ISOVF in anterior limb of internal capsule on FA skeleton left	25457

Mean ISOVF in posterior limb of internal capsule on FA skeleton right	25458
Mean ISOVF in posterior limb of internal capsule on FA skeleton left	25459
Mean ISOVF in retrolenticular part of internal capsule on FA skeleton right	25460
Mean ISOVF in retrolenticular part of internal capsule on FA skeleton left	25461
Mean ISOVF in anterior corona radiata on FA skeleton right	25462
Mean ISOVF in anterior corona radiata on FA skeleton left	25463
Mean ISOVF in superior corona radiata on FA skeleton right	25464
Mean ISOVF in superior corona radiata on FA skeleton left	25465
Mean ISOVF in posterior corona radiata on FA skeleton right	25466
Mean ISOVF in posterior corona radiata on FA skeleton left	25467
Mean ISOVF in posterior thalamic radiation on FA skeleton right	25468
Mean ISOVF in posterior thalamic radiation on FA skeleton left	25469
Mean ISOVF in sagittal stratum on FA skeleton right	25470
Mean ISOVF in sagittal stratum on FA skeleton left	25471
Mean ISOVF in external capsule on FA skeleton right	25472
Mean ISOVF in external capsule on FA skeleton left	25473
Mean ISOVF in cingulum cingulate gyrus on FA skeleton right	25474
Mean ISOVF in cingulum cingulate gyrus on FA skeleton left	25475
Mean ISOVF in cingulum hippocampus on FA skeleton right	25476
Mean ISOVF in cingulum hippocampus on FA skeleton left	25477
Mean ISOVF in fornix cres/stria terminalis on FA skeleton right	25478
Mean ISOVF in fornix cres/stria terminalis on FA skeleton left	25479
Mean ISOVF in superior longitudinal fasciculus on FA skeleton right	25480
Mean ISOVF in superior longitudinal fasciculus on FA skeleton left	25481
Mean ISOVF in superior frontooccipital fasciculus on FA skeleton right	25482
Mean ISOVF in superior frontooccipital fasciculus on FA skeleton left	25483
Mean ISOVF in uncinate fasciculus on FA skeleton right	25484
Mean ISOVF in uncinate fasciculus on FA skeleton left	25485
Mean ISOVF in tapetum on FA skeleton right	25486
Mean ISOVF in tapetum on FA skeleton left	25487
Weighted mean FA in tract acoustic radiation left	25488

Weighted mean FA in tract acoustic radiation right	25489
Weighted mean FA in tract anterior thalamic radiation left	25490
Weighted mean FA in tract anterior thalamic radiation right	25491
Weighted mean FA in tract cingulate gyrus part of cingulum left	25492
Weighted mean FA in tract cingulate gyrus part of cingulum right	25493
Weighted mean FA in tract parahippocampal part of cingulum left	25494
Weighted mean FA in tract parahippocampal part of cingulum right	25495
Weighted mean FA in tract corticospinal tract left	25496
Weighted mean FA in tract corticospinal tract right	25497
Weighted mean FA in tract forceps major	25498
Weighted mean FA in tract forceps minor	25499
Weighted mean FA in tract inferior frontooccipital fasciculus left	25500
Weighted mean FA in tract inferior frontooccipital fasciculus right	25501
Weighted mean FA in tract inferior longitudinal fasciculus left	25502
Weighted mean FA in tract inferior longitudinal fasciculus right	25503
Weighted mean FA in tract middle cerebellar peduncle	25504
Weighted mean FA in tract medial lemniscus left	25505
Weighted mean FA in tract medial lemniscus right	25506
Weighted mean FA in tract posterior thalamic radiation left	25507
Weighted mean FA in tract posterior thalamic radiation right	25508
Weighted mean FA in tract superior longitudinal fasciculus left	25509
Weighted mean FA in tract superior longitudinal fasciculus right	25510
Weighted mean FA in tract superior thalamic radiation left	25511
Weighted mean FA in tract superior thalamic radiation right	25512
Weighted mean FA in tract uncinate fasciculus left	25513
Weighted mean FA in tract uncinate fasciculus right	25514
Weighted mean MD in tract acoustic radiation left	25515
Weighted mean MD in tract acoustic radiation right	25516
Weighted mean MD in tract anterior thalamic radiation left	25517
Weighted mean MD in tract anterior thalamic radiation right	25518
Weighted mean MD in tract cingulate gyrus part of cingulum left	25519
Weighted mean MD in tract cingulate gyrus part of cingulum right	25520
Weighted mean MD in tract parahippocampal part of cingulum left	25521
Weighted mean MD in tract parahippocampal part of cingulum right	25522

Weighted mean MD in tract corticospinal tract left	25523
Weighted mean MD in tract corticospinal tract right	25524
Weighted mean MD in tract forceps major	25525
Weighted mean MD in tract forceps minor	25526
Weighted mean MD in tract inferior frontooccipital fasciculus left	25527
Weighted mean MD in tract inferior frontooccipital fasciculus right	25528
Weighted mean MD in tract inferior longitudinal fasciculus left	25529
Weighted mean MD in tract inferior longitudinal fasciculus right	25530
Weighted mean MD in tract middle cerebellar peduncle	25531
Weighted mean MD in tract medial lemniscus left	25532
Weighted mean MD in tract medial lemniscus right	25533
Weighted mean MD in tract posterior thalamic radiation left	25534
Weighted mean MD in tract posterior thalamic radiation right	25535
Weighted mean MD in tract superior longitudinal fasciculus left	25536
Weighted mean MD in tract superior longitudinal fasciculus right	25537
Weighted mean MD in tract superior thalamic radiation left	25538
Weighted mean MD in tract superior thalamic radiation right	25539
Weighted mean MD in tract uncinate fasciculus left	25540
Weighted mean MD in tract uncinate fasciculus right	25541
Weighted mean MO in tract acoustic radiation left	25542
Weighted mean MO in tract acoustic radiation right	25543
Weighted mean MO in tract anterior thalamic radiation left	25544
Weighted mean MO in tract anterior thalamic radiation right	25545
Weighted mean MO in tract cingulate gyrus part of cingulum left	25546
Weighted mean MO in tract cingulate gyrus part of cingulum right	25547
Weighted mean MO in tract parahippocampal part of cingulum left	25548
Weighted mean MO in tract parahippocampal part of cingulum right	25549
Weighted mean MO in tract corticospinal tract left	25550
Weighted mean MO in tract corticospinal tract right	25551
Weighted mean MO in tract forceps major	25552
Weighted mean MO in tract forceps minor	25553
Weighted mean MO in tract inferior frontooccipital fasciculus left	25554
Weighted mean MO in tract inferior frontooccipital fasciculus right	25555
Weighted mean MO in tract inferior longitudinal fasciculus left	25556

Weighted mean MO in tract inferior longitudinal fasciculus right	25557
Weighted mean MO in tract middle cerebellar peduncle	25558
Weighted mean MO in tract medial lemniscus left	25559
Weighted mean MO in tract medial lemniscus right	25560
Weighted mean MO in tract posterior thalamic radiation left	25561
Weighted mean MO in tract posterior thalamic radiation right	25562
Weighted mean MO in tract superior longitudinal fasciculus left	25563
Weighted mean MO in tract superior longitudinal fasciculus right	25564
Weighted mean MO in tract superior thalamic radiation left	25565
Weighted mean MO in tract superior thalamic radiation right	25566
Weighted mean MO in tract uncinate fasciculus left	25567
Weighted mean MO in tract uncinate fasciculus right	25568
Weighted mean L1 in tract acoustic radiation left	25569
Weighted mean L1 in tract acoustic radiation right	25570
Weighted mean L1 in tract anterior thalamic radiation left	25571
Weighted mean L1 in tract anterior thalamic radiation right	25572
Weighted mean L1 in tract cingulate gyrus part of cingulum left	25573
Weighted mean L1 in tract cingulate gyrus part of cingulum right	25574
Weighted mean L1 in tract parahippocampal part of cingulum left	25575
Weighted mean L1 in tract parahippocampal part of cingulum right	25576
Weighted mean L1 in tract corticospinal tract left	25577
Weighted mean L1 in tract corticospinal tract right	25578
Weighted mean L1 in tract forceps major	25579
Weighted mean L1 in tract forceps minor	25580
Weighted mean L1 in tract inferior frontooccipital fasciculus left	25581
Weighted mean L1 in tract inferior frontooccipital fasciculus right	25582
Weighted mean L1 in tract inferior longitudinal fasciculus left	25583
Weighted mean L1 in tract inferior longitudinal fasciculus right	25584
Weighted mean L1 in tract middle cerebellar peduncle	25585
Weighted mean L1 in tract medial lemniscus left	25586
Weighted mean L1 in tract medial lemniscus right	25587
Weighted mean L1 in tract posterior thalamic radiation left	25588
Weighted mean L1 in tract posterior thalamic radiation right	25589
Weighted mean L1 in tract superior longitudinal fasciculus left	25590

Weighted mean L1 in tract superior longitudinal fasciculus right	25591
Weighted mean L1 in tract superior thalamic radiation left	25592
Weighted mean L1 in tract superior thalamic radiation right	25593
Weighted mean L1 in tract uncinate fasciculus left	25594
Weighted mean L1 in tract uncinate fasciculus right	25595
Weighted mean L2 in tract acoustic radiation left	25596
Weighted mean L2 in tract acoustic radiation right	25597
Weighted mean L2 in tract anterior thalamic radiation left	25598
Weighted mean L2 in tract anterior thalamic radiation right	25599
Weighted mean L2 in tract cingulate gyrus part of cingulum left	25600
Weighted mean L2 in tract cingulate gyrus part of cingulum right	25601
Weighted mean L2 in tract parahippocampal part of cingulum left	25602
Weighted mean L2 in tract parahippocampal part of cingulum right	25603
Weighted mean L2 in tract corticospinal tract left	25604
Weighted mean L2 in tract corticospinal tract right	25605
Weighted mean L2 in tract forceps major	25606
Weighted mean L2 in tract forceps minor	25607
Weighted mean L2 in tract inferior frontooccipital fasciculus left	25608
Weighted mean L2 in tract inferior frontooccipital fasciculus right	25609
Weighted mean L2 in tract inferior longitudinal fasciculus left	25610
Weighted mean L2 in tract inferior longitudinal fasciculus right	25611
Weighted mean L2 in tract middle cerebellar peduncle	25612
Weighted mean L2 in tract medial lemniscus left	25613
Weighted mean L2 in tract medial lemniscus right	25614
Weighted mean L2 in tract posterior thalamic radiation left	25615
Weighted mean L2 in tract posterior thalamic radiation right	25616
Weighted mean L2 in tract superior longitudinal fasciculus left	25617
Weighted mean L2 in tract superior longitudinal fasciculus right	25618
Weighted mean L2 in tract superior thalamic radiation left	25619
Weighted mean L2 in tract superior thalamic radiation right	25620
Weighted mean L2 in tract uncinate fasciculus left	25621
Weighted mean L2 in tract uncinate fasciculus right	25622
Weighted mean L3 in tract acoustic radiation left	25623
Weighted mean L3 in tract acoustic radiation right	25624

Weighted mean L3 in tract anterior thalamic radiation left	25625
Weighted mean L3 in tract anterior thalamic radiation right	25626
Weighted mean L3 in tract cingulate gyrus part of cingulum left	25627
Weighted mean L3 in tract cingulate gyrus part of cingulum right	25628
Weighted mean L3 in tract parahippocampal part of cingulum left	25629
Weighted mean L3 in tract parahippocampal part of cingulum right	25630
Weighted mean L3 in tract corticospinal tract left	25631
Weighted mean L3 in tract corticospinal tract right	25632
Weighted mean L3 in tract forceps major	25633
Weighted mean L3 in tract forceps minor	25634
Weighted mean L3 in tract inferior frontooccipital fasciculus left	25635
Weighted mean L3 in tract inferior frontooccipital fasciculus right	25636
Weighted mean L3 in tract inferior longitudinal fasciculus left	25637
Weighted mean L3 in tract inferior longitudinal fasciculus right	25638
Weighted mean L3 in tract middle cerebellar peduncle	25639
Weighted mean L3 in tract medial lemniscus left	25640
Weighted mean L3 in tract medial lemniscus right	25641
Weighted mean L3 in tract posterior thalamic radiation left	25642
Weighted mean L3 in tract posterior thalamic radiation right	25643
Weighted mean L3 in tract superior longitudinal fasciculus left	25644
Weighted mean L3 in tract superior longitudinal fasciculus right	25645
Weighted mean L3 in tract superior thalamic radiation left	25646
Weighted mean L3 in tract superior thalamic radiation right	25647
Weighted mean L3 in tract uncinate fasciculus left	25648
Weighted mean L3 in tract uncinate fasciculus right	25649
Weighted mean ICVF in tract acoustic radiation left	25650
Weighted mean ICVF in tract acoustic radiation right	25651
Weighted mean ICVF in tract anterior thalamic radiation left	25652
Weighted mean ICVF in tract anterior thalamic radiation right	25653
Weighted mean ICVF in tract cingulate gyrus part of cingulum left	25654
Weighted mean ICVF in tract cingulate gyrus part of cingulum right	25655
Weighted mean ICVF in tract parahippocampal part of cingulum left	25656
Weighted mean ICVF in tract parahippocampal part of cingulum right	25657
Weighted mean ICVF in tract corticospinal tract left	25658

Weighted mean ICVF in tract corticospinal tract right	25659
Weighted mean ICVF in tract forceps major	25660
Weighted mean ICVF in tract forceps minor	25661
Weighted mean ICVF in tract inferior frontooccipital fasciculus left	25662
Weighted mean ICVF in tract inferior frontooccipital fasciculus right	25663
Weighted mean ICVF in tract inferior longitudinal fasciculus left	25664
Weighted mean ICVF in tract inferior longitudinal fasciculus right	25665
Weighted mean ICVF in tract middle cerebellar peduncle	25666
Weighted mean ICVF in tract medial lemniscus left	25667
Weighted mean ICVF in tract medial lemniscus right	25668
Weighted mean ICVF in tract posterior thalamic radiation left	25669
Weighted mean ICVF in tract posterior thalamic radiation right	25670
Weighted mean ICVF in tract superior longitudinal fasciculus left	25671
Weighted mean ICVF in tract superior longitudinal fasciculus right	25672
Weighted mean ICVF in tract superior thalamic radiation left	25673
Weighted mean ICVF in tract superior thalamic radiation right	25674
Weighted mean ICVF in tract uncinate fasciculus left	25675
Weighted mean ICVF in tract uncinate fasciculus right	25676
Weighted mean OD in tract acoustic radiation left	25677
Weighted mean OD in tract acoustic radiation right	25678
Weighted mean OD in tract anterior thalamic radiation left	25679
Weighted mean OD in tract anterior thalamic radiation right	25680
Weighted mean OD in tract cingulate gyrus part of cingulum left	25681
Weighted mean OD in tract cingulate gyrus part of cingulum right	25682
Weighted mean OD in tract parahippocampal part of cingulum left	25683
Weighted mean OD in tract parahippocampal part of cingulum right	25684
Weighted mean OD in tract corticospinal tract left	25685
Weighted mean OD in tract corticospinal tract right	25686
Weighted mean OD in tract forceps major	25687
Weighted mean OD in tract forceps minor	25688
Weighted mean OD in tract inferior frontooccipital fasciculus left	25689
Weighted mean OD in tract inferior frontooccipital fasciculus right	25690
Weighted mean OD in tract inferior longitudinal fasciculus left	25691
Weighted mean OD in tract inferior longitudinal fasciculus right	25692

Weighted mean OD in tract middle cerebellar peduncle	25693
Weighted mean OD in tract medial lemniscus left	25694
Weighted mean OD in tract medial lemniscus right	25695
Weighted mean OD in tract posterior thalamic radiation left	25696
Weighted mean OD in tract posterior thalamic radiation right	25697
Weighted mean OD in tract superior longitudinal fasciculus left	25698
Weighted mean OD in tract superior longitudinal fasciculus right	25699
Weighted mean OD in tract superior thalamic radiation left	25700
Weighted mean OD in tract superior thalamic radiation right	25701
Weighted mean OD in tract uncinate fasciculus left	25702
Weighted mean OD in tract uncinate fasciculus right	25703
Weighted mean ISOVF in tract acoustic radiation left	25704
Weighted mean ISOVF in tract acoustic radiation right	25705
Weighted mean ISOVF in tract anterior thalamic radiation left	25706
Weighted mean ISOVF in tract anterior thalamic radiation right	25707
Weighted mean ISOVF in tract cingulate gyrus part of cingulum left	25708
Weighted mean ISOVF in tract cingulate gyrus part of cingulum right	25709
Weighted mean ISOVF in tract parahippocampal part of cingulum left	25710
Weighted mean ISOVF in tract parahippocampal part of cingulum right	25711
Weighted mean ISOVF in tract corticospinal tract left	25712
Weighted mean ISOVF in tract corticospinal tract right	25713
Weighted mean ISOVF in tract forceps major	25714
Weighted mean ISOVF in tract forceps minor	25715
Weighted mean ISOVF in tract inferior frontooccipital fasciculus left	25716
Weighted mean ISOVF in tract inferior frontooccipital fasciculus right	25717
Weighted mean ISOVF in tract inferior longitudinal fasciculus left	25718
Weighted mean ISOVF in tract inferior longitudinal fasciculus right	25719
Weighted mean ISOVF in tract middle cerebellar peduncle	25720
Weighted mean ISOVF in tract medial lemniscus left	25721
Weighted mean ISOVF in tract medial lemniscus right	25722
Weighted mean ISOVF in tract posterior thalamic radiation left	25723
Weighted mean ISOVF in tract posterior thalamic radiation right	25724
Weighted mean ISOVF in tract superior longitudinal fasciculus left	25725
Weighted mean ISOVF in tract superior longitudinal fasciculus right	25726

Weighted mean ISOVF in tract superior thalamic radiation left	25727
Weighted mean ISOVF in tract superior thalamic radiation right	25728
Weighted mean ISOVF in tract uncinate fasciculus left	25729
Weighted mean ISOVF in tract uncinate fasciculus right	25730

ICVF = intracellular volume fraction; FA = fractional anisotropy; ISOVF = isotropic volume fraction; MO = mode of anisotropy; OD = orientation dispersion; Data filed indicates the fundamental block of data held within the UK Biobank.

Table A2. Feature importance (XGBoost)

Feature	Weight
volume_of_brain_stem_4th_ventricle	1.040
mean_fa_in_body_of_corpus_callosum_on_fa_skeleton	0.776
volume_of_grey_matter_in_ventral_striatum_left	-0.775
weightedmean_fa_in_tract_forceps_minor	-0.768
mean_isovf_in_fornix_on_fa_skeleton	0.756
mean_fa_in_superior_cerebellar_peduncle_on_fa_skeleton_right	0.699
weightedmean_md_in_tract_anterior_thalamic_radiation_right	0.695
mean_fa_in_cerebral_peduncle_on_fa_skeleton_left	-0.681
weightedmean_md_in_tract_anterior_thalamic_radiation_left	0.614
volume_of_grey_matter_in_subcallosal_cortex_right	0.607
volume_of_grey_matter_in_frontal_operculum_cortex_right	-0.600
mean_md_in_pontine_crossing_tract_on_fa_skeleton	-0.575
mean_md_in_anterior_limb_of_internal_capsule_on_fa_skeleton_right	0.574
mean_fa_in_superior_cerebellar_peduncle_on_fa_skeleton_left	0.570
mean_md_in_retrolenticular_part_of_internal_capsule_on_fa_skeleton_left	-0.562
mean_fa_in_posterior_limb_of_internal_capsule_on_fa_skeleton_right	-0.554
volume_of_grey_matter_in_crus_ii_cerebellum_right	-0.547
weightedmean_isovf_in_tract_superior_longitudinal_fasciculus_right	0.541
weightedmean_fa_in_tract_anterior_thalamic_radiation_left	0.541
weightedmean_isovf_in_tract_forceps_minor	-0.529
mean_fa_in_posterior_thalamic_radiation_on_fa_skeleton_right	-0.510
mean_md_in_posterior_thalamic_radiation_on_fa_skeleton_left	0.507
volume_of_grey_matter_in_crus_ii_cerebellum_vermis	0.487
mean_fa_in_sagittal_stratum_on_fa_skeleton_right	-0.479
volume_of_grey_matter_in_frontal_orbital_cortex_right	-0.469
mean_md_in_retrolenticular_part_of_internal_capsule_on_fa_skeleton_right	-0.467
volume_of_grey_matter_in_insular_cortex_left	0.457
weightedmean_md_in_tract_corticospinal tract_right	-0.456
mean_fa_in_fornix_cresstria_terminalis_on_fa_skeleton_left	-0.449

mean_md_in_anterior_limb_of_internal_capsule_on_fa_skeleton_left	0.447
weightedmean_isovf_in_tract_anterior_thalamic_radiation_right	-0.443
weightedmean_isovf_in_tract_anterior_thalamic_radiation_left	-0.442
mean_fa_in_fornix_cresstria_terminalis_on_fa_skeleton_right	-0.435
mean_fa_in_anterior_corona_radiata_on_fa_skeleton_left	-0.434
mean_isovf_in_tapetum_on_fa_skeleton_right	-0.427
mean_md_in_superior_longitudinal_fasciculus_on_fa_skeleton_right	-0.421
mean_fa_in_superior_longitudinal_fasciculus_on_fa_skeleton_left	-0.420
weightedmean_md_in_tract_corticospinal tract_left	-0.416
volume_of_grey_matter_in_vii_cerebellum_left	-0.407
mean_fa_in_middle_cerebellar_peduncle_on_fa_skeleton	-0.407
mean_fa_in_anterior_limb_of_internal_capsule_on_fa_skeleton_left	0.407
volume_of_grey_matter_in_putamen_left	0.400
weightedmean_md_in_tract_medial_lemniscus_right	-0.398
mean_fa_in_corticospinal_tract_on_fa_skeleton_right	0.398
volume_of_thalamus_right	-0.397
weightedmean_md_in_tract_superior_longitudinal_fasciculus_left	-0.392
weightedmean_md_in_tract_superior_thalamic_radiation_right	0.387
mean_isovf_in_inferior_cerebellar_peduncle_on_fa_skeleton_left	-0.375
volume_of_putamen_right	-0.373
volume_of_grey_matter_in_pallidum_left	0.367
mean_md_in_genu_of_corpus_callosum_on_fa_skeleton	0.366
volume_of_putamen_left	-0.365
weightedmean_fa_in_tract_anterior_thalamic_radiation_right	0.359
mean_isovf_in_corticospinal_tract_on_fa_skeleton_right	0.357
volume_of_thalamus_left	-0.355
mean_md_in_posterior_thalamic_radiation_on_fa_skeleton_right	0.351
mean_isovf_in_medial_lemniscus_on_fa_skeleton_left	0.346
weightedmean_md_in_tract_superior_longitudinal_fasciculus_right	-0.342
volume_of_grey_matter_in_insular_cortex_right	0.339
weightedmean_fa_in_tract_posterior_thalamic_radiation_left	0.337
mean_isovf_in_body_of_corpus_callosum_on_fa_skeleton	0.332

volume_of_grey_matter_in_heschls_gyrus_includes_h1_and_h2_right	-0.330
volume_of_grey_matter_in_viiib_cerebellum_left	0.328
volume_of_grey_matter_in_ix_cerebellum_left	0.328
volume_of_grey_matter_in_lateral_occipital_cortex_superior_division_right	-0.327
mean_fa_in_anterior_limb_of_internal_capsule_on_fa_skeleton_right	0.324
weightedmean_md_in_tract_posterior_thalamic_radiation_right	0.323
mean_md_in_superior_longitudinal_fasciculus_on_fa_skeleton_left	-0.323
weightedmean_isovf_in_tract_inferior_longitudinal_fasciculus_right	0.320
volume_of_grey_matter_in_vi_cerebellum_right	-0.317
weightedmean_md_in_tract_superior_thalamic_radiation_left	0.311
weightedmean_fa_in_tract_posterior_thalamic_radiation_right	0.310
mean_isovf_in_anterior_limb_of_internal_capsule_on_fa_skeleton_left	0.309
mean_fa_in_posterior_limb_of_internal_capsule_on_fa_skeleton_left	-0.308
volume_of_grey_matter_in_planum_polare_right	-0.305
volume_of_grey_matter_in_pallidum_right	-0.304
weightedmean_fa_in_tract_inferior_frontooccipital_fasciculus_left	0.302
volume_of_grey_matter_in_thalamus_right	0.297
mean_isovf_in_medial_lemniscus_on_fa_skeleton_right	0.292
weightedmean_isovf_in_tract_inferior_longitudinal_fasciculus_left	0.290
volume_of_grey_matter_in_frontal_orbital_cortex_left	-0.290
volume_of_grey_matter_in_supramarginal_gyrus_posterior_division_right	-0.290
mean_fa_in_inferior_cerebellar_peduncle_on_fa_skeleton_left	-0.289
volume_of_grey_matter_in_viiib_cerebellum_vermis	-0.288
mean_isovf_in_posterior_thalamic_radiation_on_fa_skeleton_left	-0.281
weightedmean_isovf_in_tract_uncinate_fasciculus_left	0.280
weightedmean_md_in_tract_inferior_frontooccipital_fasciculus_right	0.279
weightedmean_md_in_tract_inferior_longitudinal_fasciculus_right	-0.278
volume_of_grey_matter_in_ix_cerebellum_right	0.278
weightedmean_isovf_in_tract_middle_cerebellar_peduncle	-0.278
volume_of_grey_matter_in_frontal_pole_left	-0.275
mean_isovf_in_posterior_limb_of_internal_capsule_on_fa_skeleton_left	-0.274
weightedmean_isovf_in_tract_superior_longitudinal_fasciculus_left	0.271

volume_of_grey_matter_in_ventral_striatum_right	-0.270
mean_isovf_in_retrolenticular_part_of_internal_capsule_on_fa_skeleton_left	0.265
mean_md_in_external_capsule_on_fa_skeleton_right	-0.263
volume_of_grey_matter_in_inferior_temporal_gyrus_temporooccipital_part_left	0.262
volume_of_grey_matter_in_caudate_left	-0.261
weightedmean_isovf_in_tract_corticospinal tract_right	0.259
mean_isovf_in_corticospinal_tract_on_fa_skeleton_left	0.259
weightedmean_md_in_tract_forceps_minor	0.254
weightedmean_fa_in_tract_acoustic_radiation_left	-0.253
weightedmean_isovf_in_tract_parahippocampal_part_of_cingulum_right	0.248
volume_of_grey_matter_in_brainstem	-0.248
mean_fa_in_superior_corona_radiata_on_fa_skeleton_left	0.248
mean_md_in_tapetum_on_fa_skeleton_left	0.248
volume_of_grey_matter_in_x_cerebellum_left	-0.247
weightedmean_fa_in_tract_acoustic_radiation_right	-0.244
weightedmean_fa_in_tract_superior_thalamic_radiation_right	0.244
weightedmean_isovf_in_tract_superior_thalamic_radiation_right	0.242
mean_isovf_in_splenium_of_corpus_callosum_on_fa_skeleton	-0.241
mean_md_in_superior_frontooccipital_fasciculus_on_fa_skeleton_right	0.240
mean_isovf_in_fornix_cresstria_terminalis_on_fa_skeleton_right	-0.239
weightedmean_md_in_tract_parahippocampal_part_of_cingulum_left	-0.239
weightedmean_fa_in_tract_inferior_longitudinal_fasciculus_left	-0.239
mean_fa_in_cingulum_cingulate_gyrus_on_fa_skeleton_left	0.239
weightedmean_fa_in_tract_superior_longitudinal_fasciculus_left	-0.237
volume_of_grey_matter_in_putamen_right	0.236
weightedmean_fa_in_tract_uncinate_fasciculus_right	0.235
volume_of_grey_matter_in_frontal_operculum_cortex_left	-0.232
volume_of_grey_matter_in_inferior_frontal_gyrus_pars_trangularis_right	0.231
mean_fa_in_uncinate_fasciculus_on_fa_skeleton_left	0.230
mean_fa_in_cingulum_cingulate_gyrus_on_fa_skeleton_right	0.229
mean_md_in_sagittal_stratum_on_fa_skeleton_right	-0.227
volume_of_grey_matter_in-angular_gyrus_left	0.226

volume_of_grey_matter_in_viiib_cerebellum_right	0.225
volume_of_grey_matter_in_middle_temporal_gyrus_anterior_division_left	-0.222
mean_md_in_posterior_corona_radiata_on_fa_skeleton_left	-0.222
mean_fa_in_superior_longitudinal_fasciculus_on_fa_skeleton_right	0.221
mean_md_in_superior_frontooccipital_fasciculus_on_fa_skeleton_left	0.218
mean_isovf_in_sagittal_stratum_on_fa_skeleton_right	-0.218
volume_of_grey_matter_in_paracingulate_gyrus_right	-0.217
volume_of_caudate_right	0.216
weightedmean_fa_in_tract_middle_cerebellar_peduncle	-0.214
mean_isovf_in_posterior_limb_of_internal_capsule_on_fa_skeleton_right	-0.214
mean_md_in_tapetum_on_fa_skeleton_right	0.208
mean_fa_in_posterior_thalamic_radiation_on_fa_skeleton_left	-0.208
volume_of_grey_matter_in_planum_polare_left	-0.208
mean_isovf_in_superior_frontooccipital_fasciculus_on_fa_skeleton_right	-0.205
mean_isovf_in_superior_corona_radiata_on_fa_skeleton_right	0.204
mean_fa_in_posterior_corona_radiata_on_fa_skeleton_left	0.204
weightedmean_md_in_tract_acoustic_radiation_left	-0.203
mean_fa_in_superior_frontooccipital_fasciculus_on_fa_skeleton_right	0.202
weightedmean_fa_in_tract_cingulate_gyrus_part_of_cingulum_left	-0.202
mean_md_in_cingulum_cingulate_gyrus_on_fa_skeleton_right	-0.200
volume_of_grey_matter_in_inferior_temporal_gyrus_posterior_division_left	0.200
mean_md_in_corticospinal_tract_on_fa_skeleton_right	-0.198
mean_md_in_medial_lemniscus_on_fa_skeleton_left	-0.196
mean_isovf_in_retrolenticular_part_of_internal_capsule_on_fa_skeleton_right	0.194
mean_fa_in_retrolenticular_part_of_internal_capsule_on_fa_skeleton_right	0.194
mean_md_in_superior_corona_radiata_on_fa_skeleton_left	0.194
mean_fa_in_medial_lemniscus_on_fa_skeleton_right	0.193
mean_md_in_anterior_corona_radiata_on_fa_skeleton_left	0.193
volume_of_grey_matter_in_cingulate_gyrus_anterior_division_left	-0.191
mean_isovf_in_tapetum_on_fa_skeleton_left	-0.188
volume_of_grey_matter_in_crus_i_cerebellum_right	-0.188
volume_of_grey_matter_in_v_cerebellum_left	0.185

mean_isovf_in_superior_corona_radiata_on_fa_skeleton_left	0.182
mean_md_in_cerebral_peduncle_on_fa_skeleton_right	-0.179
volume_of_grey_matter_in_temporal_fusiform_cortex_anterior_division_right	-0.179
mean_isovf_in_posterior_corona_radiata_on_fa_skeleton_right	0.178
mean_md_in_inferior_cerebellar_peduncle_on_fa_skeleton_left	0.178
volume_of_grey_matter_in_temporal_fusiform_cortex_posterior_division_left	-0.177
volume_of_grey_matter_in_lingual_gyrus_left	-0.174
volume_of_grey_matter_in_viiia_cerebellum_left	-0.174
mean_fa_in_external_capsule_on_fa_skeleton_right	-0.173
mean_fa_in_genu_of_corpus_callosum_on_fa_skeleton	0.171
mean_fa_in_tapetum_on_fa_skeleton_right	-0.171
mean_fa_in_tapetum_on_fa_skeleton_left	-0.170
mean_md_in_anterior_corona_radiata_on_fa_skeleton_right	0.169
volume_of_grey_matter_in_lateral_occipital_cortex_inferior_division_left	0.169
mean_md_in_fornix_cresstria_terminalis_on_fa_skeleton_right	0.168
volume_of_grey_matter_in_paracingulate_gyrus_left	0.163
mean_md_in_uncinate_fasciculus_on_fa_skeleton_right	0.163
weightedmean_md_in_tract_uncinate_fasciculus_right	0.163
volume_of_grey_matter_in_hippocampus_right	-0.162
mean_md_in_cingulum_cingulate_gyrus_on_fa_skeleton_left	-0.162
volume_of_accumbens_left	0.161
volume_of_grey_matter_in_viiia_cerebellum_right	-0.161
volume_of_hippocampus_left	0.159
mean_fa_in_fornix_on_fa_skeleton	-0.158
mean_isovf_in_genu_of_corpus_callosum_on_fa_skeleton	-0.157
volume_of_grey_matter_in_temporal_occipital_fusiform_cortex_left	-0.154
weightedmean_fa_in_tract_parahippocampal_part_of_cingulum_right	0.154
mean_md_in_cingulum_hippocampus_on_fa_skeleton_left	-0.154
volume_of_grey_matter_in_viiib_cerebellum_vermis	0.153
mean_isovf_in_anterior_limb_of_internal_capsule_on_fa_skeleton_right	0.152
volume_of_grey_matter_in_crus_i_cerebellum_vermis	-0.152
volume_of_grey_matter_in_temporal_pole_left	0.151

volume_of_grey_matter_in_x_cerebellum_right	-0.150
weightedmean_md_in_tract_parahippocampal_part_of_cingulum_right	0.147
weightedmean_isovf_in_tract_inferior_frontooccipital_fasciculus_left	-0.147
mean_isovf_in_superior_frontooccipital_fasciculus_on_fa_skeleton_left	-0.147
weightedmean_md_in_tract_posterior_thalamic_radiation_left	0.147
volume_of_grey_matter_in_juxtapositional_lobule_cortex_formerly_supplementary_motor_cortex_left	-0.146
weightedmean_isovf_in_tract_cingulate_gyrus_part_of_cingulum_left	0.145
volume_of_grey_matter_in_supramarginal_gyrus_anterior_division_left	0.143
weightedmean_md_in_tract_medial_lemniscus_left	-0.142
mean_isovf_in_cingulum_cingulate_gyrus_on_fa_skeleton_left	-0.142
mean_md_in_posterior_limb_of_internal_capsule_on_fa_skeleton_left	-0.142
mean_md_in_medial_lemniscus_on_fa_skeleton_right	-0.141
mean_fa_in_medial_lemniscus_on_fa_skeleton_left	0.140
mean_isovf_in_cingulum_cingulate_gyrus_on_fa_skeleton_right	-0.136
volume_of_grey_matter_in_hippocampus_left	-0.135
volume_of_grey_matter_in_temporal_occipital_fusiform_cortex_right	0.134
weightedmean_md_in_tract_cingulate_gyrus_part_of_cingulum_right	-0.134
weightedmean_isovf_in_tract_acoustic_radiation_left	0.133
volume_of_grey_matter_in_juxtapositional_lobule_cortex_formerly_supplementary_motor_cortex_right	-0.133
mean_md_in_cingulum_hippocampus_on_fa_skeleton_right	-0.131
weightedmean_md_in_tract_inferior_longitudinal_fasciculus_left	-0.131
volume_of_grey_matter_in_occipital_fusiform_gyrus_left	0.127
mean_isovf_in_superior_cerebellar_peduncle_on_fa_skeleton_right	0.126
weightedmean_md_in_tract_uncinate_fasciculus_left	0.125
mean_md_in_posterior_limb_of_internal_capsule_on_fa_skeleton_right	0.125
mean_fa_in_pontine_crossing_tract_on_fa_skeleton	-0.124
volume_of_grey_matter_in_occipital_fusiform_gyrus_right	0.124
volume_of_grey_matter_in_cingulate_gyrus_posterior_division_right	0.123
volume_of_grey_matter_in_precentral_gyrus_left	-0.123
weightedmean_fa_in_tract_inferior_frontooccipital_fasciculus_right	0.123
volume_of_grey_matter_in_supracalcarine_cortex_right	0.123

volume_of_grey_matter_in_heschls_gyrus_includes_h1_and_h2_left	-0.122
mean_isovf_in_superior_longitudinal_fasciculus_on_fa_skeleton_left	-0.122
mean_md_in_sagittal_stratum_on_fa_skeleton_left	-0.122
weightedmean_fa_in_tract_corticospinal tract_left	-0.121
volume_of_grey_matter_in_lateral_occipital_cortex_superior_division_left	0.121
volume_of_grey_matter_in_frontal_medial_cortex_right	-0.121
volume_of_grey_matter_in_inferior_temporal_gyrus_posterior_division_right	-0.120
mean_isovf_in_anterior_corona_radiata_on_fa_skeleton_left	-0.119
volume_of_grey_matter_in_superior_temporal_gyrus_anterior_division_right	0.119
mean_fa_in_retrolenticular_part_of_internal_capsule_on_fa_skeleton_left	0.118
mean_md_in_corticospinal tract_on_fa_skeleton_left	-0.117
mean_isovf_in_cerebral_peduncle_on_fa_skeleton_left	0.115
volume_of_grey_matter_in_middle_temporal_gyrus_posterior_division_right	-0.114
volume_of_grey_matter_in_occipital_pole_right	0.114
volume_of_grey_matter_in_occipital_pole_left	-0.113
mean_md_in_middle_cerebellar_peduncle_on_fa_skeleton	-0.113
volume_of_grey_matter_in_superior_parietal_lobule_left	-0.113
mean_isovf_in_fornix_cresstria_terminalis_on_fa_skeleton_left	-0.110
weightedmean_md_in_tract_acoustic_radiation_right	-0.110
volume_of_grey_matter_in_superior_frontal_gyrus_left	-0.110
volume_of_grey_matter_in_superior_frontal_gyrus_right	0.110
volume_of_grey_matter_in_superior_temporal_gyrus_anterior_division_left	0.108
volume_of_amygdala_right	0.107
volume_of_grey_matter_in_ix_cerebellum_vermis	-0.107
weightedmean_fa_in_tract_uncinate_fasciculus_left	-0.107
volume_of_grey_matter_in_middle_temporal_gyrus_posterior_division_left	-0.106
mean_md_in_inferior_cerebellar_peduncle_on_fa_skeleton_right	0.105
mean_md_in_body_of_corpus_callosum_on_fa_skeleton	0.104
volume_of_grey_matter_in_subcallosal_cortex_left	0.104
volume_of_grey_matter_in_parahippocampal_gyrus_anterior_division_left	-0.104
volume_of_grey_matter_in_supramarginal_gyrus_anterior_division_right	0.103
weightedmean_isovf_in_tract_inferior_fronooccipital_fasciculus_right	0.103

weightedmean_fa_in_tract_forceps_major	0.102
weightedmean_isovf_in_tract_uncinate_fasciculus_right	-0.101
volume_of_grey_matter_in_iiv_cerebellum_left	-0.100
volume_of_grey_matter_in_temporal_fusiform_cortex_posterior_division_right	-0.098
volume_of_grey_matter_in_cingulate_gyrus_anterior_division_right	0.098
volume_of_grey_matter_in_lingual_gyrus_right	-0.098
volume_of_grey_matter_in_iiv_cerebellum_right	-0.098
weightedmean_fa_in_tract_medial_lemniscus_left	-0.097
mean_md_in_cerebral_peduncle_on_fa_skeleton_left	-0.095
weightedmean_isovf_in_tract_cingulate_gyrus_part_of_cingulum_right	0.095
volume_of_caudate_left	0.093
volume_of_grey_matter_in_precuneous_cortex_right	-0.091
mean_isovf_in_superior_cerebellar_peduncle_on_fa_skeleton_left	0.091
volume_of_hippocampus_right	0.091
mean_isovf_in_superior_longitudinal_fasciculus_on_fa_skeleton_right	0.089
volume_of_grey_matter_in_frontal_medial_cortex_left	0.088
volume_of_grey_matter_in_parahippocampal_gyrus_posterior_division_left	0.087
volume_of_grey_matter_in_amygdala_right	0.086
volume_of_grey_matter_in_precuneous_cortex_left	-0.086
volume_of_grey_matter_in_viiia_cerebellum_vermis	0.086
mean_isovf_in_cerebral_peduncle_on_fa_skeleton_right	0.085
volume_of_grey_matter_in_viiib_cerebellum_left	0.083
volume_of_grey_matter_in_inferior_temporal_gyrus_anterior_division_left	-0.080
volume_of_grey_matter_in_lateral_occipital_cortex_inferior_division_right	-0.080
volume_of_amygdala_left	0.077
mean_isovf_in_pontine_crossing_tract_on_fa_skeleton	0.076
mean_md_in_superior_cerebellar_peduncle_on_fa_skeleton_right	0.074
mean_fa_in_cingulum_hippocampus_on_fa_skeleton_right	-0.074
volume_of_accumbens_right	0.073
volume_of_grey_matter_in_inferior_frontal_gyrus_pars_trangularis_left	-0.072
volume_of_grey_matter_in_cuneal_cortex_right	0.071
volume_of_grey_matter_in_vi_cerebellum_vermis	-0.071

weightedmean_md_in_tract_middle_cerebellar_peduncle	0.070
weightedmean_md_in_tract_inferior_fron то occipital_fasciculus_left	0.069
mean_isovf_in_cingulum_hippocampus_on_fa_skeleton_left	0.069
volume_of_grey_matter_in_temporal_pole_right	-0.069
weightedmean_isovf_in_tract_medial_lemniscus_left	0.068
mean_isovf_in_inferior_cerebellar_peduncle_on_fa_skeleton_right	-0.068
volume_of_grey_matter_in_supramarginal_gyrus_posterior_division_left	-0.067
mean_isovf_in_middle_cerebellar_peduncle_on_fa_skeleton	-0.067
volume_of_grey_matter_in_crus_ii_cerebellum_left	-0.066
volume_of_grey_matter_in_postcentral_gyrus_right	-0.064
volume_of_grey_matter_in_inferior_temporal_gyrus_anterior_division_right	-0.064
volume_of_grey_matter_in_viiib_cerebellum_right	-0.062
mean_isovf_in_external_capsule_on_fa_skeleton_left	0.060
weightedmean_fa_in_tract_inferior_longitudinal_fasciculus_right	-0.060
volume_of_grey_matter_in_cingulate_gyrus_posterior_division_left	0.058
mean_isovf_in_anterior_corona_radiata_on_fa_skeleton_right	-0.058
mean_fa_in_sagittal_stratum_on_fa_skeleton_left	0.058
volume_of_grey_matter_in_frontal_pole_right	0.057
mean_isovf_in_posterior_corona_radiata_on_fa_skeleton_left	-0.056
mean_md_in_fornix_cresstria_terminalis_on_fa_skeleton_left	0.055
volume_of_grey_matter_in_parietal_operculum_cortex_right	0.054
mean_md_in_splenium_of_corpus_callosum_on_fa_skeleton	-0.053
mean_isovf_in_external_capsule_on_fa_skeleton_right	-0.053
weightedmean_isovf_in_tract_medial_lemniscus_right	-0.053
mean_fa_in_inferior_cerebellar_peduncle_on_fa_skeleton_right	0.051
volume_of_grey_matter_in_precentral_gyrus_right	0.050
volume_of_grey_matter_in_crus_i_cerebellum_left	0.050
volume_of_grey_matter_in_middle_frontal_gyrus_left	0.050
volume_of_grey_matter_in_supracalcarine_cortex_left	-0.047
volume_of_grey_matter_in-angular_gyrus_right	-0.044
volume_of_grey_matter_in_parahippocampal_gyrus_anterior_division_right	0.043
mean_fa_in_superior_corona_radiata_on_fa_skeleton_right	0.042

volume_of_grey_matter_in_inferior_frontal_gyrus_pars_opercularis_right	0.041
mean_isovf_in_cingulum_hippocampus_on_fa_skeleton_right	-0.041
mean_isovf_in_uncinate_fasciculus_on_fa_skeleton_left	-0.040
volume_of_grey_matter_in_planum_temporale_right	-0.040
mean_fa_in_posterior_corona_radiata_on_fa_skeleton_right	-0.039
weightedmean_isovf_in_tract_forceps_major	-0.039
mean_fa_in_superior_frontooccipital_fasciculus_on_fa_skeleton_left	0.036
volume_of_grey_matter_in_x_cerebellum_vermis	-0.036
mean_md_in_superior_cerebellar_peduncle_on_fa_skeleton_left	0.035
volume_of_grey_matter_in_middle_frontal_gyrus_right	0.034
volume_of_grey_matter_in_planum_temporale_left	-0.034
volume_of_grey_matter_in_middle_temporal_gyrus_temporooccipital_part_right	-0.033
mean_md_in_fornix_on_fa_skeleton	0.032
mean_isovf_in_sagittal_stratum_on_fa_skeleton_left	-0.031
volume_of_grey_matter_in_middle_temporal_gyrus_anterior_division_right	-0.031
weightedmean_isovf_in_tract_parahippocampal_part_of_cingulum_left	0.031
volume_of_grey_matter_in_v_cerebellum_right	-0.030
mean_fa_in_cerebral_peduncle_on_fa_skeleton_right	-0.030
mean_fa_in_uncinate_fasciculus_on_fa_skeleton_right	0.027
volume_of_pallidum_left	0.027
mean_md_in_external_capsule_on_fa_skeleton_left	0.027
volume_of_grey_matter_in_parahippocampal_gyrus_posterior_division_right	0.027
weightedmean_fa_in_tract_medial_lemniscus_right	0.025
volume_of_grey_matter_in_intracalcarine_cortex_left	0.025
weightedmean_fa_in_tract_superior_longitudinal_fasciculus_right	-0.025
weightedmean_fa_in_tract_parahippocampal_part_of_cingulum_left	-0.024
mean_fa_in_cingulum_hippocampus_on_fa_skeleton_left	-0.023
mean_fa_in_splenium_of_corpus_callosum_on_fa_skeleton	0.023
volume_of_pallidum_right	0.021
weightedmean_fa_in_tract_superior_thalamic_radiation_left	0.021
volume_of_grey_matter_in_parietal_operculum_cortex_left	-0.019
mean_isovf_in_posterior_thalamic_radiation_on_fa_skeleton_right	-0.018

volume_of_grey_matter_in_inferior_temporal_gyrus_temporooccipital_part_right	-0.017
volume_of_grey_matter_in_intracalcarine_cortex_right	-0.015
weightedmean_md_in_tract_cingulate_gyrus_part_of_cingulum_left	-0.015
volume_of_grey_matter_in_superior_parietal_lobule_right	0.012
weightedmean_fa_in_tract_corticospinal tract_right	-0.012
mean_fa_in_corticospinal_tract_on_fa_skeleton_left	-0.012
weightedmean_isovf_in_tract_superior_thalamic_radiation_left	0.011
volume_of_grey_matter_in_cuneal_cortex_left	0.011
mean_md_in_uncinate_fasciculus_on_fa_skeleton_left	0.010
volume_of_grey_matter_in_superior_temporal_gyrus_posterior_division_left	0.010
volume_of_grey_matter_in_inferior_frontal_gyrus_pars_opercularis_left	-0.009
volume_of_grey_matter_in_amygdala_left	0.009
mean_isovf_in_uncinate_fasciculus_on_fa_skeleton_right	0.008
weightedmean_isovf_in_tract_posterior_thalamic_radiation_left	-0.008
volume_of_grey_matter_in_central_opercular_cortex_left	0.008
volume_of_grey_matter_in_postcentral_gyrus_left	-0.007
mean_fa_in_external_capsule_on_fa_skeleton_left	0.007
weightedmean_isovf_in_tract_corticospinal_tract_left	-0.007
volume_of_grey_matter_in_thalamus_left	-0.005
volume_of_grey_matter_in_superior_temporal_gyrus_posterior_division_right	0.005
weightedmean_md_in_tract_forceps_major	-0.005
weightedmean_fa_in_tract_cingulate_gyrus_part_of_cingulum_right	-0.005
weightedmean_isovf_in_tract_acoustic_radiation_right	0.003
mean_fa_in_anterior_corona_radiata_on_fa_skeleton_right	-0.003
mean_md_in_posterior_corona_radiata_on_fa_skeleton_right	0.003
volume_of_grey_matter_in_caudate_right	0.002
mean_md_in_superior_corona_radiata_on_fa_skeleton_right	-0.002
volume_of_grey_matter_in_central_opercular_cortex_right	0.001
volume_of_grey_matter_in_temporal_fusiform_cortex_anterior_division_left	-0.001
volume_of_grey_matter_in_middle_temporal_gyrus_temporooccipital_part_left	0.000
weightedmean_isovf_in_tract_posterior_thalamic_radiation_right	0.000

ICVF = intracellular volume fraction; FA = fractional anisotropy; ISOVF = isotropic volume fraction;
 MO = mode of anisotropy; OD = orientation dispersion

Table A3. Results of correlational analysis for BrainAGE and health related outcomes

Traits	<i>r</i>	<i>p</i>	Cl.low	Cl.high	<i>p</i> .FDR
body mass index	0.07	4.E-41	0.063	0.084	2.E-40
diastolic blood pressure automated reading 0	0.09	2.E-55	0.082	0.105	2.E-54
diastolic blood pressure automated reading 1	0.09	1.E-49	0.077	0.101	9.E-49
systolic blood pressure automated reading 0	0.06	1.E-20	0.044	0.067	3.E-20
systolic blood pressure automated reading 1	0.05	2.E-19	0.043	0.066	4.E-19
hip circumference	0.03	1.E-07	0.018	0.039	2.E-07
weight	0.04	1.E-12	0.028	0.050	2.E-12
hand grip strength left	-0.01	1.E-02	-0.024	-0.003	1.E-02
hand grip strength right	-0.02	4.E-04	-0.030	-0.009	6.E-04
overall health rating	0.08	5.E-49	0.069	0.090	3.E-48
longstanding illness disability or infirmity	0.05	3.E-20	0.039	0.060	8.E-20
height	-0.04	4.E-16	-0.054	-0.033	9.E-16
volumetric scaling	0.11	2.E-85	0.095	0.116	4.E-84
fluid intelligence score	-0.06	3.E-27	-0.071	-0.050	9.E-27
duration to complete numeric path trail 1	0.02	1.E-03	0.009	0.034	1.E-03
duration to complete alphanumeric path trail 2	0.04	1.E-08	0.024	0.050	2.E-08
number of puzzles correctly solved	-0.05	6.E-16	-0.066	-0.040	1.E-15
duration spent answering each puzzle	-0.01	3.E-01	-0.019	0.007	4.E-01
number of puzzles correct	-0.03	3.E-06	-0.044	-0.018	4.E-06
duration of moderate activity	0.00	9.E-01	-0.012	0.011	9.E-01
duration of vigorous activity	0.00	5.E-01	-0.017	0.009	6.E-01

Cl.low = confidence interval low; Cl.high = confidence interval high; *p* = p-value; *p*.FDR = p-value using false discovery rate correction, *r* = correlation coefficient.

Table A4. eQTL results of the BrainGWAS

chr	pos	tissue	tested Allele	p	signed_stats	FDR	aligned Direction	symbol
1	43842827	Adipose_Subcutaneous	A	2.5E-26	-0.290041	2.51836E-22	-	TIE1
1	43842827	Adipose_Subcutaneous	A	2.7E-13	0.18161	3.53967E-10	+	MED8
1	43842827	Adipose_Visceral_Omentum	A	1.2E-20	-0.317656	6.89766E-17	-	TIE1
1	43842827	Whole_Blood	A	2.0E-08	0.112265	5.27554E-07	+	SZT2
1	43842827	Artery_Aorta	A	3.4E-08	-0.152584	4.42856E-05	-	TIE1
1	43842827	Artery_Aorta	A	9.0E-13	0.210367	9.26834E-10	+	MED8
1	43842827	Artery_Tibial	A	1.1E-05	-0.0723745	1.20241E-05	-	TIE1
1	43842827	Artery_Tibial	A	2.2E-12	0.164698	1.23381E-09	+	MED8
1	43842827	Brain_Caudate_basal_ganglia	A	5.4E-05	0.239834	0.00491449	+	MED8
1	43842827	Brain_Hippocampus	A	3.7E-06	-0.29052	0.00360162	-	TIE1
1	43842827	Breast_Mammary_Tissue	A	1.2E-18	-0.241274	5.28172E-15	-	TIE1
1	43842827	Breast_Mammary_Tissue	A	1.5E-07	0.119787	0.000058251	+	MED8
1	43842827	Colon_Transverse	A	3.8E-07	-0.117452	1.07034E-05	-	TIE1
1	43842827	Esophagus_Gastroesophageal_Junction	A	4.9E-09	-0.223687	5.76572E-06	-	TIE1
1	43842827	Esophagus_Mucosa	A	1.7E-07	-0.117507	6.15688E-05	-	TIE1
1	43842827	Esophagus_Mucosa	A	2.4E-05	-0.0700665	0.00409891	-	CDC20
1	43842827	Esophagus_Muscularis	A	3.6E-18	-0.269184	2.64607E-14	-	TIE1

1	43842827	Esophagus_Muscularis	A	1.0E-08	0.141538	6.70732E-06	+	MED8
1	43842827	Heart_Atrial_Appendage	A	1.4E-05	-0.173061	0.00226823	-	TIE1
1	43842827	Heart_Left_Ventricle	A	5.5E-13	-0.239484	2.41646E-10	-	TIE1
1	43842827	Heart_Left_Ventricle	A	2.2E-06	-0.175291	0.000430892	-	MED8
1	43842827	Lung	A	6.0E-12	-0.164307	3.1985E-11	-	TIE1
1	43842827	Lung	A	1.1E-05	0.0940075	0.00335966	+	MED8
1	43842827	Muscle_Skeletal	A	1.0E-29	-0.336968	2.83033E-30	-	TIE1
1	43842827	Muscle_Skeletal	A	1.6E-113	-0.576141	3.00E-117	-	MED8
1	43842827	Nerve_Tibial	A	1.5E-16	-0.233026	6.89368E-14	-	TIE1
1	43842827	Nerve_Tibial	A	1.8E-15	0.231773	4.80209E-12	+	MED8
1	43842827	Ovary	A	1.7E-05	0.241018	0.0222646	+	MED8
1	43842827	Pancreas	A	9.5E-05	-0.197874	0.00911807	-	TIE1
1	43842827	Pituitary	A	1.4E-05	0.387565	0.00876902	+	CDC20
1	43842827	Pituitary	A	3.8E-05	0.174848	0.0284268	+	MED8
1	43842827	Prostate	A	6.6E-06	-0.21342	0.0087838	-	TIE1
1	43842827	Prostate	A	1.3E-05	0.240741	0.022027	+	MED8
1	43842827	Skin_Not_Sun_Exposed_Suprapubic	A	2.0E-12	-0.166483	1.05781E-09	-	TIE1
1	43842827	Skin_Sun_Exposed_Lower_leg	A	4.9E-21	-0.199567	3.54887E-17	-	TIE1
1	43842827	Skin_Sun_Exposed_Lower_leg	A	2.1E-04	-0.0746866	0.000127434	-	PTPRF
1	43842827	Stomach	A	1.9E-07	-0.185999	0.000113735	-	TIE1
1	43842827	Testis	A	3.5E-08	0.29853	1.47213E-05	+	MPL

1	43842827	Testis	A	3.8E-17	-0.365397	2.73978E-13	-	MED8
1	43842827	Testis	A	8.6E-07	0.160257	0.000131163	+	SZT2
1	43842827	Thyroid	A	3.5E-07	-0.198802	6.91131E-05	-	TIE1
1	43842827	Thyroid	A	9.8E-06	0.150127	0.00024488	+	CDC20
1	43842827	Thyroid	A	6.3E-25	0.261341	4.87493E-20	+	MED8
2	203720745	Adipose_Subcutaneous	A	3.7E-09	0.165512	1.69739E-13	+	CARF
2	203720745	Adipose_Subcutaneous	A	1.1E-08	0.165268	1.65694E-15	+	NBEAL1
2	203720745	Adipose_Subcutaneous	A	7.5E-05	-0.125383	1.2693E-08	-	ICA1L
2	203720745	Whole_Blood	A	3.3E-05	0.155262	2.05888E-44	+	FAM117B
2	203720745	Artery_Aorta	A	1.8E-19	0.388651	7.19034E-43	+	NBEAL1
2	203720745	Artery_Coronary	A	4.7E-12	0.43964	1.84554E-10	+	NBEAL1
2	203720745	Artery_Tibial	A	6.9E-09	0.13305	1.30069E-11	+	CARF
2	203720745	Artery_Tibial	A	1.4E-31	0.393655	4.09296E-57	+	NBEAL1
2	203720745	Artery_Tibial	A	1.6E-04	-0.120766	8.14785E-06	-	ICA1L
2	203720745	Brain_Nucleus_accumbens_basal_ganglia	A	5.6E-05	0.143229	0.00741269	+	WDR12
2	203720745	Breast_Mammary_Tissue	A	1.2E-07	0.157226	2.82058E-09	+	CARF
2	203720745	Breast_Mammary_Tissue	A	8.2E-06	-0.188583	2.99441E-05	-	ICA1L
2	203720745	Esophagus_Mucosa	A	5.0E-05	-0.156516	2.94894E-08	-	FAM117B
2	203720745	Esophagus_Mucosa	A	2.4E-04	0.101882	0.000593774	+	NBEAL1
2	203720745	Esophagus_Mucosa	A	1.7E-06	-0.172905	0.000565241	-	ICA1L
2	203720745	Esophagus_Muscularis	A	2.3E-04	0.10664	2.02779E-08	+	CARF

2	203720745	Lung	A	2.8E-04	0.0978187	2.84473E-09	+	CARF
2	203720745	Lung	A	5.0E-05	0.128377	2.6634E-08	+	NBEAL1
2	203720745	Muscle_Skeletal	A	2.4E-04	0.0867002	0.00535383	+	WDR12
2	203720745	Muscle_Skeletal	A	4.1E-16	-0.294512	5.29972E-23	-	ICA1L
2	203720745	Nerve_Tibial	A	1.6E-04	0.0956746	7.37866E-10	+	CARF
2	203720745	Nerve_Tibial	A	7.1E-07	0.148761	6.93027E-12	+	NBEAL1
2	203720745	Nerve_Tibial	A	4.8E-08	-0.130223	1.99263E-15	-	ICA1L
2	203720745	Pancreas	A	3.7E-10	-0.295093	2.31867E-11	-	ICA1L
2	203720745	Cells_Cultured_fibroblasts	A	3.2E-06	0.088591	4.18E-12	+	CARF
2	203720745	Cells_Cultured_fibroblasts	A	2.1E-12	-0.276873	7.10008E-18	-	ICA1L
2	203720745	Skin_Not_Sun_Exposed_Suprapubic	A	1.3E-07	0.151418	2.76545E-15	+	CARF
2	203720745	Skin_Not_Sun_Exposed_Suprapubic	A	2.3E-07	0.172131	1.4007E-14	+	NBEAL1
2	203720745	Skin_Not_Sun_Exposed_Suprapubic	A	6.2E-10	-0.215241	3.57938E-13	-	ICA1L
2	203720745	Skin_Sun_Exposed_Lower_leg	A	2.3E-06	0.126002	1.27743E-13	+	CARF
2	203720745	Skin_Sun_Exposed_Lower_leg	A	4.8E-08	-0.157451	4.97554E-09	-	ICA1L
2	203720745	Stomach	A	7.1E-08	0.200776	0.000084695	+	CARF
2	203720745	Testis	A	1.4E-15	0.337322	1.43632E-29	+	CARF
2	203720745	Thyroid	A	5.3E-04	0.0867839	4.68105E-14	+	CARF
2	203720745	Thyroid	A	4.6E-05	-0.145435	1.55963E-05	-	FAM117B
2	203720745	Thyroid	A	1.9E-15	-0.258545	1.67666E-26	-	ICA1L
4	38634757	Esophagus_Mucosa	G	1.9E-05	0.156169	6.15853E-26	+	TLR1

17	43919073	Adipose_Subcutaneous	T	2.0E-11	0.37874	1.5414E-26	+	WNT3
17	43919073	Adipose_Subcutaneous	T	7.6E-10	0.28901	5.7284E-39	+	KANSL1
17	43919073	Adipose_Subcutaneous	T	2.2E-17	0.497152	4.83764E-14	+	CRHR1
17	43919073	Adipose_Subcutaneous	T	5.7E-05	0.160563	3.59451E-26	+	DCAKD
17	43919073	Adipose_Subcutaneous	T	2.6E-34	0.795792	1.19942E-67	+	LRRC37A
17	43919073	Adipose_Subcutaneous	T	2.6E-16	0.534389	6.22486E-21	+	ARL17A
17	43919073	Adipose_Subcutaneous	T	3.5E-05	0.12331	0.0026298	+	MAPT
17	43919073	Adipose_Subcutaneous	T	1.3E-08	0.17257	3.72801E-10	+	PLEKHM1
17	43919073	Adipose_Subcutaneous	T	1.6E-118	1.19501	1.5183E-103	+	LRRC37A2
17	43919073	Adipose_Visceral_Omentum	T	6.3E-05	0.239591	3.08779E-26	+	WNT3
17	43919073	Adipose_Visceral_Omentum	T	1.8E-07	0.23477	5.01622E-18	+	KANSL1
17	43919073	Adipose_Visceral_Omentum	T	1.6E-20	0.51364	2.70499E-18	+	CRHR1
17	43919073	Adipose_Visceral_Omentum	T	2.6E-21	0.602452	1.04784E-51	+	LRRC37A
17	43919073	Adipose_Visceral_Omentum	T	1.1E-16	0.580694	4.61062E-19	+	ARL17A
17	43919073	Adipose_Visceral_Omentum	T	1.0E-06	0.172464	0.000432139	+	MAPT
17	43919073	Adipose_Visceral_Omentum	T	2.8E-06	0.176128	0.000305673	+	PLEKHM1
17	43919073	Adipose_Visceral_Omentum	T	1.4E-85	0.987074	3.95887E-76	+	LRRC37A2
17	43919073	Adrenal_Gland	T	6.8E-12	0.612275	7.19125E-11	+	WNT3
17	43919073	Adrenal_Gland	T	1.4E-06	0.54728	2.79493E-31	+	LRRC37A
17	43919073	Adrenal_Gland	T	3.1E-17	0.87712	8.65853E-14	+	ARL17A
17	43919073	Adrenal_Gland	T	3.6E-11	0.417316	5.44951E-08	+	PLEKHM1

17	43919073	Adrenal_Gland	T	5.5E-35	1.1064	1.28946E-29	+	LRRC37A2
17	43919073	Cells_EBV-transformed_lymphocytes	T	3.5E-10	0.666044	6.2468E-07	+	KANSL1
17	43919073	Cells_EBV-transformed_lymphocytes	T	2.6E-12	-0.520948	1.32016E-08	-	ARHGAP27
17	43919073	Cells_EBV-transformed_lymphocytes	T	2.6E-05	0.581171	3.55316E-13	+	ARL17A
17	43919073	Cells_EBV-transformed_lymphocytes	T	2.0E-13	0.882053	1.7299E-10	+	LRRC37A2
17	43919073	Whole_Blood	T	8.9E-12	0.222736	4.18444E-29	+	KANSL1
17	43919073	Whole_Blood	T	8.3E-15	0.467206	1.42983E-36	+	LRRC37A
17	43919073	Whole_Blood	T	3.1E-06	0.284694	2.53511E-39	+	ARL17A
17	43919073	Whole_Blood	T	1.4E-05	-0.0656968	0.000665585	-	PLEKHM1
17	43919073	Whole_Blood	T	7.1E-05	-0.268873	1.08354E-28	-	ARL17B
17	43919073	Whole_Blood	T	1.9E-60	0.840672	2.85759E-52	+	LRRC37A2
17	43919073	Artery_Aorta	T	1.3E-06	-0.168408	6.59179E-05	-	NSF
17	43919073	Artery_Aorta	T	2.1E-14	0.503276	1.86333E-19	+	WNT3
17	43919073	Artery_Aorta	T	1.2E-04	0.116346	0.00119664	+	ARHGAP27
17	43919073	Artery_Aorta	T	2.9E-18	0.644823	2.76E-30	+	LRRC37A
17	43919073	Artery_Aorta	T	3.9E-11	0.441631	4.19549E-08	+	ARL17A
17	43919073	Artery_Aorta	T	3.7E-09	-0.323721	2.71903E-20	-	MAPT
17	43919073	Artery_Aorta	T	2.8E-75	1.07296	4.68859E-66	+	LRRC37A2
17	43919073	Artery_Coronary	T	6.1E-09	0.520818	1.46044E-06	+	WNT3
17	43919073	Artery_Coronary	T	8.1E-16	0.782459	6.1015E-23	+	LRRC37A
17	43919073	Artery_Coronary	T	5.4E-09	0.597321	1.46921E-06	+	ARL17A

17	43919073	Artery_Coronary	T	1.6E-36	1.04683	1.73412E-30	+	LRRC37A2
17	43919073	Artery_Tibial	T	1.2E-06	-0.16979	1.00477E-08	-	NSF
17	43919073	Artery_Tibial	T	6.4E-13	0.359175	2.12359E-17	+	WNT3
17	43919073	Artery_Tibial	T	5.4E-07	0.236737	6.72547E-40	+	KANSL1
17	43919073	Artery_Tibial	T	2.9E-05	0.190848	2.68979E-32	+	DCAKD
17	43919073	Artery_Tibial	T	1.1E-43	0.866401	3.25263E-65	+	LRRC37A
17	43919073	Artery_Tibial	T	1.0E-10	0.40441	1.521E-10	+	ARL17A
17	43919073	Artery_Tibial	T	6.8E-07	-0.19387	8.33164E-12	-	MAPT
17	43919073	Artery_Tibial	T	1.5E-04	0.0903745	0.0014	+	PLEKHM1
17	43919073	Artery_Tibial	T	5.9E-108	1.16011	9.58893E-94	+	LRRC37A2
17	43919073	Brain_Amygdala	T	6.3E-07	0.679567	2.4924E-20	+	LRRC37A
17	43919073	Brain_Amygdala	T	6.2E-10	0.816611	1.19361E-06	+	ARL17A
17	43919073	Brain_Amygdala	T	1.7E-05	0.337383	0.00225518	+	PLEKHM1
17	43919073	Brain_Amygdala	T	9.0E-26	1.10433	7.12462E-22	+	LRRC37A2
17	43919073	Brain_Anterior_cingulate_cortex_BA24	T	1.2E-07	0.67051	3.11336E-25	+	LRRC37A
17	43919073	Brain_Anterior_cingulate_cortex_BA24	T	4.6E-13	0.892391	1.03581E-09	+	ARL17A
17	43919073	Brain_Anterior_cingulate_cortex_BA24	T	6.2E-08	0.386642	9.34763E-05	+	PLEKHM1
17	43919073	Brain_Anterior_cingulate_cortex_BA24	T	1.2E-29	1.22552	2.20599E-23	+	LRRC37A2
17	43919073	Brain_Caudate_basal_ganglia	T	6.6E-05	-0.263963	0.0041038	-	CRHR1
17	43919073	Brain_Caudate_basal_ganglia	T	4.8E-09	0.240715	4.55561E-06	+	ARHGAP27
17	43919073	Brain_Caudate_basal_ganglia	T	4.8E-10	0.715212	3.07662E-32	+	LRRC37A

17	43919073	Brain_Caudate_basal_ganglia	T	2.2E-17	0.856008	8.68241E-14	+	ARL17A
17	43919073	Brain_Caudate_basal_ganglia	T	4.7E-08	0.313105	3.83119E-07	+	PLEKHM1
17	43919073	Brain_Caudate_basal_ganglia	T	7.5E-41	1.22199	7.06782E-35	+	LRRC37A2
17	43919073	Brain_Cerebellar_Hemisphere	T	1.3E-05	0.353543	1.08545E-09	+	KANSL1
17	43919073	Brain_Cerebellar_Hemisphere	T	7.9E-05	-0.227737	0.00258696	-	NMT1
17	43919073	Brain_Cerebellar_Hemisphere	T	2.8E-25	1.12453	1.15957E-23	+	LRRC37A
17	43919073	Brain_Cerebellar_Hemisphere	T	5.1E-19	-0.640966	1.75905E-15	-	FMNL1
17	43919073	Brain_Cerebellar_Hemisphere	T	8.3E-20	0.67929	1.38828E-15	+	SPPL2C
17	43919073	Brain_Cerebellar_Hemisphere	T	8.2E-33	1.10786	8.40967E-27	+	ARL17A
17	43919073	Brain_Cerebellar_Hemisphere	T	1.3E-27	-0.839202	4.68594E-23	-	PLEKHM1
17	43919073	Brain_Cerebellar_Hemisphere	T	2.1E-42	1.30629	1.0494E-34	+	LRRC37A2
17	43919073	Brain_Cerebellum	T	1.7E-04	-0.14865	2.14459E-10	-	NSF
17	43919073	Brain_Cerebellum	T	1.1E-05	0.331017	1.35458E-08	+	KANSL1
17	43919073	Brain_Cerebellum	T	6.3E-27	1.04178	1.32888E-33	+	LRRC37A
17	43919073	Brain_Cerebellum	T	1.6E-22	-0.703595	7.89257E-19	-	FMNL1
17	43919073	Brain_Cerebellum	T	5.5E-24	0.760892	5.44181E-19	+	SPPL2C
17	43919073	Brain_Cerebellum	T	1.8E-36	1.11953	7.41812E-31	+	ARL17A
17	43919073	Brain_Cerebellum	T	7.9E-07	-0.285805	7.42082E-05	-	MAPT
17	43919073	Brain_Cerebellum	T	5.5E-40	-1.0217	8.79568E-35	-	PLEKHM1
17	43919073	Brain_Cerebellum	T	1.4E-51	1.18601	7.9119E-44	+	LRRC37A2
17	43919073	Brain_Cortex	T	2.8E-06	0.317929	0.000186356	+	ARHGAP27

17	43919073	Brain_Cortex	T	1.1E-13	0.782074	4.8669E-42	+	LRRC37A
17	43919073	Brain_Cortex	T	8.9E-28	1.06058	8.50282E-24	+	ARL17A
17	43919073	Brain_Cortex	T	9.2E-14	0.440667	5.24864E-12	+	PLEKHM1
17	43919073	Brain_Cortex	T	6.8E-42	1.20536	4.81353E-35	+	LRRC37A2
17	43919073	Brain_Frontal_Cortex_BA9	T	5.1E-11	0.766885	3.82005E-31	+	LRRC37A
17	43919073	Brain_Frontal_Cortex_BA9	T	9.0E-06	0.3708	0.00224603	+	SPPL2C
17	43919073	Brain_Frontal_Cortex_BA9	T	3.2E-26	1.12952	2.13049E-20	+	ARL17A
17	43919073	Brain_Frontal_Cortex_BA9	T	8.0E-07	0.324298	0.000032641	+	PLEKHM1
17	43919073	Brain_Frontal_Cortex_BA9	T	4.3E-35	1.23549	1.94581E-30	+	LRRC37A2
17	43919073	Brain_Hippocampus	T	7.4E-05	-0.229731	0.0137363	-	CRHR1
17	43919073	Brain_Hippocampus	T	3.2E-09	0.715883	5.42655E-23	+	LRRC37A
17	43919073	Brain_Hippocampus	T	3.8E-10	0.683399	5.4462E-07	+	ARL17A
17	43919073	Brain_Hippocampus	T	9.3E-34	1.19171	1.29741E-27	+	LRRC37A2
17	43919073	Brain_Hypothalamus	T	7.3E-13	0.893178	3.00905E-29	+	LRRC37A
17	43919073	Brain_Hypothalamus	T	7.9E-21	1.0354	2.17212E-16	+	ARL17A
17	43919073	Brain_Hypothalamus	T	6.6E-41	1.30353	2.48811E-35	+	LRRC37A2
17	43919073	Brain_Nucleus_accumbens_basal_ganglia	T	9.5E-05	-0.256662	0.00117547	-	CRHR1
17	43919073	Brain_Nucleus_accumbens_basal_ganglia	T	4.1E-18	0.427502	7.23313E-14	+	ARHGAP27
17	43919073	Brain_Nucleus_accumbens_basal_ganglia	T	7.6E-09	0.651052	2.07654E-40	+	LRRC37A
17	43919073	Brain_Nucleus_accumbens_basal_ganglia	T	2.6E-23	0.989819	2.05259E-18	+	ARL17A
17	43919073	Brain_Nucleus_accumbens_basal_ganglia	T	1.5E-13	0.409056	3.42523E-13	+	PLEKHM1

17	43919073	Brain_Nucleus_accumbens_basal_ganglia	T	2.0E-44	1.20528	4.14936E-37	+	LRRC37A2
17	43919073	Brain_Putamen_basal_ganglia	T	8.6E-08	0.681975	1.62202E-31	+	LRRC37A
17	43919073	Brain_Putamen_basal_ganglia	T	2.2E-12	0.776594	8.98679E-09	+	ARL17A
17	43919073	Brain_Putamen_basal_ganglia	T	2.3E-07	0.338848	7.91819E-07	+	PLEKHM1
17	43919073	Brain_Putamen_basal_ganglia	T	1.5E-35	1.20334	1.78933E-29	+	LRRC37A2
17	43919073	Brain_Spinal_cord_cervical_c-1	T	7.2E-10	0.908005	1.09702E-10	+	LRRC37A
17	43919073	Brain_Spinal_cord_cervical_c-1	T	1.1E-21	1.11361	2.48143E-16	+	LRRC37A2
17	43919073	Brain_Substantia_nigra	T	2.0E-08	0.914186	1.2137E-10	+	LRRC37A
17	43919073	Brain_Substantia_nigra	T	2.5E-20	1.24082	3.09413E-15	+	LRRC37A2
17	43919073	Breast_Mammary_Tissue	T	2.7E-07	0.303217	3.37586E-09	+	WNT3
17	43919073	Breast_Mammary_Tissue	T	5.3E-23	0.437239	1.60577E-18	+	CRHR1
17	43919073	Breast_Mammary_Tissue	T	4.2E-18	0.682612	3.99656E-46	+	LRRC37A
17	43919073	Breast_Mammary_Tissue	T	2.2E-13	0.541358	4.90715E-16	+	ARL17A
17	43919073	Breast_Mammary_Tissue	T	1.3E-07	0.191984	5.6696E-06	+	PLEKHM1
17	43919073	Breast_Mammary_Tissue	T	1.4E-68	1.11414	8.26068E-60	+	LRRC37A2
17	43919073	Colon_Sigmoid	T	2.0E-10	0.481385	1.40022E-12	+	WNT3
17	43919073	Colon_Sigmoid	T	4.5E-08	0.373246	1.8484E-17	+	KANSL1
17	43919073	Colon_Sigmoid	T	2.6E-15	0.673123	8.60644E-40	+	LRRC37A
17	43919073	Colon_Sigmoid	T	8.0E-14	0.647243	1.41963E-11	+	ARL17A
17	43919073	Colon_Sigmoid	T	5.4E-25	-0.669112	3.0403E-32	-	MAPT
17	43919073	Colon_Sigmoid	T	8.6E-54	1.079	1.87165E-46	+	LRRC37A2

17	43919073	Colon_Transverse	T	2.6E-09	0.44435	1.09903E-16	+	WNT3
17	43919073	Colon_Transverse	T	1.7E-07	0.358103	3E-14	+	KANSL1
17	43919073	Colon_Transverse	T	4.9E-07	0.458253	1.53695E-41	+	LRRC37A
17	43919073	Colon_Transverse	T	8.6E-16	0.688539	1.49032E-20	+	ARL17A
17	43919073	Colon_Transverse	T	2.3E-07	-0.172316	2.42823E-21	-	MAPT
17	43919073	Colon_Transverse	T	1.8E-53	1.074	9.29476E-46	+	LRRC37A2
17	43919073	Esophagus_Gastroesophageal_Junction	T	7.1E-13	0.505828	6.76072E-16	+	WNT3
17	43919073	Esophagus_Gastroesophageal_Junction	T	4.5E-06	0.373159	0.00052326	+	CRHR1
17	43919073	Esophagus_Gastroesophageal_Junction	T	1.6E-17	0.650444	3.08892E-41	+	LRRC37A
17	43919073	Esophagus_Gastroesophageal_Junction	T	2.2E-08	0.459146	7.42458E-07	+	ARL17A
17	43919073	Esophagus_Gastroesophageal_Junction	T	1.2E-60	1.00691	3.96604E-54	+	LRRC37A2
17	43919073	Esophagus_Mucosa	T	1.1E-09	-0.159537	2.93494E-08	-	NSF
17	43919073	Esophagus_Mucosa	T	5.0E-18	0.352579	3.96159E-16	+	KANSL1
17	43919073	Esophagus_Mucosa	T	3.6E-17	-0.165835	1.70981E-13	-	ARHGAP27
17	43919073	Esophagus_Mucosa	T	2.7E-04	0.160237	4.29651E-69	+	DCAKD
17	43919073	Esophagus_Mucosa	T	4.7E-08	0.401429	4.64588E-62	+	LRRC37A
17	43919073	Esophagus_Mucosa	T	7.5E-15	0.556693	1.00973E-28	+	ARL17A
17	43919073	Esophagus_Mucosa	T	7.5E-73	0.685238	3.482E-64	+	MAPT
17	43919073	Esophagus_Mucosa	T	2.1E-24	-0.310509	1.41572E-20	-	PLEKHM1
17	43919073	Esophagus_Mucosa	T	7.2E-67	0.952711	3.28068E-59	+	LRRC37A2
17	43919073	Esophagus_Muscularis	T	2.4E-07	-0.189037	4.20909E-09	-	NSF

17	43919073	Esophagus_Muscularis	T	6.2E-15	0.440557	5.30688E-22	+	WNT3
17	43919073	Esophagus_Muscularis	T	1.1E-09	0.376154	4.14314E-07	+	CRHR1
17	43919073	Esophagus_Muscularis	T	2.5E-29	0.749313	1.1165E-65	+	LRRC37A
17	43919073	Esophagus_Muscularis	T	2.0E-17	0.590487	3.80217E-15	+	ARL17A
17	43919073	Esophagus_Muscularis	T	1.1E-05	-0.20584	2.41112E-23	-	MAPT
17	43919073	Esophagus_Muscularis	T	1.5E-09	0.155702	7.71557E-09	+	PLEKHM1
17	43919073	Esophagus_Muscularis	T	6.8E-91	1.06724	8.81618E-80	+	LRRC37A2
17	43919073	Heart_Atrial_Appendage	T	8.3E-07	-0.198169	7.66562E-08	-	NSF
17	43919073	Heart_Atrial_Appendage	T	7.8E-08	0.399948	4.34098E-09	+	WNT3
17	43919073	Heart_Atrial_Appendage	T	5.7E-06	0.370625	1.24085E-45	+	LRRC37A
17	43919073	Heart_Atrial_Appendage	T	4.4E-14	0.655937	3.40411E-16	+	ARL17A
17	43919073	Heart_Atrial_Appendage	T	1.9E-53	0.975712	9.52955E-47	+	LRRC37A2
17	43919073	Heart_Left_Ventricle	T	6.9E-10	0.491294	2.31458E-10	+	WNT3
17	43919073	Heart_Left_Ventricle	T	1.7E-09	0.491499	7.7567E-42	+	LRRC37A
17	43919073	Heart_Left_Ventricle	T	4.2E-14	0.639015	2.73636E-13	+	ARL17A
17	43919073	Heart_Left_Ventricle	T	2.3E-16	-0.479266	4.84413E-68	-	MAPT
17	43919073	Heart_Left_Ventricle	T	1.1E-56	1.02807	1.71954E-48	+	LRRC37A2
17	43919073	Kidney_Cortex	T	9.7E-13	1.00072	3.20719E-08	+	LRRC37A2
17	43919073	Liver	T	2.7E-09	0.64893	1.10549E-07	+	ARL17A
17	43919073	Liver	T	5.7E-24	0.892327	7.58113E-19	+	LRRC37A2
17	43919073	Lung	T	4.9E-16	0.338392	2.34993E-20	+	WNT3

17	43919073	Lung	T	2.8E-06	0.284962	1.17216E-24	+	KANSL1
17	43919073	Lung	T	5.8E-19	0.561007	2.04353E-60	+	LRRC37A
17	43919073	Lung	T	5.2E-15	0.547791	5.82485E-24	+	ARL17A
17	43919073	Lung	T	3.4E-32	0.593659	8.36707E-29	+	MAPT
17	43919073	Lung	T	3.7E-08	0.182784	4.485E-11	+	PLEKHM1
17	43919073	Lung	T	2.3E-82	0.952209	7.62411E-74	+	LRRC37A2
17	43919073	Muscle_Skeletal	T	1.5E-05	0.243584	3.34436E-08	+	WNT3
17	43919073	Muscle_Skeletal	T	3.9E-22	0.403345	1.95739E-20	+	KANSL1
17	43919073	Muscle_Skeletal	T	2.4E-07	0.249628	2.24321E-05	+	CRHR1
17	43919073	Muscle_Skeletal	T	3.0E-14	0.475484	1.73283E-93	+	LRRC37A
17	43919073	Muscle_Skeletal	T	5.5E-28	0.609483	1.94622E-23	+	ARL17A
17	43919073	Muscle_Skeletal	T	3.9E-33	0.308483	8.86045E-30	+	PLEKHM1
17	43919073	Muscle_Skeletal	T	3.2E-05	-0.271833	2.22867E-37	-	ARL17B
17	43919073	Muscle_Skeletal	T	5.2E-73	0.977669	2.28068E-84	+	LRRC37A2
17	43919073	Nerve_Tibial	T	3.0E-13	0.425428	1.02693E-20	+	WNT3
17	43919073	Nerve_Tibial	T	3.9E-13	0.500413	9.94377E-11	+	CRHR1
17	43919073	Nerve_Tibial	T	1.1E-04	0.190645	8.62603E-41	+	DCAKD
17	43919073	Nerve_Tibial	T	9.4E-44	0.951019	1.40037E-51	+	LRRC37A
17	43919073	Nerve_Tibial	T	2.1E-04	-0.115693	3.30948E-18	-	ACBD4
17	43919073	Nerve_Tibial	T	9.9E-13	0.507332	6.68568E-21	+	ARL17A
17	43919073	Nerve_Tibial	T	7.3E-96	1.17926	2.13473E-84	+	LRRC37A2

17	43919073	Ovary	T	2.5E-06	-0.249112	0.000940674	-	NSF
17	43919073	Ovary	T	4.8E-09	0.642613	2.74478E-09	+	LRRC37A
17	43919073	Ovary	T	1.2E-09	0.718312	3.84783E-07	+	ARL17A
17	43919073	Ovary	T	2.8E-21	0.924083	3.0287E-17	+	LRRC37A2
17	43919073	Pancreas	T	1.1E-17	0.719009	2.01234E-21	+	WNT3
17	43919073	Pancreas	T	9.2E-15	0.736311	1.10237E-15	+	ARL17A
17	43919073	Pancreas	T	1.2E-35	1.00423	1.41591E-30	+	LRRC37A2
17	43919073	Pituitary	T	2.9E-16	0.541039	1.75695E-16	+	WNT3
17	43919073	Pituitary	T	4.3E-05	0.374929	6.52535E-15	+	KANSL1
17	43919073	Pituitary	T	3.0E-12	0.732584	9.01513E-54	+	LRRC37A
17	43919073	Pituitary	T	1.1E-25	0.986333	1.42234E-23	+	ARL17A
17	43919073	Pituitary	T	4.5E-50	1.23217	4.0241E-43	+	LRRC37A2
17	43919073	Prostate	T	2.2E-12	0.745588	3.69025E-26	+	LRRC37A
17	43919073	Prostate	T	4.7E-11	0.693283	9.61203E-08	+	ARL17A
17	43919073	Prostate	T	8.2E-06	-0.275737	0.00073194	-	MAPT
17	43919073	Prostate	T	6.9E-37	1.05011	7.4008E-32	+	LRRC37A2
17	43919073	Minor_Salivary_Gland	T	4.2E-08	0.773661	3.54555E-12	+	ARL17A
17	43919073	Minor_Salivary_Gland	T	3.9E-19	1.11366	1.0265E-14	+	LRRC37A2
17	43919073	Cells_Cultured_fibroblasts	T	4.4E-08	0.18589	3.12586E-07	+	NSF
17	43919073	Cells_Cultured_fibroblasts	T	1.6E-16	0.266291	1.39037E-13	+	KANSL1
17	43919073	Cells_Cultured_fibroblasts	T	2.6E-06	-0.135548	1.05938E-23	-	NMT1

17	43919073	Cells_Cultured_fibroblasts	T	3.3E-20	0.686644	3.65165E-40	+	ARL17A
17	43919073	Cells_Cultured_fibroblasts	T	1.9E-08	0.111655	5.73949E-10	+	PLEKHM1
17	43919073	Cells_Cultured_fibroblasts	T	3.6E-47	0.934614	8.9085E-41	+	LRRC37A2
17	43919073	Skin_Not_Sun_Exposed_Suprapubic	T	2.1E-14	0.318583	5.37067E-20	+	KANSL1
17	43919073	Skin_Not_Sun_Exposed_Suprapubic	T	3.9E-35	0.388141	2.5924E-36	+	ARHGAP27
17	43919073	Skin_Not_Sun_Exposed_Suprapubic	T	3.3E-34	0.736864	1.61134E-29	+	LRRC37A
17	43919073	Skin_Not_Sun_Exposed_Suprapubic	T	3.1E-11	0.444699	2.26113E-39	+	ARL17A
17	43919073	Skin_Not_Sun_Exposed_Suprapubic	T	2.1E-09	0.292927	1.72116E-07	+	MAPT
17	43919073	Skin_Not_Sun_Exposed_Suprapubic	T	1.4E-06	0.362481	1.63552E-14	+	ARL17B
17	43919073	Skin_Not_Sun_Exposed_Suprapubic	T	4.7E-65	0.908035	1.40757E-55	+	LRRC37A2
17	43919073	Skin_Sun_Exposed_Lower_leg	T	4.1E-16	0.31288	1.63734E-20	+	KANSL1
17	43919073	Skin_Sun_Exposed_Lower_leg	T	4.3E-33	0.400227	4.93528E-39	+	ARHGAP27
17	43919073	Skin_Sun_Exposed_Lower_leg	T	6.8E-39	0.758874	1.00775E-36	+	LRRC37A
17	43919073	Skin_Sun_Exposed_Lower_leg	T	2.0E-12	0.438088	5.39841E-36	+	ARL17A
17	43919073	Skin_Sun_Exposed_Lower_leg	T	1.1E-21	0.491257	1.28633E-17	+	MAPT
17	43919073	Skin_Sun_Exposed_Lower_leg	T	1.4E-05	0.312931	3.681E-15	+	ARL17B
17	43919073	Skin_Sun_Exposed_Lower_leg	T	1.4E-81	0.981155	4.44256E-72	+	LRRC37A2
17	43919073	Small_Intestine_Terminal_Ileum	T	1.8E-05	0.301981	0.00242943	+	KANSL1
17	43919073	Small_Intestine_Terminal_Ileum	T	1.5E-06	0.622306	1.56947E-24	+	LRRC37A
17	43919073	Small_Intestine_Terminal_Ileum	T	3.3E-07	0.537006	1.42325E-05	+	ARL17A
17	43919073	Small_Intestine_Terminal_Ileum	T	2.4E-27	1.08265	6.45694E-22	+	LRRC37A2

17	43919073	Spleen	T	1.8E-06	0.540752	4.14024E-26	+	LRRC37A
17	43919073	Spleen	T	3.2E-08	0.691722	2.70721E-09	+	ARL17A
17	43919073	Spleen	T	1.3E-05	0.46364	2.85241E-05	+	MAPT
17	43919073	Spleen	T	2.2E-29	1.09372	1.88326E-24	+	LRRC37A2
17	43919073	Stomach	T	2.0E-07	0.332121	2.07295E-11	+	WNT3
17	43919073	Stomach	T	1.3E-07	0.473412	1.69991E-31	+	LRRC37A
17	43919073	Stomach	T	9.4E-15	0.669788	2.81675E-15	+	ARL17A
17	43919073	Stomach	T	1.2E-51	1.03004	1.58182E-44	+	LRRC37A2
17	43919073	Testis	T	3.8E-09	0.222098	9.74137E-08	+	NSF
17	43919073	Testis	T	6.8E-08	0.314087	6.93428E-11	+	WNT3
17	43919073	Testis	T	4.9E-10	-0.341408	1.17626E-11	-	ARHGAP27
17	43919073	Testis	T	2.0E-04	0.10561	0.00399745	+	SPPL2C
17	43919073	Testis	T	4.4E-12	0.604936	4.92591E-22	+	ARL17A
17	43919073	Testis	T	3.7E-117	1.22397	2.2324E-103	+	MAPT
17	43919073	Testis	T	1.0E-09	-0.345761	6.07257E-10	-	PLEKHM1
17	43919073	Testis	T	5.5E-34	1.05753	2.73138E-30	+	ARL17B
17	43919073	Thyroid	T	1.7E-41	0.661905	1.63707E-60	+	WNT3
17	43919073	Thyroid	T	2.1E-04	-0.178893	0.000272096	-	CRHR1
17	43919073	Thyroid	T	4.5E-06	-0.137389	5.30846E-37	-	NMT1
17	43919073	Thyroid	T	5.0E-16	0.542655	3.06278E-93	+	LRRC37A
17	43919073	Thyroid	T	2.1E-47	0.884613	1.50873E-41	+	ARL17A

17	43919073	Thyroid	T	5.4E-05	-0.186288	1.14749E-15	-	MAPT
17	43919073	Thyroid	T	1.2E-113	1.09508	7.6994E-99	+	LRRC37A2
17	43919073	Uterus	T	1.7E-12	0.695797	4.39044E-10	+	LRRC37A
17	43919073	Uterus	T	3.6E-08	0.698685	1.61159E-05	+	ARL17A
17	43919073	Uterus	T	1.4E-20	0.905106	1.57915E-16	+	LRRC37A2
17	43919073	Vagina	T	5.1E-07	0.562084	1.66874E-10	+	LRRC37A
17	43919073	Vagina	T	5.0E-05	0.484048	6.20603E-05	+	ARL17A
17	43919073	Vagina	T	2.6E-19	0.890036	1.24149E-15	+	LRRC37A2

Abbreviation. SNP, single nucleotide polymorphism; tissue, tissue type; testedAllele, tested allele obtained from the input GWAS summary statistics; p, P-value of eQTLs; signed_stats, signed statistics, the actual value depends on the data source; alignedDirection, the direction of effect to gene expression after aligning risk increasing allele of GWAS and tested allele of eQTLs; chr, chromosome; pos, position on hg19; symbol, gene symbol.

Table A5. Enrichment for heritability partitioned based on 53 functional genomic annotation

Category	Prop. SNPs	Prop. h2	Prop. h2 se	Enrichment	Enrichment se	Enrichment p	Coefficient se	Coefficient p	Coefficient p_FDR
Conserved_LindbladToh	0.03	0.39	0.09	15.10	3.59	0.00	0.00	0.00	0.00
UTR_5_UCSC	0.01	0.10	0.04	17.94	7.11	0.01	0.00	0.00	0.02
DHS_peaks_Trynka	0.11	0.39	0.20	3.57	1.82	0.15	0.00	0.00	0.03
Repressed_Hoffman	0.46	0.52	0.15	1.12	0.32	0.70	0.00	0.00	0.03
Enhancer_Hoffman	0.04	0.25	0.09	6.01	2.23	0.03	0.00	0.00	0.05
TSS_Hoffman	0.02	0.11	0.06	6.42	3.40	0.11	0.00	0.00	0.05
H3K4me1_peaks_Trynka	0.17	0.73	0.20	4.27	1.18	0.01	0.00	0.00	0.05
Coding_UCSC.extend.500	0.06	0.31	0.06	4.81	0.92	0.00	0.00	0.00	0.06
H3K4me3_peaks_Trynka	0.04	0.28	0.11	6.66	2.71	0.04	0.00	0.00	0.07
PromoterFlanking_Hoffman	0.01	0.07	0.06	8.36	7.05	0.29	0.00	0.00	0.07
H3K27ac_PGC2.extend.500	0.34	0.78	0.10	2.34	0.29	0.00	0.00	0.00	0.07
CTCF_Hoffman.extend.500	0.07	0.17	0.11	2.42	1.57	0.37	0.00	0.00	0.08
Intron_UCSC	0.39	0.48	0.06	1.23	0.15	0.13	0.00	0.00	0.08
TFBS_ENCODE.extend.500	0.34	0.65	0.15	1.90	0.44	0.05	0.00	0.00	0.15
H3K9ac_Trynka.extend.500	0.23	0.67	0.11	2.91	0.46	0.00	0.00	0.00	0.15
H3K4me3_Trynka.extend.500	0.26	0.54	0.13	2.12	0.50	0.03	0.00	0.00	0.18
DGF_ENCODE.extend.500	0.54	0.86	0.14	1.60	0.26	0.02	0.00	0.00	0.19
Transcribed_Hoffman	0.35	0.39	0.13	1.12	0.37	0.75	0.00	0.00	0.58

H3K4me1_Trynka	0.42	0.96	0.18	2.26	0.42	0.00	0.00	0.00	0.22	0.62
UTR_3_UCSC	0.01	0.09	0.04	7.85	3.55	0.05	0.00	0.00	0.27	0.71
Coding_UCSC	0.01	0.15	0.05	10.51	3.56	0.01	0.00	0.00	0.28	0.72
Conserved_LindbladToh extend.500	0.33	0.77	0.11	2.33	0.32	0.00	0.00	0.00	0.32	0.76
Promoter_UCSC	0.05	0.10	0.08	2.17	1.72	0.49	0.00	0.00	0.34	0.79
H3K9ac_Trynka	0.13	0.44	0.12	3.48	0.94	0.01	0.00	0.00	0.38	0.81
H3K27ac_Hniszext end.500	0.42	0.73	0.09	1.74	0.20	0.00	0.00	0.00	0.39	0.81
WeakEnhancer_Hoffman	0.02	0.04	0.08	2.01	3.81	0.79	0.00	0.00	0.40	0.81
SuperEnhancer_Hnisz	0.17	0.35	0.05	2.12	0.28	0.00	0.00	0.00	0.41	0.81
FetalDHS_Trynka extend.500	0.28	0.44	0.14	1.56	0.48	0.25	0.00	0.00	0.48	0.87
H3K9ac_peaks_Trynka	0.04	0.18	0.12	4.65	3.03	0.24	0.00	0.00	0.55	0.97
SuperEnhancer_Hnisz extend.500	0.17	0.35	0.05	2.06	0.28	0.00	0.00	0.00	0.59	0.97
H3K27ac_Hnisz	0.39	0.67	0.08	1.73	0.21	0.00	0.00	0.00	0.65	0.97
DGF_ENCODE	0.14	0.21	0.22	1.54	1.59	0.73	0.00	0.00	0.72	0.97
Promoter_UCSC.extend.500	0.06	0.08	0.05	1.33	0.91	0.72	0.00	0.00	0.72	0.97
Enhancer_Andersson	0.00	-0.04	0.04	-9.09	9.63	0.30	0.00	0.00	0.75	0.97
DHS_Trynka.extend.500	0.50	0.65	0.17	1.30	0.34	0.38	0.00	0.00	0.76	0.97
UTR_5_UCSC.extend.500	0.03	0.12	0.05	4.50	1.87	0.07	0.00	0.00	0.76	0.97
Enhancer_Hoffman extend.500	0.09	0.21	0.09	2.33	1.00	0.18	0.00	0.00	0.76	0.97

UTR_3_UCSC extend.500	0.03	0.10	0.05	3.82	1.74	0.10	0.00	0.00	0.77	0.97
Transcribed_Hoffman extend.500	0.76	0.64	0.09	0.84	0.11	0.17	0.00	0.00	0.79	0.97
WeakEnhancer_Hoffman extend.500	0.09	0.09	0.09	0.99	0.96	0.99	0.00	0.00	0.80	0.97
Enhancer_Andersson extend.500	0.02	-0.05	0.04	-2.87	2.32	0.10	0.00	0.00	0.80	0.97
TFBS_ENCODE	0.13	0.10	0.18	0.80	1.38	0.88	0.00	0.00	0.84	0.97
H3K4me1_Trynka extend.500	0.61	0.86	0.09	1.42	0.15	0.01	0.00	0.00	0.85	0.97
FetalDHS_Trynka	0.08	0.08	0.16	0.94	1.91	0.97	0.00	0.00	0.86	0.97
DHS_Trynka	0.17	0.21	0.21	1.24	1.27	0.85	0.00	0.00	0.89	0.97
H3K27ac_PGC2	0.27	0.52	0.12	1.94	0.44	0.04	0.00	0.00	0.89	0.97
CTCF_Hoffman	0.02	-0.10	0.10	-4.15	4.14	0.21	0.00	0.00	0.91	0.97
TSS_Hoffman extend.500	0.03	0.04	0.06	1.24	1.85	0.90	0.00	0.00	0.92	0.97
Intron_UCSC extend.500	0.40	0.51	0.05	1.28	0.12	0.02	0.00	0.00	0.92	0.97
Repressed_Hoffman extend.500	0.72	0.38	0.07	0.53	0.10	0.00	0.00	0.00	0.93	0.97
H3K4me3_Trynka	0.13	0.18	0.11	1.38	0.83	0.65	0.00	0.00	0.97	0.98
PromoterFlanking_Hoffman extend.500	0.03	-0.05	0.06	-1.62	1.87	0.15	0.00	0.00	0.98	0.98

Note. BOLD indicates FDR < 0.05 passed results.

Table A6. Results from the Multiple-tissue of gene expression analysis

Name	Coefficient	Coefficient se	Coefficient P	Tissue Category	Coefficient P FDR
A08.186.211.730.885.287.249.487.Corpus.Striatum	3.54E-08	8.02E-09	5.09E-06	CNS	1.04E-03
Brain_Spinal_cord_(cervical_c-1)	2.33E-08	6.50E-09	1.68E-04	CNS	1.72E-02
Brain_Amygdala	1.98E-08	6.21E-09	7.08E-04	CNS	3.93E-02
Brain_Substantia_nigra	1.96E-08	6.17E-09	7.67E-04	CNS	3.93E-02
A08.186.211.730.885.287.249.Basal.Ganglia	2.22E-08	7.75E-09	2.11E-03	CNS	8.67E-02
A08.186.211.653.Mesencephalon	1.81E-08	7.46E-09	7.61E-03	CNS	2.60E-01
A11.443.Erythroid.Cells	1.89E-08	8.84E-09	1.62E-02	Blood/Immune	3.31E-01
A08.186.211.464.710.225.Entorhinal.Cortex	1.29E-08	6.99E-09	3.24E-02	CNS	3.31E-01
A08.186.211.Brain	1.54E-08	6.99E-09	1.38E-02	CNS	3.31E-01
Brain_Anterior_cingulate_cortex_(BA24)	1.08E-08	5.86E-09	3.32E-02	CNS	3.31E-01
Brain_Caudate_(basal_ganglia)	1.42E-08	6.32E-09	1.23E-02	CNS	3.31E-01
Brain_Cerebellum	1.27E-08	6.63E-09	2.76E-02	CNS	3.31E-01
Brain_Cortex	1.24E-08	6.21E-09	2.31E-02	CNS	3.31E-01
Brain_Frontal_Cortex_(BA9)	1.07E-08	5.60E-09	2.82E-02	CNS	3.31E-01
Brain_Hippocampus	1.34E-08	6.16E-09	1.49E-02	CNS	3.31E-01
Brain_Hypothalamus	1.32E-08	6.53E-09	2.13E-02	CNS	3.31E-01
Brain_Putamen_(basal_ganglia)	1.25E-08	6.23E-09	2.24E-02	CNS	3.31E-01
A03.556.249.124.Ileum	2.08E-08	1.03E-08	2.24E-02	Digestive	3.31E-01
A03.556.875.875.Stomach	1.77E-08	9.43E-09	3.02E-02	Digestive	3.31E-01
A03.556.875.Upper.Gastrointestinal.Tract	1.84E-08	1.02E-08	3.55E-02	Digestive	3.31E-01
A04.411.Lung	1.69E-08	8.76E-09	2.67E-02	Other	3.31E-01
A11.872.700.500.Induced.Prunipotent.Stem.Cells	1.50E-08	8.28E-09	3.53E-02	Other	3.31E-01
A05.360.319.887.Vulva	1.94E-08	1.10E-08	3.94E-02	Other	3.51E-01
A03.556.875.500.Esophagus	1.61E-08	9.28E-09	4.17E-02	Digestive	3.56E-01
A08.186.211.730.317.Diencephalon	1.66E-08	9.86E-09	4.58E-02	CNS	3.75E-01

A11.872.040.Adult.Stem.Cells	1.52E-08	9.12E-09	4.79E-02	Other	3.78E-01
Artery_Coronary	1.34E-08	8.23E-09	5.14E-02	Cardiovascular	3.90E-01
Brain_Nucleus_accumbens_(basal_ganglia)	1.02E-08	6.35E-09	5.47E-02	CNS	4.01E-01
Brain_Cerebellar_Hemisphere	1.09E-08	6.96E-09	5.90E-02	CNS	4.17E-01
A11.118.637.555.567.569.T.Lymphocytes	1.34E-08	9.31E-09	7.53E-02	Blood/Immune	4.29E-01
A07.231.Blood.Vessels	1.39E-08	9.29E-09	6.79E-02	Cardiovascular	4.29E-01
A08.186.211.464.405.Hippocampus	9.90E-09	6.85E-09	7.43E-02	CNS	4.29E-01
A08.186.211.464.Limbic.System	1.06E-08	7.27E-09	7.30E-02	CNS	4.29E-01
A08.186.211.730.885.287.500.Cerebral.Cortex	1.04E-08	7.11E-09	7.26E-02	CNS	4.29E-01
A03.556.124.684.Intestine..Small	1.38E-08	9.09E-09	6.48E-02	Digestive	4.29E-01
A17.815.Skin	1.29E-08	8.70E-09	6.88E-02	Other	4.29E-01
A08.186.211.132.Brain.Stem	9.46E-09	6.66E-09	7.79E-02	CNS	4.32E-01
A08.186.211.730.885.287.500.670.Parietal.Lobe	9.28E-09	6.78E-09	8.56E-02	CNS	4.62E-01
A08.186.211.730.317.357.Hypothalamus	1.29E-08	9.83E-09	9.42E-02	CNS	4.86E-01
A08.186.211.730.885.287.500.270.Frontal.Lobe	9.61E-09	7.41E-09	9.72E-02	CNS	4.86E-01
Colon_Transverse	1.08E-08	8.33E-09	9.72E-02	Digestive	4.86E-01
A07.541.560.Heart.Ventricles	8.87E-09	7.65E-09	1.23E-01	Cardiovascular	5.73E-01
Esophagus_Muscularis	1.02E-08	8.63E-09	1.19E-01	Digestive	5.73E-01
A05.360.319.679.Uterus	1.02E-08	8.68E-09	1.20E-01	Other	5.73E-01
A05.360.319.114.373.Fallopian.Tubes	1.03E-08	9.71E-09	1.45E-01	Other	6.60E-01
A15.382.490.555.567.537.Killer.Cells..Natural	9.47E-09	1.04E-08	1.81E-01	Blood/Immune	8.04E-01
Bladder	6.02E-09	6.69E-09	1.84E-01	Other	8.04E-01
A15.145.229.188.Blood.Platelets	6.70E-09	8.57E-09	2.17E-01	Blood/Immune	8.10E-01
A07.231.114.Arteries	7.59E-09	8.65E-09	1.90E-01	Cardiovascular	8.10E-01
A07.231.908.Veins	7.23E-09	8.86E-09	2.07E-01	Cardiovascular	8.10E-01
A07.541.510.110.Aortic.Valve	6.16E-09	7.63E-09	2.10E-01	Cardiovascular	8.10E-01
Artery_Tibial	5.89E-09	7.37E-09	2.12E-01	Cardiovascular	8.10E-01
A08.186.211.865.428.Metencephalon	5.46E-09	6.83E-09	2.12E-01	CNS	8.10E-01
Esophagus_Gastroesophageal_Junction	7.02E-09	8.13E-09	1.94E-01	Digestive	8.10E-01
Esophagus_Mucosa	6.68E-09	8.53E-09	2.17E-01	Digestive	8.10E-01

A11.627.340.360.Granulocyte.Precursor.Cells	6.17E-09	9.69E-09	2.62E-01	Blood/Immune	8.81E-01
A15.145.Blood	6.13E-09	9.40E-09	2.57E-01	Blood/Immune	8.81E-01
A07.231.908.670.874.Umbilical.Veins	5.43E-09	8.53E-09	2.62E-01	Cardiovascular	8.81E-01
A09.371.729.Retina	4.69E-09	7.32E-09	2.61E-01	CNS	8.81E-01
A05.360.444.492.362.Foreskin	6.01E-09	8.79E-09	2.47E-01	Other	8.81E-01
A11.872.190.Embryonic.Stem.Cells	5.03E-09	7.84E-09	2.61E-01	Other	8.81E-01
Artery_Aorta	5.41E-09	8.75E-09	2.68E-01	Cardiovascular	8.87E-01
A11.118.637.555.567.569.200.700.T.Lymphocytes..Regulatory	3.85E-09	9.52E-09	3.43E-01	Blood/Immune	8.88E-01
A11.872.378.590.817.Megakaryocyte.Erythroid.Progenitor.Cells	4.28E-09	7.77E-09	2.91E-01	Blood/Immune	8.88E-01
A15.145.229.637.555.567.569.200.CD4.Positive.T.Lymphocytes	4.67E-09	9.77E-09	3.16E-01	Blood/Immune	8.88E-01
A15.382.490.315.583.Neutrophils	4.41E-09	9.26E-09	3.17E-01	Blood/Immune	8.88E-01
Heart_Left_Ventricle	3.77E-09	7.45E-09	3.06E-01	Cardiovascular	8.88E-01
A08.186.211.132.810.428.200.Cerebellum	3.91E-09	6.90E-09	2.85E-01	CNS	8.88E-01
A08.186.211.730.317.357.352.435.Hypothalamo.Hypophyseal.System	4.60E-09	9.39E-09	3.12E-01	CNS	8.88E-01
A03.556.124.369.Intestinal.Mucosa	3.64E-09	9.05E-09	3.44E-01	Digestive	8.88E-01
A03.556.249.249.356.668.Colon..Sigmoid	3.90E-09	8.82E-09	3.29E-01	Digestive	8.88E-01
Small_Intestine_Terminal_Ileum	2.98E-09	8.42E-09	3.62E-01	Digestive	8.88E-01
A03.620.Liver	5.11E-09	9.04E-09	2.86E-01	Liver	8.88E-01
Liver	4.10E-09	8.07E-09	3.06E-01	Liver	8.88E-01
A02.835.232.834.151.Cervical.Vertrebrae	3.28E-09	8.69E-09	3.53E-01	Musculoskeletal/Connective	8.88E-01
A02.835.583.443.800.Synovial.Membrane	3.21E-09	9.28E-09	3.65E-01	Musculoskeletal/Connective	8.88E-01
A05.360.319.Genitalia..Female	4.51E-09	8.45E-09	2.97E-01	Other	8.88E-01
A05.810.453.324.Kidney.Cortex	3.89E-09	7.88E-09	3.11E-01	Other	8.88E-01
A05.810.890.Urinary.Bladder	4.06E-09	9.15E-09	3.29E-01	Other	8.88E-01
A06.407.312.782.Testis	2.53E-09	7.53E-09	3.68E-01	Other	8.88E-01
A10.336.707.Prostate	3.05E-09	7.92E-09	3.50E-01	Other	8.88E-01
A11.436.294.064.Glucagon.Secreting.Cells	4.50E-09	9.01E-09	3.09E-01	Other	8.88E-01
A14.549.167.646.Periodontium	3.16E-09	8.14E-09	3.49E-01	Other	8.88E-01
Ovary	3.59E-09	8.37E-09	3.34E-01	Other	8.88E-01
Skin_Sun_Exposed_(Lower_leg)	3.07E-09	8.42E-09	3.58E-01	Other	8.88E-01

A05.360.319.679.256.Cervix.Uteri	2.76E-09	8.92E-09	3.79E-01	Other	8.92E-01
A05.360.Genitalia	2.73E-09	8.65E-09	3.76E-01	Other	8.92E-01
A10.165.114.830.750.Subcutaneous.Fat	2.01E-09	7.91E-09	3.99E-01	Adipose	9.10E-01
A07.541.Heart	1.99E-09	7.47E-09	3.95E-01	Cardiovascular	9.10E-01
Heart_Atrial_Appendage	1.73E-09	6.72E-09	3.98E-01	Cardiovascular	9.10E-01
A05.360.319.679.690.Myometrium	1.69E-09	7.75E-09	4.14E-01	Musculoskeletal/Connective	9.22E-01
Vagina	1.81E-09	8.27E-09	4.13E-01	Other	9.22E-01
Spleen	1.56E-09	9.08E-09	4.32E-01	Blood/Immune	9.42E-01
A11.872.Stem.Cells	1.76E-09	1.00E-08	4.30E-01	Other	9.42E-01
A11.118.637.555.567.562.440.Precursor.Cells..B.Lymphoid	1.55E-09	1.03E-08	4.40E-01	Blood/Immune	9.50E-01
A15.382.520.604.700.Spleen	1.22E-09	9.55E-09	4.49E-01	Blood/Immune	9.56E-01
A11.872.190.260.Embryoid.Bodies	1.02E-09	8.53E-09	4.52E-01	Other	9.56E-01
A06.407.Endocrine.Glands	8.89E-10	8.69E-09	4.59E-01	Other	9.61E-01
A10.165.114.830.500.750.Subcutaneous.Fat..Abdominal	-6.09E-09	8.16E-09	7.73E-01	Adipose	9.61E-01
Adipose_Subcutaneous	-3.32E-09	7.87E-09	6.64E-01	Adipose	9.61E-01
A02.835.583.443.800.800.Synovial.Fluid	5.04E-10	9.94E-09	4.80E-01	Blood/Immune	9.61E-01
A10.549.400.Lymph.Nodes	-1.75E-09	9.17E-09	5.76E-01	Blood/Immune	9.61E-01
A10.549.Lymphoid.Tissue	-1.44E-09	1.00E-08	5.57E-01	Blood/Immune	9.61E-01
A11.118.637.Leukocytes	-5.62E-09	8.68E-09	7.41E-01	Blood/Immune	9.61E-01
A11.627.624.249.Monocyte.Macrophage.Precursor.Cells	-3.12E-09	9.05E-09	6.35E-01	Blood/Immune	9.61E-01
A11.627.635.Myeloid.Progenitor.Cells	-6.63E-09	8.84E-09	7.74E-01	Blood/Immune	9.61E-01
A11.872.378.590.635.Granulocyte.Macrophage.Progenitor.Cells	-4.89E-09	1.00E-08	6.87E-01	Blood/Immune	9.61E-01
A11.872.378.Hematopoietic.Stem.Cells	-8.57E-10	9.28E-09	5.37E-01	Blood/Immune	9.61E-01
A15.145.229.637.555.Leukocytes..Mononuclear	-4.90E-09	1.01E-08	6.86E-01	Blood/Immune	9.61E-01
A15.145.229.Blood.Cells	-4.86E-09	9.74E-09	6.91E-01	Blood/Immune	9.61E-01
A15.145.300.Fetal.Blood	-3.40E-09	9.82E-09	6.35E-01	Blood/Immune	9.61E-01
A15.145.846.Serum	-6.77E-09	9.42E-09	7.64E-01	Blood/Immune	9.61E-01
A15.382.490.555.567.622.Lymphocytes..Null	-5.17E-09	8.95E-09	7.18E-01	Blood/Immune	9.61E-01
A15.382.490.555.567.Lymphocytes	-7.47E-09	1.00E-08	7.72E-01	Blood/Immune	9.61E-01
A15.382.520.604.800.Palatine.Tonsil	-5.60E-09	9.69E-09	7.18E-01	Blood/Immune	9.61E-01

A15.382.Immune.System	-6.33E-09	8.80E-09	7.64E-01	Blood/Immune	9.61E-01
Whole_Blood	-5.76E-09	8.93E-09	7.41E-01	Blood/Immune	9.61E-01
A07.541.358.100.Atrial.Appendage	-2.93E-09	7.44E-09	6.53E-01	Cardiovascular	9.61E-01
A08.186.211.730.885.287.500.571.735.Visual.Cortex	-1.99E-09	7.09E-09	6.10E-01	CNS	9.61E-01
A11.872.653.Neural.Stem.Cells	-2.65E-09	8.13E-09	6.28E-01	CNS	9.61E-01
A03.556.124.526.767.Rectum	-3.78E-09	8.99E-09	6.63E-01	Digestive	9.61E-01
A03.556.124.Intestines	-2.29E-09	9.55E-09	5.95E-01	Digestive	9.61E-01
A03.556.249.249.356.Colon	-3.57E-09	8.60E-09	6.61E-01	Digestive	9.61E-01
A03.556.Gastrointestinal.T tract	-3.75E-09	8.85E-09	6.64E-01	Digestive	9.61E-01
Colon_Sigmoid	-2.76E-09	7.84E-09	6.38E-01	Digestive	9.61E-01
A11.436.348.Hepatocytes	-4.22E-09	9.72E-09	6.68E-01	Liver	9.61E-01
A02.165.Cartilage	-1.71E-09	8.09E-09	5.84E-01	Musculoskeletal/Connective	9.61E-01
A02.633.567.850.Quadriceps.Muscle	-3.25E-09	9.29E-09	6.37E-01	Musculoskeletal/Connective	9.61E-01
A10.690.467.Muscle..Smooth	-4.81E-09	8.74E-09	7.09E-01	Musculoskeletal/Connective	9.61E-01
A10.690.Muscles	-1.63E-09	9.01E-09	5.72E-01	Musculoskeletal/Connective	9.61E-01
A11.329.171.Chondrocytes	-2.34E-09	8.25E-09	6.12E-01	Musculoskeletal/Connective	9.61E-01
A11.329.228.Fibroblasts	-7.07E-10	8.37E-09	5.34E-01	Musculoskeletal/Connective	9.61E-01
A11.329.629.Osteoblasts	-2.02E-09	7.83E-09	6.02E-01	Musculoskeletal/Connective	9.61E-01
A11.329.830.Stromal.Cells	-7.80E-11	8.24E-09	5.04E-01	Musculoskeletal/Connective	9.61E-01
A11.620.520.Myocytes..Smooth.Muscle	-3.91E-09	8.83E-09	6.71E-01	Musculoskeletal/Connective	9.61E-01
Cells_Transformed_fibroblasts	5.14E-10	7.92E-09	4.74E-01	Musculoskeletal/Connective	9.61E-01
Muscle_Skeletal	-3.76E-10	7.59E-09	5.20E-01	Musculoskeletal/Connective	9.61E-01
A05.360.319.114.630.Ovary	-1.07E-09	8.90E-09	5.48E-01	Other	9.61E-01
A05.360.319.679.490.Endometrium	-4.55E-09	8.65E-09	7.01E-01	Other	9.61E-01
A05.360.444.Genitalia..Male	-9.09E-10	7.50E-09	5.48E-01	Other	9.61E-01
A05.810.453.Kidney	-4.51E-09	8.23E-09	7.08E-01	Other	9.61E-01
A06.407.071.140.Adrenal.Cortex	-5.84E-09	8.83E-09	7.46E-01	Other	9.61E-01
A06.407.071.Adrenal.Glands	-2.20E-09	9.36E-09	5.93E-01	Other	9.61E-01
A06.407.312.Gonads	7.97E-10	8.92E-09	4.64E-01	Other	9.61E-01
A06.407.900.Thyroid.Gland	-1.92E-09	7.05E-09	6.07E-01	Other	9.61E-01

A10.272.497.Epidermis	5.47E-11	9.24E-09	4.98E-01	Other	9.61E-01
A10.615.550.599.Mouth.Mucosa	-5.85E-09	8.66E-09	7.50E-01	Other	9.61E-01
A10.615.550.Mucous.Membrane	-3.84E-09	9.58E-09	6.56E-01	Other	9.61E-01
A10.615.789.Serous.Membrane	2.42E-10	9.59E-09	4.90E-01	Other	9.61E-01
A10.615.Membranes	-6.17E-09	9.18E-09	7.49E-01	Other	9.61E-01
A11.382.Endocrine.Cells	-4.52E-09	8.46E-09	7.03E-01	Other	9.61E-01
A11.436.275.Endothelial.Cells	-1.40E-09	8.73E-09	5.64E-01	Other	9.61E-01
A14.549.167.Dentition	-1.90E-10	8.17E-09	5.09E-01	Other	9.61E-01
A14.549.885.Tongue	-6.58E-09	9.11E-09	7.65E-01	Other	9.61E-01
A14.549.Mouth	-4.47E-09	9.34E-09	6.84E-01	Other	9.61E-01
Adrenal_Gland	-2.82E-09	8.02E-09	6.38E-01	Other	9.61E-01
Breast_Mammary_Tissue	-2.74E-09	7.93E-09	6.35E-01	Other	9.61E-01
Cervix_Ectocervix	-3.83E-09	7.51E-09	6.95E-01	Other	9.61E-01
Cervix_Endocervix	-1.07E-09	7.79E-09	5.54E-01	Other	9.61E-01
Minor_Salivary_Gland	-4.60E-09	7.61E-09	7.27E-01	Other	9.61E-01
Nerve_Tibial	-3.00E-09	7.41E-09	6.57E-01	Other	9.61E-01
Skin_Not_Sun_Exposed_(Suprapubic)	-4.18E-09	8.46E-09	6.89E-01	Other	9.61E-01
Uterus	2.81E-10	8.02E-09	4.86E-01	Other	9.61E-01
A03.734.414.Islets.of.Langerhans	-4.27E-09	8.61E-09	6.90E-01	Pancreas	9.61E-01
A03.734.Pancreas	-1.53E-09	8.96E-09	5.68E-01	Pancreas	9.61E-01
Adipose_Visceral_(Omentum)	-7.69E-09	7.97E-09	8.33E-01	Adipose	9.75E-01
A11.118.637.555.567.562.B.Lymphocytes	-7.74E-09	8.49E-09	8.19E-01	Blood/Immune	9.75E-01
A07.541.358.Heart.Atria	-6.32E-09	7.46E-09	8.02E-01	Cardiovascular	9.75E-01
A03.556.249.249.209.Cecum	-6.94E-09	8.60E-09	7.90E-01	Digestive	9.75E-01
A11.329.Connective.Tissue.Cells	-7.56E-09	8.34E-09	8.18E-01	Musculoskeletal/Connective	9.75E-01
A11.436.329.Granulosa.Cells	-7.85E-09	8.71E-09	8.16E-01	Other	9.75E-01
A11.872.580.Mesenchymal.Stem.Cells	-6.91E-09	7.80E-09	8.12E-01	Other	9.75E-01
Kidney_Cortex	-7.46E-09	7.82E-09	8.30E-01	Other	9.75E-01
Lung	-6.71E-09	7.73E-09	8.07E-01	Other	9.75E-01
Testis	-7.26E-09	7.78E-09	8.25E-01	Other	9.75E-01

A11.329.114.Adipocytes	-8.91E-09	7.68E-09	8.77E-01	Adipose	9.99E-01
A11.329.372.600.Macrophages..Alveolar	-2.55E-08	8.30E-09	9.99E-01	Blood/Immune	9.99E-01
A15.145.229.637.555.567.562.725.Plasma.Cells	-9.96E-09	8.17E-09	8.89E-01	Blood/Immune	9.99E-01
A15.378.316.580.Monocytes	-2.09E-08	8.72E-09	9.92E-01	Blood/Immune	9.99E-01
A15.378.316.Bone.Marrow.Cells	-2.01E-08	9.52E-09	9.82E-01	Blood/Immune	9.99E-01
A15.382.680.Phagocytes	-2.20E-08	9.18E-09	9.92E-01	Blood/Immune	9.99E-01
A15.382.812.260.Dendritic.Cells	-2.26E-08	7.76E-09	9.98E-01	Blood/Immune	9.99E-01
A15.382.812.522.Macrophages	-2.18E-08	7.82E-09	9.97E-01	Blood/Immune	9.99E-01
A15.382.812.Mononuclear.Phagocyte.System	-2.00E-08	7.66E-09	9.96E-01	Blood/Immune	9.99E-01
Cells_EBV-transformed_lymphocytes	-1.21E-08	8.36E-09	9.26E-01	Blood/Immune	9.99E-01
A03.556.500.760.464.Parotid.Gland	-1.27E-08	7.16E-09	9.62E-01	Digestive	9.99E-01
A03.556.500.760.Salivary.Glands	-1.24E-08	7.25E-09	9.56E-01	Digestive	9.99E-01
Stomach	-2.20E-08	8.79E-09	9.94E-01	Digestive	9.99E-01
A10.165.450.300.425.Keloid	-1.43E-08	7.74E-09	9.68E-01	Musculoskeletal/Connective	9.99E-01
A10.165.450.300.Cicatrix	-1.67E-08	7.71E-09	9.85E-01	Musculoskeletal/Connective	9.99E-01
A04.531.520.Nasal.Mucosa	-1.68E-08	8.62E-09	9.74E-01	Other	9.99E-01
A05.360.490.Germ.Cells	-1.24E-08	7.72E-09	9.45E-01	Other	9.99E-01
A09.371.Eye	-9.53E-09	8.01E-09	8.83E-01	Other	9.99E-01
A10.272.Epithelium	-1.84E-08	8.96E-09	9.80E-01	Other	9.99E-01
A10.615.284.473.Chorion	-1.09E-08	7.07E-09	9.38E-01	Other	9.99E-01
A11.436.397.Keratinocytes	-1.34E-08	9.28E-09	9.25E-01	Other	9.99E-01
A11.436.Epithelial.Cells	-1.42E-08	8.23E-09	9.58E-01	Other	9.99E-01
A11.497.497.600.Oocytes	-1.20E-08	7.88E-09	9.36E-01	Other	9.99E-01
A14.724.557.Nasopharynx	-1.35E-08	7.63E-09	9.62E-01	Other	9.99E-01
A14.724.Pharynx	-1.16E-08	7.46E-09	9.39E-01	Other	9.99E-01
Fallopian_Tube	-1.10E-08	8.91E-09	8.91E-01	Other	9.99E-01
Pituitary	-8.48E-09	7.53E-09	8.70E-01	Other	9.99E-01
Prostate	-1.88E-08	8.42E-09	9.87E-01	Other	9.99E-01
Thyroid	-1.85E-08	6.84E-09	9.97E-01	Other	9.99E-01
Pancreas	-8.69E-09	7.22E-09	8.85E-01	Pancreas	9.99E-01

Note. BOLD indicates FDR < 0.05 passed results.

Table A7. Results from the Multiple-tissue analysis of chromatin data (validation)

Name	Coefficient	Coefficient se	Coefficient p	Tissue Category	Coefficient p_FDR
Brain_Hippocampus_Middle_H3K27ac	2.28E-07	6.81E-08	0.00	CNS	0.058
Brain_Angular_Gyrus_H3K4me1	2.89E-07	8.82E-08	0.00	CNS	0.058
Brain_Substantia_Nigra_H3K27ac	2.00E-07	6.18E-08	0.00	CNS	0.058
Brain_Angular_Gyrus_H3K27ac	2.50E-07	7.82E-08	0.00	CNS	0.058
Brain_Anterior_Caudate_H3K27ac	2.29E-07	7.23E-08	0.00	CNS	0.058
Brain_Dorsolateral_Prefrontal_Cortex_H3K4me1	3.32E-07	1.06E-07	0.00	CNS	0.058
Brain_Substantia_Nigra_H3K4me1	2.02E-07	6.49E-08	0.00	CNS	0.058
Brain_Substantia_Nigra_H3K9ac	5.45E-07	1.78E-07	0.00	CNS	0.058
Brain_Hippocampus_Middle_H3K4me1	1.75E-07	5.73E-08	0.00	CNS	0.058
Brain_Anterior_Caudate_H3K4me1	2.32E-07	7.67E-08	0.00	CNS	0.058
Brain_Cingulate_Gyrus_H3K27ac	2.16E-07	7.19E-08	0.00	CNS	0.058
Brain_Dorsolateral_Prefrontal_Cortex_H3K27ac	2.54E-07	8.54E-08	0.00	CNS	0.059
Brain_Cingulate_Gyrus_H3K4me1	2.20E-07	7.48E-08	0.00	CNS	0.062
Brain_Inferior_Temporal_Lobe_H3K4me1	2.59E-07	9.70E-08	0.00	CNS	0.131
Brain_Inferior_Temporal_Lobe_H3K27ac	1.68E-07	6.50E-08	0.00	CNS	0.153
Heart-LV_ENTEX_H3K36me3	2.59E-07	1.01E-07	0.01	Cardiovascular	0.153
Ovary_H3K4me3	7.68E-07	3.01E-07	0.01	Other	0.153

Brain_Anterior_Caudate__H3K9ac	4.06E-07	1.61E-07	0.01	CNS	0.157
Brain_Dorsolateral_Prefrontal_Cortex__H3K4me3	5.55E-07	2.32E-07	0.01	CNS	0.213
Aorta__H3K4me3	8.17E-07	3.45E-07	0.01	Cardiovascular	0.220
Esoph-Muscularis_ENTEX__H3K36me3	1.82E-07	8.29E-08	0.01	Digestive	0.330
Artery-Tibial_ENTEX__H3K36me3	1.63E-07	8.15E-08	0.02	Cardiovascular	0.505
Primary_hematopoietic_stem_cells_G-CSF-mobilized_Male__H3K4me3	2.91E-07	1.47E-07	0.02	Blood/Immune	0.511
Primary_hematopoietic_stem_cells_G-CSF-mobilized_Female__H3K4me3	4.24E-07	2.21E-07	0.03	Blood/Immune	0.553
Fetal_Brain_Female__H3K36me3	1.92E-07	1.01E-07	0.03	CNS	0.553
Esoph-Muscularis_ENTEX__H3K4me3	4.80E-07	2.56E-07	0.03	Digestive	0.571
Lung_ENTEX__H3K36me3	1.62E-07	9.00E-08	0.04	Other	0.636
Fetal_Kidney__H3K4me1	3.48E-07	1.95E-07	0.04	Other	0.636
Aorta_ENTEX__H3K36me3	1.10E-07	6.19E-08	0.04	Cardiovascular	0.636
Fetal_Stomach__H3K4me3	5.98E-07	3.43E-07	0.04	Digestive	0.661
Brain_Hippocampus_Middle__H3K4me3	2.92E-07	1.70E-07	0.04	CNS	0.669
Rectal_Smooth_Muscle__H3K4me3	4.30E-07	2.60E-07	0.05	Musculoskeletal/Connective	0.751
Aorta_ENTEX__H3K4me3	1.93E-07	1.22E-07	0.06	Cardiovascular	0.825
Artery-Coronary_ENTEX__H3K4me3	2.19E-07	1.39E-07	0.06	Cardiovascular	0.825
Fetal_Kidney__DNase	2.77E-07	1.81E-07	0.06	Other	0.829
Brain_Inferior_Temporal_Lobe__H3K4me3	3.23E-07	2.12E-07	0.06	CNS	0.829
Brain_Inferior_Temporal_Lobe__H3K9ac	2.20E-07	1.46E-07	0.07	CNS	0.829
Small_Intestine__H3K36me3	3.65E-07	2.45E-07	0.07	Digestive	0.829
Brain_Germinal_Matrix__H3K36me3	2.00E-07	1.34E-07	0.07	CNS	0.829

Brain_Angular_Gyrus__H3K36me3	2.09E-07	1.42E-07	0.07	CNS	0.829
Duodenum_Smooth_Muscle__H3K4me1	1.68E-07	1.14E-07	0.07	Musculoskeletal/Connective	0.829
Fetal_Thymus__H3K36me3	9.30E-08	6.34E-08	0.07	Blood/Immune	0.829
Fetal_Adrenal_Gland__H3K4me3	5.68E-07	3.92E-07	0.07	Other	0.840
Brain_Angular_Gyrus__H3K9ac	2.78E-07	1.95E-07	0.08	CNS	0.850
Fetal_Brain_Male__DNase	2.17E-07	1.53E-07	0.08	CNS	0.850
Fetal_Intestine_Large__H3K36me3	1.19E-07	8.48E-08	0.08	Digestive	0.862
Brain_Anterior_Caudate__H3K4me3	2.79E-07	2.03E-07	0.08	CNS	0.866
Primary_hematopoietic_stem_cells_G-CSF-mobilized_Female__DNase	2.58E-07	1.88E-07	0.08	Blood/Immune	0.866
Right_Atrium__H3K4me3	3.99E-07	2.95E-07	0.09	Cardiovascular	0.866
Brain_Dorsolateral_Prefrontal_Cortex__H3K9ac	2.68E-07	2.03E-07	0.09	CNS	0.866
Sigmoid_Colon__H3K36me3	1.62E-07	1.24E-07	0.10	Digestive	0.866
Brain_Hippocampus_Middle__H3K36me3	1.40E-07	1.07E-07	0.10	CNS	0.866
Brain_Angular_Gyrus__H3K4me3	3.27E-07	2.51E-07	0.10	CNS	0.866
Fetal_Stomach__H3K36me3	9.00E-08	6.92E-08	0.10	Digestive	0.866
NHDF-Ad_Adult_Dermal_Fibroblast_Primary_Cells__DNase	1.92E-07	1.48E-07	0.10	Musculoskeletal/Connective	0.866
Brain_Cingulate_Gyrus__H3K4me3	2.89E-07	2.28E-07	0.10	CNS	0.872
Brain_Dorsolateral_Prefrontal_Cortex__H3K36me3	1.66E-07	1.33E-07	0.10	CNS	0.872
Vagina_ENTEX__H3K4me3	4.01E-07	3.20E-07	0.11	Other	0.872
Fetal_Brain_Female__DNase	1.76E-07	1.41E-07	0.11	CNS	0.872
Brain_Cingulate_Gyrus__H3K36me3	1.46E-07	1.18E-07	0.11	CNS	0.881
Rectal_Mucosa_Donor_31__H3K36me3	1.15E-07	9.47E-08	0.11	Digestive	0.886

Primary_hematopoietic_stem_cells_G-CSF-mobilized_Female_H3K4me1	6.81E-08	5.64E-08	0.11	Blood/Immune	0.886
Primary_hematopoietic_stem_cells_G-CSF-mobilized_Male_H3K4me1	7.57E-08	6.29E-08	0.11	Blood/Immune	0.886
NHDF-Ad_Adult_Dermal_Fibroblast_Primary_Cells_H3K4me1	1.08E-07	9.15E-08	0.12	Musculoskeletal/Connective	0.903
Uterus_ENTEX_H3K4me3	4.03E-07	3.45E-07	0.12	Other	0.903
Liver_H3K36me3	7.49E-08	6.43E-08	0.12	Liver	0.903
Esoph-Mucosa_ENTEX_H3K4me3	2.14E-07	1.87E-07	0.13	Digestive	0.907
Spleen_H3K27ac	1.16E-07	1.01E-07	0.13	Blood/Immune	0.907
Aorta_ENTEX_H3K4me1	4.13E-08	3.64E-08	0.13	Cardiovascular	0.907
Aorta_ENTEX_H3K27ac	4.23E-08	3.83E-08	0.13	Cardiovascular	0.940
Primary_neutrophils_from_peripheral_blood_H3K4me3	1.35E-07	1.23E-07	0.14	Blood/Immune	0.942
Esoph-Mucosa_ENTEX_H3K4me1	7.94E-08	7.43E-08	0.14	Digestive	0.963
Fetal_Kidney_H3K9ac	3.31E-07	3.11E-07	0.14	Other	0.963
Aorta_H3K36me3	2.43E-07	2.36E-07	0.15	Cardiovascular	0.989
Primary_hematopoietic_stem_cells_H3K4me1	1.21E-07	1.19E-07	0.15	Blood/Immune	0.989
Spleen_ENTEX_H3K4me3	9.75E-08	9.65E-08	0.16	Blood/Immune	0.989
Aorta_H3K4me1	1.78E-07	1.77E-07	0.16	Cardiovascular	0.989
Brain_Cingulate_Gyrus_H3K9ac	1.96E-07	1.95E-07	0.16	CNS	0.989
Artery-Coronary_ENTEX_H3K27ac	6.44E-08	6.47E-08	0.16	Cardiovascular	0.989
Vagina_ENTEX_H3K27ac	6.39E-08	6.53E-08	0.16	Other	0.994
HMEC_Mammary_Epithelial_Primary_Cells_H3K36me3	1.21E-07	1.25E-07	0.17	Other	0.994
Fetal_Kidney_H3K4me3	3.02E-07	3.17E-07	0.17	Other	0.994
Fetal_Stomach_H3K27ac	8.51E-08	9.00E-08	0.17	Digestive	0.994

Stomach_Smooth_Muscle__H3K4me3	1.71E-07	1.82E-07	0.17	Musculoskeletal/Connective	0.994
Ganglion_Eminence_derived_primary_cultured_neurospheres__H3K36me3	1.17E-07	1.24E-07	0.17	CNS	0.994
Fetal_Intestine_Small__H3K36me3	5.19E-08	5.57E-08	0.18	Digestive	0.994
Primary_T_helper_memory_cells_from_peripheral_blood_1__H3K36me3	1.05E-07	1.13E-07	0.18	Blood/Immune	0.994
Colon_Smooth_Muscle__H3K4me3	1.94E-07	2.11E-07	0.18	Musculoskeletal/Connective	0.994
Foreskin_Melanocyte_Primary_Cells_skin01__DNase	1.02E-07	1.12E-07	0.18	Other	0.994
Primary_T_helper_memory_cells_from_peripheral_blood_2__H3K36me3	1.35E-07	1.53E-07	0.19	Blood/Immune	1.000
Fetal_Intestine_Large__H3K27ac	6.61E-08	7.51E-08	0.19	Digestive	1.000
Esoph-GJ_ENTEX__H3K4me3	2.07E-07	2.38E-07	0.19	Digestive	1.000
Primary_T_killer_memory_cells_from_peripheral_blood__H3K36me3	1.11E-07	1.30E-07	0.20	Blood/Immune	1.000
Brain_Inferior_Temporal_Lobe__H3K36me3	9.45E-08	1.11E-07	0.20	CNS	1.000
Fetal_Stomach__H3K4me1	6.06E-08	7.13E-08	0.20	Digestive	1.000
Ovary__DNase	1.38E-07	1.64E-07	0.20	Other	1.000
Breast_Myoepithelial_Primary_Cells__H3K36me3	5.99E-08	7.16E-08	0.20	Other	1.000
Brain_Substantia_Nigra__H3K4me3	1.73E-07	2.10E-07	0.20	CNS	1.000
Foreskin_Melanocyte_Primary_Cells_skin01__H3K4me3	2.16E-07	2.64E-07	0.21	Other	1.000
Skeletal_Muscle_Female__H3K4me1	5.15E-08	6.31E-08	0.21	Musculoskeletal/Connective	1.000
SI-Term-Ileum_ENTEX__H3K27ac	5.54E-08	6.80E-08	0.21	Digestive	1.000
Foreskin_Melanocyte_Primary_Cells_skin01__H3K4me1	1.50E-07	1.85E-07	0.21	Other	1.000
Rectal_Smooth_Muscle__H3K4me1	7.25E-08	9.10E-08	0.21	Musculoskeletal/Connective	1.000
Fetal_Adrenal_Gland__H3K36me3	5.90E-08	7.57E-08	0.22	Other	1.000
Rectal_Mucosa_Donor_29__H3K36me3	8.43E-08	1.08E-07	0.22	Digestive	1.000

Aorta_H3K27ac	8.98E-08	1.16E-07	0.22	Cardiovascular	1.000
Foreskin_Fibroblast_Primary_Cells_skin02_DNase	1.23E-07	1.61E-07	0.22	Musculoskeletal/Connective	1.000
Fetal_Intestine_Small_DNase	1.42E-07	1.88E-07	0.22	Digestive	1.000
Nerve-Tibial_ENTEX_H3K4me1	4.73E-08	6.39E-08	0.23	Other	1.000
Colon_Smooth_Muscle_H3K36me3	8.56E-08	1.16E-07	0.23	Musculoskeletal/Connective	1.000
Mammary_ENTEX_H3K27ac	4.98E-08	6.80E-08	0.23	Other	1.000
Liver_H3K9ac	8.74E-08	1.24E-07	0.24	Liver	1.000
Fetal_Intestine_Large_H3K4me3	1.96E-07	2.79E-07	0.24	Digestive	1.000
Fetal_Intestine_Large_H3K4me1	4.41E-08	6.38E-08	0.24	Digestive	1.000
Nerve-Tibial_ENTEX_H3K27ac	2.85E-08	4.12E-08	0.24	Other	1.000
Duodenum_Mucosa_H3K36me3	6.81E-08	1.00E-07	0.25	Digestive	1.000
Primary_T_killer_naive_cells_from_peripheral_blood_H3K36me3	8.50E-08	1.26E-07	0.25	Blood/Immune	1.000
Primary_T_helper_naive_cells_from_peripheral_blood_1_H3K36me3	7.24E-08	1.08E-07	0.25	Blood/Immune	1.000
Fetal_Lung_DNase	7.88E-08	1.19E-07	0.25	Other	1.000
Stomach_Smooth_Muscle_H3K36me3	7.75E-08	1.18E-07	0.26	Musculoskeletal/Connective	1.000
Testis_ENTEX_H3K4me3	8.49E-08	1.32E-07	0.26	Other	1.000
NHDF-Ad_Adult_Dermal_Fibroblast_Primary_Cells_H3K4me3	1.92E-07	3.03E-07	0.26	Musculoskeletal/Connective	1.000
Colon-TV_ENTEX_H3K4me1	1.18E-07	1.87E-07	0.26	Digestive	1.000
Osteoblast_Primary_Cells_H3K4me3	1.23E-07	1.98E-07	0.27	Musculoskeletal/Connective	1.000
Primary_T_cells_from_cord_blood_H3K36me3	8.27E-08	1.35E-07	0.27	Blood/Immune	1.000
Mammary_ENTEX_H3K4me3	1.02E-07	1.67E-07	0.27	Other	1.000
Colon_Smooth_Muscle_H3K4me1	3.81E-08	6.27E-08	0.27	Musculoskeletal/Connective	1.000

Primary_monocytes_from_peripheral_blood__H3K4me3	1.90E-07	3.23E-07	0.28	Blood/Immune	1.000
Skeletal_Muscle_Female__H3K4me3	1.05E-07	1.83E-07	0.28	Musculoskeletal/Connective	1.000
Heart-Atrial_ENTEX__H3K4me3	1.52E-07	2.65E-07	0.28	Cardiovascular	1.000
Fetal_Intestine_Small__H3K4me1	3.51E-08	6.19E-08	0.29	Digestive	1.000
Psoas_Muscle__DNase	8.61E-08	1.56E-07	0.29	Musculoskeletal/Connective	1.000
Foreskin_Melanocyte_Primary_Cells_skin03__H3K4me3	1.64E-07	2.96E-07	0.29	Other	1.000
Primary_hematopoietic_stem_cells_G-CSF-mobilized_Female__H3K27ac	5.52E-08	1.00E-07	0.29	Blood/Immune	1.000
Primary_hematopoietic_stem_cells_short_term_culture__H3K4me1	4.07E-08	7.39E-08	0.29	Blood/Immune	1.000
Foreskin_Fibroblast_Primary_Cells_skin02__H3K4me3	5.80E-08	1.06E-07	0.29	Musculoskeletal/Connective	1.000
Foreskin_Fibroblast_Primary_Cells_skin01__DNase	8.16E-08	1.50E-07	0.29	Musculoskeletal/Connective	1.000
Primary_B_cells_from_peripheral_blood__DNase	8.25E-08	1.53E-07	0.30	Blood/Immune	1.000
Fetal_Brain_Male__H3K4me1	3.26E-08	6.07E-08	0.30	CNS	1.000
Primary_monocytes_from_peripheral_blood__H3K4me1	2.90E-08	5.43E-08	0.30	Blood/Immune	1.000
Breast_variant_Human_Mammary_Epithelial_Cells_(vHMEC)__H3K36me3	3.32E-08	6.34E-08	0.30	Other	1.000
Psoas_Muscle__H3K4me1	5.91E-08	1.14E-07	0.30	Musculoskeletal/Connective	1.000
Placenta_Amniotrophoblast__H3K4me1	3.56E-08	6.87E-08	0.30	Other	1.000
Esoph-Mucosa_ENTEX__H3K36me3	5.69E-08	1.10E-07	0.30	Digestive	1.000
Foreskin_Melanocyte_Primary_Cells_skin03__H3K27ac	4.87E-08	9.79E-08	0.31	Other	1.000
Cortex_derived_primary_cultured_neurospheres__H3K4me3	1.54E-07	3.16E-07	0.31	CNS	1.000
Primary_hematopoietic_stem_cells_short_term_culture__H3K36me3	3.10E-08	6.34E-08	0.31	Blood/Immune	1.000
Stomach_ENTEX__H3K4me3	8.99E-08	1.86E-07	0.31	Digestive	1.000
skeletal_muscle_ENTEX__H3K4me1	1.80E-08	3.79E-08	0.32	Musculoskeletal/Connective	1.000

Foreskin_Melanocyte_Primary_Cells_skin03__H3K4me1	2.72E-08	5.77E-08	0.32	Other	1.000
Ovary__H3K4me1	4.41E-08	9.87E-08	0.33	Other	1.000
Right_Atrium__H3K4me1	5.93E-08	1.33E-07	0.33	Cardiovascular	1.000
Right_Ventricle__H3K4me3	1.25E-07	2.88E-07	0.33	Cardiovascular	1.000
Primary_hematopoietic_stem_cells_G-CSF-mobilized_Male__DNase	9.15E-08	2.15E-07	0.34	Blood/Immune	1.000
Primary_hematopoietic_stem_cells_short_term_culture__H3K4me3	9.99E-08	2.39E-07	0.34	Blood/Immune	1.000
Small_Intestine__H3K4me1	5.54E-08	1.33E-07	0.34	Digestive	1.000
Fetal_Brain_Female__H3K4me3	8.53E-08	2.07E-07	0.34	CNS	1.000
Osteoblast_Primary_Cells__H3K4me1	2.47E-08	6.07E-08	0.34	Musculoskeletal/Connective	1.000
Skeletal_Muscle_Male__H3K4me1	3.07E-08	7.55E-08	0.34	Musculoskeletal/Connective	1.000
Primary_hematopoietic_stem_cells_G-CSF-mobilized_Female__H3K36me3	2.77E-08	6.85E-08	0.34	Blood/Immune	1.000
Fetal_Intestine_Small__H3K4me3	1.12E-07	2.78E-07	0.34	Digestive	1.000
NHLF_Lung_Fibroblast_Primary_Cells__H3K4me3	1.42E-07	3.51E-07	0.34	Musculoskeletal/Connective	1.000
Lung_ENTEX__H3K27ac	2.62E-08	6.77E-08	0.35	Other	1.000
Nerve-Tibial_ENTEX__H3K4me3	1.08E-07	2.84E-07	0.35	Other	1.000
Ovary__H3K27ac	4.51E-08	1.20E-07	0.35	Other	1.000
liver_ENTEX__H3K27ac	1.98E-08	5.29E-08	0.35	Liver	1.000
SI-Term-Ileum_ENTEX__H3K4me3	6.43E-08	1.75E-07	0.36	Digestive	1.000
Uterus_ENTEX__H3K27ac	2.05E-08	5.60E-08	0.36	Other	1.000
Lung_ENTEX__H3K4me1	2.78E-08	7.67E-08	0.36	Other	1.000
Foreskin_Fibroblast_Primary_Cells_skin01__H3K4me1	2.26E-08	6.27E-08	0.36	Musculoskeletal/Connective	1.000
Foreskin_Fibroblast_Primary_Cells_skin01__H3K4me3	5.17E-08	1.47E-07	0.36	Musculoskeletal/Connective	1.000

Brain_Substantia_Nigra__H3K36me3	6.04E-08	1.73E-07	0.36	CNS	1.000
Fetal_Kidney__H3K36me3	9.29E-08	2.69E-07	0.37	Other	1.000
Primary_T_cells_effector_memory_enriched_from_peripheral_blood__H3K4me3	7.76E-08	2.28E-07	0.37	Blood/Immune	1.000
Primary_T_helper_17_cells_PMA-I_stimulated__H3K36me3	2.75E-08	8.17E-08	0.37	Blood/Immune	1.000
Right_Atrium__H3K27ac	4.08E-08	1.24E-07	0.37	Cardiovascular	1.000
Skeletal_Muscle_Female__H3K27ac	2.48E-08	7.60E-08	0.37	Musculoskeletal/Connective	1.000
Esophagus__H3K27ac	3.42E-08	1.05E-07	0.37	Digestive	1.000
Sigmoid_Colon__H3K4me1	6.37E-08	1.96E-07	0.37	Digestive	1.000
liver_ENTEX__H3K36me3	2.77E-08	8.75E-08	0.38	Liver	1.000
Breast_Myoepithelial_Primary_Cells__H3K4me1	1.83E-08	5.81E-08	0.38	Other	1.000
Stomach_Mucosa__H3K36me3	6.73E-08	2.18E-07	0.38	Digestive	1.000
Foreskin_Keratinocyte_Primary_Cells_skin03__H3K4me3	6.40E-08	2.09E-07	0.38	Other	1.000
Right_Ventricle__H3K36me3	3.54E-08	1.19E-07	0.38	Cardiovascular	1.000
Brain_Anterior_Caudate__H3K36me3	3.51E-08	1.18E-07	0.38	CNS	1.000
Placenta_Amnion__H3K36me3	3.29E-08	1.14E-07	0.39	Other	1.000
Fetal_Hart__DNase	2.83E-08	1.02E-07	0.39	Cardiovascular	1.000
Stomach_Mucosa__H3K4me1	1.80E-08	6.54E-08	0.39	Digestive	1.000
liver_ENTEX__H3K4me1	6.65E-08	2.46E-07	0.39	Liver	1.000
Duodenum_Smooth_Muscle__H3K27ac	3.40E-08	1.30E-07	0.40	Musculoskeletal/Connective	1.000
Brain_Germinal_Matrix__H3K4me3	6.30E-08	2.46E-07	0.40	CNS	1.000
Liver__H3K4me1	1.42E-08	5.69E-08	0.40	Liver	1.000
Thymus__H3K36me3	2.92E-08	1.21E-07	0.40	Blood/Immune	1.000

Cortex_derived_primary_cultured_neurospheres__H3K4me1	2.09E-08	9.00E-08	0.41	CNS	1.000
Heart-Atrial_ENTEX__H3K27ac	1.18E-08	5.29E-08	0.41	Cardiovascular	1.000
Esoph-GJ_ENTEX__H3K4me1	1.32E-08	6.12E-08	0.41	Digestive	1.000
Lung__H3K4me1	2.59E-08	1.23E-07	0.42	Other	1.000
Placenta_Amniot__H3K27ac	3.23E-08	1.60E-07	0.42	Other	1.000
Primary_B_cells_from_cord_blood__H3K4me1	1.29E-08	7.08E-08	0.43	Blood/Immune	1.000
Primary_neutrophils_from_peripheral_blood__H3K4me1	8.50E-09	4.71E-08	0.43	Blood/Immune	1.000
Cortex_derived_primary_cultured_neurospheres__H3K36me3	2.01E-08	1.15E-07	0.43	CNS	1.000
Breast_Myoepithelial_Primary_Cells__H3K4me3	3.22E-08	2.01E-07	0.44	Other	1.000
Fetal_Muscle_Trunk__DNase	2.28E-08	1.43E-07	0.44	Musculoskeletal/Connective	1.000
Brain_Germinal_Matrix__H3K4me1	2.30E-08	1.54E-07	0.44	CNS	1.000
Fetal_Lung__H3K36me3	1.19E-08	8.12E-08	0.44	Other	1.000
Fetal_Intestine_Small__H3K27ac	1.11E-08	7.63E-08	0.44	Digestive	1.000
Colonic_Mucosa__H3K36me3	1.78E-08	1.27E-07	0.44	Digestive	1.000
Rectal_Mucosa_Donor_31__H3K4me3	3.23E-08	2.36E-07	0.45	Digestive	1.000
Foreskin_Keratinocyte_Primary_Cells_skin03__H3K36me3	7.35E-09	5.56E-08	0.45	Other	1.000
Primary_B_cells_from_cord_blood__H3K4me3	3.66E-08	2.81E-07	0.45	Blood/Immune	1.000
Pancreas_ENTEX__H3K36me3	1.08E-08	8.80E-08	0.45	Pancreas	1.000
Fetal_Intestine_Large__DNase	1.83E-08	1.50E-07	0.45	Digestive	1.000
Ovary_ENTEX__H3K4me3	4.05E-08	3.43E-07	0.45	Other	1.000
Primary_hematopoietic_stem_cells__H3K36me3	1.68E-08	1.44E-07	0.45	Blood/Immune	1.000
NHEK-Epidermal_Keratinocyte_Primary_Cells__H3K36me3	1.07E-08	9.23E-08	0.45	Other	1.000

Skeletal_Muscle_Male_H3K9ac	1.17E-08	1.19E-07	0.46	Musculoskeletal/Connective	1.000
Fetal_Muscle_Trunk_H3K36me3	9.80E-09	1.00E-07	0.46	Musculoskeletal/Connective	1.000
Sigmoid_Colon_H3K4me3	3.07E-08	3.39E-07	0.46	Digestive	1.000
Rectal_Mucosa_Donor_29_H3K4me3	1.64E-08	1.89E-07	0.47	Digestive	1.000
Colon_Smooth_Muscle_H3K27ac	5.46E-09	7.00E-08	0.47	Musculoskeletal/Connective	1.000
Fetal_Stomach_DNase	1.44E-08	2.10E-07	0.47	Digestive	1.000
Fetal_Muscle_Leg_H3K4me3	2.26E-08	3.53E-07	0.47	Musculoskeletal/Connective	1.000
Primary_T_helper_cells_PMA-I_stimulated_H3K36me3	4.28E-09	6.89E-08	0.48	Blood/Immune	1.000
Foreskin_Keratinocyte_Primary_Cells_skin02_H3K4me1	6.42E-09	1.05E-07	0.48	Other	1.000
Primary_hematopoietic_stem_cells_H3K4me3	1.33E-08	2.98E-07	0.48	Blood/Immune	1.000
Rectal_Mucosa_Donor_29_H3K4me1	5.44E-09	1.43E-07	0.48	Digestive	1.000
Stomach_ENTEX_H3K36me3	2.14E-09	6.97E-08	0.49	Digestive	1.000
Left_Ventricle_H3K4me3	4.56E-09	3.59E-07	0.49	Cardiovascular	1.000
Fetal_Muscle_Leg_H3K27ac	1.05E-09	8.82E-08	0.50	Musculoskeletal/Connective	1.000
Heart-Atrial_ENTEX_H3K36me3	7.11E-10	8.31E-08	0.50	Cardiovascular	1.000
Small_Intestine_H3K27ac	-2.52E-10	1.24E-07	0.50	Digestive	1.000
Primary_T_cells_effector_memory_enriched_from_peripheral_blood_H3K36me3	-2.42E-09	9.31E-08	0.51	Blood/Immune	1.000
Heart-LV_ENTEX_H3K27ac	-1.87E-09	6.00E-08	0.51	Cardiovascular	1.000
Fetal_Muscle_Leg_DNase	-3.75E-09	1.17E-07	0.51	Musculoskeletal/Connective	1.000
Fetal_Muscle_Trunk_H3K27ac	-3.52E-09	1.08E-07	0.51	Musculoskeletal/Connective	1.000
liver_ENTEX_H3K4me3	-5.46E-09	1.46E-07	0.51	Liver	1.000
Esophagus_H3K4me3	-1.09E-08	2.86E-07	0.52	Digestive	1.000

Colon_Smooth_Muscle__H3K9ac	-7.63E-09	1.98E-07	0.52	Musculoskeletal/Connective	1.000
Stomach_Smooth_Muscle__H3K4me1	-3.72E-09	7.73E-08	0.52	Musculoskeletal/Connective	1.000
Stomach_ENTEX__H3K4me1	-4.03E-09	7.11E-08	0.52	Digestive	1.000
NHLF_Lung_Fibroblast_Primary_Cells__H3K4me1	-9.87E-09	1.28E-07	0.53	Musculoskeletal/Connective	1.000
HMEC_Mammary_Epithelial_Primary_Cells__H3K9ac	-1.47E-08	1.66E-07	0.54	Other	1.000
Fetal_Adrenal_Gland__DNase	-1.43E-08	1.57E-07	0.54	Other	1.000
Primary_T_helper_cells_from_peripheral_blood__H3K4me3	-2.11E-08	2.17E-07	0.54	Blood/Immune	1.000
Foreskin_Keratinocyte_Primary_Cells_skin03__H3K4me1	-7.25E-09	6.74E-08	0.54	Other	1.000
Pancreatic_Islets__H3K9ac	-3.67E-08	3.36E-07	0.54	Pancreas	1.000
NHEK-Epidermal_Keratinocyte_Primary_Cells__H3K27ac	-8.76E-09	7.96E-08	0.54	Other	1.000
Fetal_Brain_Male__H3K4me3	-5.34E-08	4.55E-07	0.55	CNS	1.000
skeletal_muscle_ENTEX__H3K27ac	-3.91E-09	3.33E-08	0.55	Musculoskeletal/Connective	1.000
Foreskin_Fibroblast_Primary_Cells_skin02__H3K4me1	-9.61E-09	7.62E-08	0.55	Musculoskeletal/Connective	1.000
Primary_monocytes_from_peripheral_blood__H3K36me3	-7.55E-09	5.82E-08	0.55	Blood/Immune	1.000
Ganglion_Eminence_derived_primary_cultured_neurospheres__H3K4me3	-3.24E-08	2.27E-07	0.56	CNS	1.000
Esoph-Muscularis_ENTEX__H3K27ac	-1.02E-08	7.04E-08	0.56	Digestive	1.000
Primary_monocytes_from_peripheral_blood__H3K27ac	-1.52E-08	1.01E-07	0.56	Blood/Immune	1.000
Fetal_Muscle_Leg__H3K36me3	-1.32E-08	8.69E-08	0.56	Musculoskeletal/Connective	1.000
NHEK-Epidermal_Keratinocyte_Primary_Cells__H3K4me3	-2.84E-08	1.85E-07	0.56	Other	1.000
Thyroid_gland_ENTEX__H3K36me3	-1.31E-08	8.35E-08	0.56	Other	1.000
Placenta__H3K27ac	-1.04E-08	6.14E-08	0.57	Other	1.000
Primary_mononuclear_cells_from_peripheral_blood__H3K9ac	-3.22E-08	1.86E-07	0.57	Blood/Immune	1.000

Ganglion_Eminence_derived_primary_cultured_neurospheres__H3K4me1	-2.16E-08	1.23E-07	0.57	CNS	1.000
Rectal_Mucosa_Donor_31__H3K9ac	-2.79E-08	1.58E-07	0.57	Digestive	1.000
Placenta_Amnion__H3K4me3	-7.04E-08	3.78E-07	0.57	Other	1.000
Stomach_Smooth_Muscle__H3K27ac	-1.38E-08	7.29E-08	0.57	Musculoskeletal/Connective	1.000
Adipose_Nuclei__H3K4me1	-1.29E-08	6.70E-08	0.58	Adipose	1.000
NHLF_Lung_Fibroblast_Primary_Cells__DNase	-3.13E-08	1.61E-07	0.58	Musculoskeletal/Connective	1.000
Esoph-Mucosa_ENTEX__H3K27ac	-1.73E-08	8.68E-08	0.58	Digestive	1.000
Primary_neutrophils_from_peripheral_blood__H3K36me3	-1.07E-08	5.32E-08	0.58	Blood/Immune	1.000
Rectal_Smooth_Muscle__H3K36me3	-3.85E-08	1.81E-07	0.58	Musculoskeletal/Connective	1.000
Primary_T_cells_from_peripheral_blood__H3K36me3	-1.65E-08	7.70E-08	0.58	Blood/Immune	1.000
Psoas_Muscle__H3K4me3	-7.02E-08	3.16E-07	0.59	Musculoskeletal/Connective	1.000
Foreskin_Melanocyte_Primary_Cells_skin01__H3K27ac	-4.51E-08	2.00E-07	0.59	Other	1.000
Pancreas__H3K4me1	-2.25E-08	9.82E-08	0.59	Pancreas	1.000
Fetal_Brain_Male__H3K36me3	-8.35E-08	3.45E-07	0.60	CNS	1.000
Small_Intestine__DNase	-3.51E-08	1.44E-07	0.60	Digestive	1.000
Rectal_Mucosa_Donor_31__H3K4me1	-2.23E-08	8.93E-08	0.60	Digestive	1.000
Adipose_Nuclei__H3K36me3	-2.20E-08	8.71E-08	0.60	Adipose	1.000
Colon-Sigm_ENTEX__H3K27ac	-1.82E-08	7.19E-08	0.60	Digestive	1.000
Placenta__H3K4me3	-8.36E-08	3.23E-07	0.60	Other	1.000
Skeletal_Muscle_Female__H3K9ac	-4.27E-08	1.63E-07	0.60	Musculoskeletal/Connective	1.000
Heart-LV_ENTEX__H3K4me1	-2.35E-08	8.93E-08	0.60	Cardiovascular	1.000
Fetal_Brain_Female__H3K4me1	-2.77E-08	1.04E-07	0.60	CNS	1.000

HMEC_Mammary_Epithelial_Primary_Cells__H3K4me1	-2.29E-08	8.15E-08	0.61	Other	1.000
Duodenum_Smooth_Muscle__H3K36me3	-2.89E-08	1.02E-07	0.61	Musculoskeletal/Connective	1.000
Duodenum_Mucosa__H3K4me1	-2.55E-08	8.97E-08	0.61	Digestive	1.000
Fetal_Muscle_Trunk__H3K4me1	-1.78E-08	6.21E-08	0.61	Musculoskeletal/Connective	1.000
NHEK-Epidermal_Keratinocyte_Primary_Cells__H3K4me1	-1.90E-08	6.54E-08	0.61	Other	1.000
Heart-Atrial_ENTEX__H3K4me1	-9.45E-08	3.01E-07	0.62	Cardiovascular	1.000
Right_Ventricle__H3K4me1	-3.34E-08	1.05E-07	0.62	Cardiovascular	1.000
Left_Ventricle__H3K36me3	-3.77E-08	1.18E-07	0.62	Cardiovascular	1.000
Thymus__H3K4me3	-7.55E-08	2.36E-07	0.63	Blood/Immune	1.000
Primary_T_helper_cells_from_peripheral_blood__H3K36me3	-2.15E-08	6.59E-08	0.63	Blood/Immune	1.000
Right_Atrium__H3K36me3	-5.92E-08	1.80E-07	0.63	Cardiovascular	1.000
SI-Term-Ileum_ENTEX__H3K4me1	-3.61E-08	1.09E-07	0.63	Digestive	1.000
Pancreatic_Islets__H3K27ac	-6.19E-08	1.86E-07	0.63	Pancreas	1.000
Fetal_Adrenal_Gland__H3K4me1	-2.37E-08	6.81E-08	0.64	Other	1.000
Adrenal_gland_ENTEX__H3K27ac	-1.95E-08	5.57E-08	0.64	Other	1.000
Primary_T_cells_from_peripheral_blood__H3K4me3	-7.67E-08	2.18E-07	0.64	Blood/Immune	1.000
Colon-Sigm_ENTEX__H3K4me3	-1.17E-07	3.31E-07	0.64	Digestive	1.000
Placenta__H3K4me1	-2.65E-08	7.35E-08	0.64	Other	1.000
Esophagus__H3K36me3	-4.64E-08	1.29E-07	0.64	Digestive	1.000
Right_Ventricle__H3K27ac	-3.72E-08	9.87E-08	0.65	Cardiovascular	1.000
Gastric__DNase	-8.29E-08	2.12E-07	0.65	Digestive	1.000
Rectal_Smooth_Muscle__H3K27ac	-2.77E-08	7.05E-08	0.65	Musculoskeletal/Connective	1.000

Fetal_Lung__H3K4me1	-2.56E-08	6.37E-08	0.66	Other	1.000
Breast_variant_Human_Mammary_Epithelial_Cells_(vHMEC)__H3K4me1	-3.00E-08	7.37E-08	0.66	Other	1.000
Skeletal_Muscle_Male__H3K4me3	-8.25E-08	2.02E-07	0.66	Musculoskeletal/Connective	1.000
NHEK-Epidermal_Keratinocyte_Primary_Cells__H3K9ac	-5.17E-08	1.26E-07	0.66	Other	1.000
Esophagus__H3K4me1	-5.40E-08	1.31E-07	0.66	Digestive	1.000
Colon-TV_ENTEX__H3K27ac	-2.70E-08	6.49E-08	0.66	Digestive	1.000
Left_Ventricle__H3K27ac	-3.10E-08	7.35E-08	0.66	Cardiovascular	1.000
Rectal_Mucosa_Donor_29__H3K9ac	-9.93E-08	2.29E-07	0.67	Digestive	1.000
Thyroid_gland_ENTEX__H3K4me1	-2.05E-08	4.69E-08	0.67	Other	1.000
Spleen_ENTEX__H3K27ac	-2.05E-08	4.58E-08	0.67	Blood/Immune	1.000
Primary_mononuclear_cells_from_peripheral_blood__H3K36me3	-3.84E-08	8.52E-08	0.67	Blood/Immune	1.000
Primary_T_helper_memory_cells_from_peripheral_blood_1__H3K4me3	-9.58E-08	2.11E-07	0.67	Blood/Immune	1.000
Primary_B_cells_from_peripheral_blood__H3K4me3	-1.21E-07	2.65E-07	0.68	Blood/Immune	1.000
Liver__H3K27ac	-2.99E-08	6.44E-08	0.68	Liver	1.000
Primary_B_cells_from_peripheral_blood__H3K27ac	-4.62E-08	9.87E-08	0.68	Blood/Immune	1.000
Stomach_Smooth_Muscle__H3K9ac	-1.20E-07	2.52E-07	0.68	Musculoskeletal/Connective	1.000
Primary_T_regulatory_cells_from_peripheral_blood__H3K36me3	-3.50E-08	7.27E-08	0.68	Blood/Immune	1.000
Ovary__H3K36me3	-6.06E-08	1.14E-07	0.70	Other	1.000
Left_Ventricle__H3K4me1	-5.40E-08	1.00E-07	0.70	Cardiovascular	1.000
Stomach_Mucosa__H3K9ac	-9.25E-08	1.71E-07	0.71	Digestive	1.000
NHDF-Ad_Adult_Dermal_Fibroblast_Primary_Cells__H3K27ac	-7.06E-08	1.30E-07	0.71	Musculoskeletal/Connective	1.000
Artery-Tibial_ENTEX__H3K4me1	-1.18E-07	2.14E-07	0.71	Cardiovascular	1.000

Sigmoid_Colon__H3K27ac	-6.87E-08	1.23E-07	0.71	Digestive	1.000
Colonic_Mucosa__H3K9ac	-1.42E-07	2.56E-07	0.71	Digestive	1.000
HMEC_Mammary_Epithelial_Primary_Cells__H3K4me3	-1.46E-07	2.60E-07	0.71	Other	1.000
Small_Intestine__H3K4me3	-1.92E-07	3.33E-07	0.72	Digestive	1.000
Thyroid_gland_ENTEX__H3K27ac	-2.31E-08	3.95E-08	0.72	Other	1.000
Colon-Sigm_ENTEX__H3K36me3	-8.74E-08	1.47E-07	0.72	Digestive	1.000
Placenta__H3K36me3	-4.60E-08	7.50E-08	0.73	Other	1.000
Spleen__H3K4me3	-1.14E-07	1.85E-07	0.73	Blood/Immune	1.000
Primary_T_helper_naive_cells_from_peripheral_blood_2__H3K36me3	-5.46E-08	8.80E-08	0.73	Blood/Immune	1.000
NHDF-Ad_Adult_Dermal_Fibroblast_Primary_Cells__H3K9ac	-1.45E-07	2.30E-07	0.74	Musculoskeletal/Connective	1.000
Primary_Natural_Killer_cells_from_peripheral_blood__H3K4me3	-1.60E-07	2.54E-07	0.74	Blood/Immune	1.000
Esoph-Muscularis_ENTEX__H3K4me1	-3.69E-08	5.84E-08	0.74	Digestive	1.000
Skin_tissue_ENTEX__H3K4me3	-1.55E-07	2.39E-07	0.74	Other	1.000
Pancreatic_Islets__H3K4me3	-2.00E-07	3.04E-07	0.74	Pancreas	1.000
Primary_mononuclear_cells_from_peripheral_blood__H3K4me3	-2.06E-07	3.14E-07	0.74	Blood/Immune	1.000
NHDF-Ad_Adult_Dermal_Fibroblast_Primary_Cells__H3K36me3	-1.32E-07	1.96E-07	0.75	Musculoskeletal/Connective	1.000
Fetal_Muscle_Trunk__H3K4me3	-2.58E-07	3.82E-07	0.75	Musculoskeletal/Connective	1.000
Esoph-GJ_ENTEX__H3K27ac	-4.46E-08	6.55E-08	0.75	Digestive	1.000
Mammary_ENTEX__H3K36me3	-5.60E-08	8.13E-08	0.75	Other	1.000
Rectal_Mucosa_Donor_31__H3K27ac	-6.67E-08	9.65E-08	0.76	Digestive	1.000
HMEC_Mammary_Epithelial_Primary_Cells__H3K27ac	-6.41E-08	9.18E-08	0.76	Other	1.000
Foreskin_Keratinocyte_Primary_Cells_skin02__H3K4me3	-1.77E-07	2.52E-07	0.76	Other	1.000

Lung_H3K27ac	-8.94E-08	1.23E-07	0.77	Other	1.000
Pancreas_ENTEX_H3K4me1	-2.90E-08	3.93E-08	0.77	Pancreas	1.000
Duodenum_Smooth_Muscle_H3K4me3	-8.52E-08	1.14E-07	0.77	Musculoskeletal/Connective	1.000
NHEK-Epidermal_Keratinocyte_Primary_Cells_DNase	-9.90E-08	1.31E-07	0.77	Other	1.000
Prostate_ENTEX_H3K27ac	-6.22E-08	8.18E-08	0.78	Other	1.000
Primary_monocytes_from_peripheral_blood_DNase	-1.36E-07	1.72E-07	0.79	Blood/Immune	1.000
Primary_B_cells_from_peripheral_blood_H3K4me1	-4.61E-08	5.52E-08	0.80	Blood/Immune	1.000
Fetal_Muscle_Leg_H3K4me1	-5.77E-08	6.90E-08	0.80	Musculoskeletal/Connective	1.000
Fetal_Heart_H3K36me3	-1.84E-07	2.17E-07	0.80	Cardiovascular	1.000
Duodenum_Mucosa_H3K4me3	-1.36E-07	1.56E-07	0.81	Digestive	1.000
Fetal_Thymus_H3K27ac	-7.62E-08	8.76E-08	0.81	Blood/Immune	1.000
Foreskin_Keratinocyte_Primary_Cells_skin03_H3K27ac	-7.64E-08	8.73E-08	0.81	Other	1.000
Testis_ENTEX_H3K27ac	-4.62E-08	5.25E-08	0.81	Other	1.000
Adipose_Nuclei_H3K4me3	-1.25E-07	1.41E-07	0.81	Adipose	1.000
skeletal_muscle_ENTEX_H3K36me3	-4.91E-08	5.50E-08	0.81	Musculoskeletal/Connective	1.000
Primary_hematopoietic_stem_cells_G-CSF-mobilized_Male_H3K36me3	-5.07E-08	5.67E-08	0.81	Blood/Immune	1.000
Primary_Natural_Killer_cells_from_peripheral_blood_H3K4me1	-5.82E-08	6.49E-08	0.81	Blood/Immune	1.000
Primary_T_helper_memory_cells_from_peripheral_blood_2_H3K27ac	-9.66E-08	1.07E-07	0.82	Blood/Immune	1.000
Psoas_Muscle_H3K27ac	-1.07E-07	1.19E-07	0.82	Musculoskeletal/Connective	1.000
Lung_H3K36me3	-1.24E-07	1.36E-07	0.82	Other	1.000
Primary_T_helper_memory_cells_from_peripheral_blood_2_H3K4me3	-2.23E-07	2.42E-07	0.82	Blood/Immune	1.000
Adipose_Nuclei_H3K9ac	-1.46E-07	1.56E-07	0.83	Adipose	1.000

Psoas_Muscle__H3K36me3	-1.58E-07	1.69E-07	0.83	Musculoskeletal/Connective	1.000
Colon-TV_ENTEX__H3K36me3	-1.05E-07	1.12E-07	0.83	Digestive	1.000
Primary_Natural_Killer_cells_from_peripheral_blood__DNase	-1.57E-07	1.67E-07	0.83	Blood/Immune	1.000
Spleen__H3K4me1	-9.59E-08	1.02E-07	0.83	Blood/Immune	1.000
Primary_Natural_Killer_cells_from_peripheral_blood__H3K36me3	-7.88E-08	8.28E-08	0.83	Blood/Immune	1.000
Fetal_Adrenal_Gland__H3K27ac	-5.95E-08	6.25E-08	0.83	Other	1.000
Vagina_ENTEX__H3K36me3	-2.38E-07	2.49E-07	0.83	Other	1.000
Primary_T_killer_memory_cells_from_peripheral_blood__H3K4me3	-2.09E-07	2.19E-07	0.83	Blood/Immune	1.000
Primary_T_helper_naive_cells_from_peripheral_blood_2__H3K4me3	-1.79E-07	1.81E-07	0.84	Blood/Immune	1.000
NHLF_Lung_Fibroblast_Primary_Cells__H3K9ac	-2.93E-07	2.97E-07	0.84	Musculoskeletal/Connective	1.000
Pancreatic_Islets__H3K36me3	-1.72E-07	1.73E-07	0.84	Pancreas	1.000
Gastric__H3K4me1	-1.34E-07	1.35E-07	0.84	Digestive	1.000
Primary_T_helper_cells_PMA-I_stimulated__H3K27ac	-6.95E-08	7.00E-08	0.84	Blood/Immune	1.000
Liver__H3K4me3	-1.14E-07	1.14E-07	0.84	Liver	1.000
Fetal_Thymus__H3K4me1	-5.66E-08	5.65E-08	0.84	Blood/Immune	1.000
Primary_T_helper_17_cells_PMA-I_stimulated__H3K4me3	-1.94E-07	1.94E-07	0.84	Blood/Immune	1.000
Rectal_Mucosa_Donor_29__H3K27ac	-1.02E-07	9.82E-08	0.85	Digestive	1.000
Adipose_Nuclei__H3K27ac	-5.34E-08	5.13E-08	0.85	Adipose	1.000
Fetal_Lung__H3K9ac	-2.07E-07	1.96E-07	0.85	Other	1.000
Foreskin_Melanocyte_Primary_Cells_skin03__H3K36me3	-5.98E-08	5.64E-08	0.86	Other	1.000
Adrenal_gland_ENTEX__H3K4me1	-7.96E-08	7.50E-08	0.86	Other	1.000
Fetal_Heart__H3K9ac	-1.03E-07	9.71E-08	0.86	Cardiovascular	1.000

HMEC_Mammary_Epithelial_Primary_Cells__DNase	-1.37E-07	1.29E-07	0.86	Other	1.000
Nerve-Tibial_ENTEX_H3K36me3	-1.07E-07	1.00E-07	0.86	Other	1.000
Osteoblast_Primary_Cells__H3K27ac	-6.66E-08	6.17E-08	0.86	Musculoskeletal/Connective	1.000
Foreskin_Keratinocyte_Primary_Cells_skin02__H3K36me3	-1.02E-07	9.42E-08	0.86	Other	1.000
Primary_B_cells_from_cord_blood__H3K36me3	-2.61E-07	2.34E-07	0.87	Blood/Immune	1.000
Colonic_Mucosa__H3K27ac	-1.42E-07	1.26E-07	0.87	Digestive	1.000
Placenta__DNase	-1.47E-07	1.30E-07	0.87	Other	1.000
Primary_T_cells_effector_memory_enriched_from_peripheral_blood__H3K4me1	-1.23E-07	1.08E-07	0.87	Blood/Immune	1.000
Heart-LV_ENTEX_H3K4me3	-2.65E-07	2.31E-07	0.87	Cardiovascular	1.000
Fetal_Lung__H3K4me3	-2.50E-07	2.16E-07	0.88	Other	1.000
Colonic_Mucosa__H3K4me1	-1.75E-07	1.51E-07	0.88	Digestive	1.000
Primary_T_helper_memory_cells_from_peripheral_blood_1__H3K27ac	-1.42E-07	1.22E-07	0.88	Blood/Immune	1.000
Primary_T_cells_from_peripheral_blood__DNase	-1.78E-07	1.52E-07	0.88	Blood/Immune	1.000
Lung__H3K4me3	-4.03E-07	3.32E-07	0.89	Other	1.000
Fetal_Heart__H3K4me1	-5.89E-08	4.81E-08	0.89	Cardiovascular	1.000
Stomach_ENTEX_H3K27ac	-8.00E-08	6.42E-08	0.89	Digestive	1.000
Pancreatic_Islets__H3K4me1	-8.53E-08	6.81E-08	0.89	Pancreas	1.000
Skeletal_Muscle_Male__H3K36me3	-1.37E-07	1.07E-07	0.90	Musculoskeletal/Connective	1.000
Pancreas_ENTEX_H3K27ac	-6.71E-08	5.25E-08	0.90	Pancreas	1.000
Pancreas__H3K36me3	-1.76E-07	1.37E-07	0.90	Pancreas	1.000
Fetal_Thymus__DNase	-1.74E-07	1.34E-07	0.90	Blood/Immune	1.000
Breast_Myoepithelial_Primary_Cells__H3K9ac	-2.40E-07	1.85E-07	0.90	Other	1.000

Stomach_Mucosa__H3K4me3	-3.59E-07	2.76E-07	0.90	Digestive	1.000
Primary_T_helper_17_cells_PMA-I_stimulated__H3K27ac	-1.53E-07	1.16E-07	0.91	Blood/Immune	1.000
Breast_variant_Human_Mammary_Epithelial_Cells_(vHMEC)_H3K4me3	-3.52E-07	2.66E-07	0.91	Other	1.000
SI-Term-Ileum_ENTEX_H3K36me3	-2.75E-07	2.08E-07	0.91	Digestive	1.000
Primary_mononuclear_cells_from_peripheral_blood_H3K4me1	-2.95E-07	2.22E-07	0.91	Blood/Immune	1.000
Breast_variant_Human_Mammary_Epithelial_Cells_(vHMEC)_DNase	-1.80E-07	1.34E-07	0.91	Other	1.000
Gastric_H3K4me3	-4.38E-07	3.21E-07	0.91	Digestive	1.000
Primary_T_killer_memory_cells_from_peripheral_blood_H3K27ac	-1.69E-07	1.24E-07	0.91	Blood/Immune	1.000
Fetal_Thymus_H3K4me3	-3.29E-07	2.39E-07	0.92	Blood/Immune	1.000
Gastric_H3K36me3	-1.60E-07	1.15E-07	0.92	Digestive	1.000
Prostate_ENTEX_H3K4me3	-5.11E-07	3.60E-07	0.92	Other	1.000
skeletal_muscle_ENTEX_H3K4me3	-1.47E-07	1.02E-07	0.93	Musculoskeletal/Connective	1.000
Primary_T_killer_naive_cells_from_peripheral_blood_H3K4me3	-3.09E-07	2.14E-07	0.93	Blood/Immune	1.000
Adrenal_gland_ENTEX_H3K36me3	-1.34E-07	9.14E-08	0.93	Other	1.000
Primary_T_cells_from_cord_blood_DNase	-2.77E-07	1.88E-07	0.93	Blood/Immune	1.000
Gastric_H3K27ac	-2.23E-07	1.51E-07	0.93	Digestive	1.000
Rectal_Smooth_Muscle_H3K9ac	-4.42E-07	2.98E-07	0.93	Musculoskeletal/Connective	1.000
Foreskin_Melanocyte_Primary_Cells_skin01_H3K36me3	-2.15E-07	1.44E-07	0.93	Other	1.000
Primary_T_regulatory_cells_from_peripheral_blood_H3K4me3	-2.54E-07	1.68E-07	0.93	Blood/Immune	1.000
NHLF_Lung_Fibroblast_Primary_Cells_H3K27ac	-1.90E-07	1.25E-07	0.94	Musculoskeletal/Connective	1.000
Primary_T_helper_naive_cells_from_peripheral_blood_1_H3K4me3	-3.03E-07	1.96E-07	0.94	Blood/Immune	1.000
Primary_T_cells_from_cord_blood_H3K4me3	-3.98E-07	2.55E-07	0.94	Blood/Immune	1.000

Mammary_ENTEX_H3K4me1	-2.48E-07	1.59E-07	0.94	Other	1.000
Primary_T_helper_17_cells_PMA-I_stimulated_H3K4me1	-1.15E-07	7.35E-08	0.94	Blood/Immune	1.000
Spleen_ENTEX_H3K4me1	-2.50E-07	1.56E-07	0.95	Blood/Immune	1.000
Primary_T_helper_naive_cells_from_peripheral_blood_1_H3K4me1	-1.15E-07	7.19E-08	0.95	Blood/Immune	1.000
Primary_T_helper_cells_from_peripheral_blood_H3K27ac	-1.79E-07	1.11E-07	0.95	Blood/Immune	1.000
Foreskin_Keratinocyte_Primary_Cells_skin02_DNase	-1.97E-07	1.21E-07	0.95	Other	1.000
Foreskin_Fibroblast_Primary_Cells_skin01_H3K27ac	-1.60E-07	9.86E-08	0.95	Musculoskeletal/Connective	1.000
Primary_T_regulatory_cells_from_peripheral_blood_H3K4me1	-1.30E-07	7.91E-08	0.95	Blood/Immune	1.000
Colonic_Mucosa_H3K4me3	-4.08E-07	2.44E-07	0.95	Digestive	1.000
Primary_T_killer_naive_cells_from_peripheral_blood_H3K27ac	-2.69E-07	1.57E-07	0.96	Blood/Immune	1.000
Thymus_H3K4me1	-1.81E-07	1.06E-07	0.96	Blood/Immune	1.000
Pancreas_H3K4me3	-4.99E-07	2.91E-07	0.96	Pancreas	1.000
Primary_T_helper_memory_cells_from_peripheral_blood_1_H3K4me1	-1.12E-07	6.53E-08	0.96	Blood/Immune	1.000
Primary_Natural_Killer_cells_from_peripheral_blood_H3K27ac	-1.58E-07	9.19E-08	0.96	Blood/Immune	1.000
Primary_T_helper_naive_cells_from_peripheral_blood_2_H3K4me1	-1.03E-07	5.96E-08	0.96	Blood/Immune	1.000
Skeletal_Muscle_Female_H3K36me3	-1.34E-07	7.71E-08	0.96	Musculoskeletal/Connective	1.000
Colon-Sigm_ENTEX_H3K4me1	-7.11E-07	4.06E-07	0.96	Digestive	1.000
Primary_T_cells_from_cord_blood_H3K4me1	-1.99E-07	1.14E-07	0.96	Blood/Immune	1.000
Osteoblast_Primary_Cells_H3K36me3	-1.09E-07	6.19E-08	0.96	Musculoskeletal/Connective	1.000
Foreskin_Fibroblast_Primary_Cells_skin02_H3K27ac	-1.82E-07	1.03E-07	0.96	Musculoskeletal/Connective	1.000
Pancreas_H3K27ac	-2.98E-07	1.67E-07	0.96	Pancreas	1.000
Pancreas_DNase	-3.02E-07	1.69E-07	0.96	Pancreas	1.000

Primary_mononuclear_cells_from_peripheral_blood__H3K27ac	-4.12E-07	2.28E-07	0.96	Blood/Immune	1.000
Primary_T_killer_naive_cells_from_peripheral_blood__H3K4me1	-1.15E-07	6.30E-08	0.97	Blood/Immune	1.000
Duodenum_Mucosa__H3K9ac	-3.45E-07	1.89E-07	0.97	Digestive	1.000
Spleen__H3K36me3	-1.80E-07	9.64E-08	0.97	Blood/Immune	1.000
Primary_T_helper_naive_cells_from_peripheral_blood__H3K9ac	-3.27E-07	1.75E-07	0.97	Blood/Immune	1.000
Primary_T_helper_cells_from_peripheral_blood__H3K4me1	-1.12E-07	5.90E-08	0.97	Blood/Immune	1.000
Foreskin_Fibroblast_Primary_Cells_skin01__H3K36me3	-1.24E-07	6.49E-08	0.97	Musculoskeletal/Connective	1.000
Primary_T_helper_cells_PMA-I_stimulated__H3K4me3	-2.63E-07	1.37E-07	0.97	Blood/Immune	1.000
Ovary_ENTEX__H3K36me3	-6.25E-07	3.16E-07	0.98	Other	1.000
Primary_T_cells_from_peripheral_blood__H3K27ac	-1.91E-07	9.51E-08	0.98	Blood/Immune	1.000
Spleen_ENTEX__H3K36me3	-1.02E-07	5.09E-08	0.98	Blood/Immune	1.000
Adrenal_gland_ENTEX__H3K4me3	-3.87E-07	1.91E-07	0.98	Other	1.000
Thyroid_gland_ENTEX__H3K4me3	-4.53E-07	2.22E-07	0.98	Other	1.000
NHLF_Lung_Fibroblast_Primary_Cells__H3K36me3	-3.12E-07	1.52E-07	0.98	Musculoskeletal/Connective	1.000
Primary_T_cells_effector_memory_enriched_from_peripheral_blood__H3K27ac	-2.15E-07	1.04E-07	0.98	Blood/Immune	1.000
Primary_T_helper_naive_cells_from_peripheral_blood_1__H3K27ac	-3.61E-07	1.73E-07	0.98	Blood/Immune	1.000
Thymus__H3K27ac	-3.18E-07	1.50E-07	0.98	Blood/Immune	1.000
Lung_ENTEX__H3K4me3	-6.39E-07	2.99E-07	0.98	Other	1.000
Primary_B_cells_from_peripheral_blood__H3K36me3	-1.26E-07	5.67E-08	0.99	Blood/Immune	1.000
Primary_T_helper_cells_PMA-I_stimulated__H3K4me1	-1.17E-07	5.22E-08	0.99	Blood/Immune	1.000
Primary_T_helper_naive_cells_from_peripheral_blood_2__H3K27ac	-1.97E-07	8.66E-08	0.99	Blood/Immune	1.000
Fetal_Heart__H3K4me3	-2.95E-07	1.28E-07	0.99	Cardiovascular	1.000

Primary_T_cells_from_peripheral_blood__H3K4me1	-1.60E-07	6.90E-08	0.99	Blood/Immune	1.000
Primary_T_killer_memory_cells_from_peripheral_blood__H3K4me1	-1.79E-07	7.74E-08	0.99	Blood/Immune	1.000
Primary_T_regulatory_cells_from_peripheral_blood__H3K27ac	-1.83E-07	7.69E-08	0.99	Blood/Immune	1.000
Primary_T_helper_memory_cells_from_peripheral_blood_2__H3K4me1	-1.49E-07	6.25E-08	0.99	Blood/Immune	1.000
Foreskin_Fibroblast_Primary_Cells_skin02__H3K36me3	-1.77E-07	7.30E-08	0.99	Musculoskeletal/Connective	1.000
Primary_T_killer_naive_cells_from_peripheral_blood__H3K9ac	-6.01E-07	2.32E-07	1.00	Blood/Immune	1.000
Colon-TV_ENTEX__H3K4me3	-6.86E-07	2.38E-07	1.00	Digestive	1.000
Prostate_ENTEX__H3K36me3	-1.29E-06	3.83E-07	1.00	Other	1.000
Pancreas_ENTEX__H3K4me3	-7.07E-07	2.08E-07	1.00	Pancreas	1.000
Testis_ENTEX__H3K36me3	-1.14E-06	2.90E-07	1.00	Other	1.000

Table A8. Results from the central nervous system (Cahoy) type of gene expression

Name	Coefficient	Coefficient se	Coefficient p	Coefficient p_FDR
Oligodendrocyte	7.73E-09	9.45E-09	0.207	0.357
Astrocyte	5.31E-09	8.26E-09	0.260	0.357
Neuron	3.05E-09	8.3E-09	0.357	0.357

Table A9. Results from the ImmGen dataset

Name	Coefficient	Coefficient se	Coefficient p	Coefficient p_FDR
ILC2.SI	2E-08	9E-09	1E-02	8E-01
NK.Sp	2E-08	1E-08	1E-02	8E-01
GN.UrAc.PC	2E-08	9E-09	2E-02	8E-01
BA.Sp	2E-08	1E-08	2E-02	8E-01
NK.49H-.Sp	2E-08	9E-09	3E-02	8E-01
T.4Mem.Sp	2E-08	9E-09	3E-02	8E-01
T.8Eff.Sp.OT1.d6.LisOva	2E-08	1E-08	3E-02	8E-01
T.8Eff.Sp.OT1.d6.VSVova	2E-08	1E-08	3E-02	8E-01
Tgd.vg2-.Sp.TCRbko	2E-08	9E-09	3E-02	8E-01
T.DPsm.Th	2E-08	1E-08	3E-02	8E-01
GN.BI	2E-08	9E-09	4E-02	8E-01
GN.BM	1E-08	8E-09	4E-02	8E-01
Tgd.vg2+24ahi.Th	2E-08	1E-08	4E-02	8E-01
GN.Arth.BM	2E-08	9E-09	5E-02	8E-01
GN.Thio.PC	2E-08	1E-08	5E-02	8E-01
MF.Microglia.CNS	1E-08	9E-09	5E-02	8E-01
BA.BI	2E-08	9E-09	5E-02	8E-01
T.DP.Th.v2	1E-08	9E-09	5E-02	8E-01

GN.Arth.SynF	2E-08	1E-08	6E-02	8E-01
NK.H+.MCMV7.Sp	1E-08	9E-09	6E-02	8E-01
T.4.Pa.BDC	1E-08	9E-09	6E-02	8E-01
BEC.SLN.OT	1E-08	9E-09	7E-02	8E-01
T.8Eff.Sp.OT1.d15.VSVova	2E-08	1E-08	7E-02	8E-01
T.8Eff.Sp.OT1.d8.VSVova	1E-08	9E-09	8E-02	8E-01
preB.FrD.FL	1E-08	9E-09	8E-02	8E-01
ABD.TR.14w.B6	1E-08	8E-09	8E-02	8E-01
T.8Eff.Sp.OT1.d15.LisOva	1E-08	1E-08	9E-02	8E-01
SC.LT34F.BM	1E-08	9E-09	9E-02	8E-01
SC.STSL.FL	1E-08	9E-09	1E-01	8E-01
T.4Eff49d+11a+.Sp.d8.LCMV	1E-08	9E-09	1E-01	8E-01
T.4FP3+25+.Sp	1E-08	9E-09	1E-01	8E-01
T.8Nve.PP	1E-08	1E-08	1E-01	8E-01
Tgd.Sp	1E-08	1E-08	1E-01	8E-01
LEC.SLN.OT	1E-08	9E-09	1E-01	8E-01
T.4Mem44h62I.LN	1E-08	9E-09	1E-01	8E-01
T.8Nve.Sp	1E-08	9E-09	1E-01	8E-01
preT.ETP-2A.Th	1E-08	9E-09	1E-01	8E-01
B.T2.Sp	1E-08	9E-09	1E-01	8E-01
Tgd.vg2-.act.Sp	1E-08	9E-09	1E-01	8E-01
T.DP.Th	1E-08	1E-08	1E-01	8E-01

Tgd.vg5-.IEL	1E-08	9E-09	1E-01	8E-01
Tgd.vg5-.act.IEL	1E-08	9E-09	1E-01	8E-01
T.8Mem.Sp.OT1.d45.VSVOva	1E-08	1E-08	1E-01	8E-01
SC.LTSL.FL	1E-08	9E-09	1E-01	8E-01
Tgd.vg2+24ahi.e17.Th.v2	1E-08	1E-08	1E-01	8E-01
NK.MCMV7.Sp	1E-08	1E-08	1E-01	8E-01
EO.AT.v2	1E-08	9E-09	2E-01	8E-01
BEC.SLN	9E-09	9E-09	2E-01	8E-01
Tgd.vg2+.Sp.TCRbko	1E-08	1E-08	2E-01	8E-01
Mo.6C-II-.BL	9E-09	1E-08	2E-01	8E-01
T.8Nve.MLN	1E-08	1E-08	2E-01	8E-01
Tgd.vg5+.IEL	1E-08	1E-08	2E-01	8E-01
NKT.44+NK1.1-.Th	8E-09	9E-09	2E-01	8E-01
preT.ETP.Th	1E-08	1E-08	2E-01	8E-01
Mo.6+2-.BL	9E-09	9E-09	2E-01	8E-01
NK.b2m-.Sp	9E-09	9E-09	2E-01	8E-01
B.FrF.BM	9E-09	1E-08	2E-01	8E-01
Tgd.vg4+24ahi.e17.Th	9E-09	1E-08	2E-01	8E-01
Tgd.vg2+.act.Sp	9E-09	1E-08	2E-01	8E-01
T.8Mem.Sp.OT1.d106.VSVOva	9E-09	1E-08	2E-01	8E-01
B.Fo.Sp	8E-09	1E-08	2E-01	8E-01
B.Fo.LN	8E-09	9E-09	2E-01	8E-01

St.31-38-44-.SLN	7E-09	8E-09	2E-01	8E-01
MF.480int.LV.Naive	7E-09	9E-09	2E-01	8E-01
T.4Mem.LN	7E-09	9E-09	2E-01	8E-01
NKT.4+.Lv	7E-09	9E-09	2E-01	8E-01
T.4Nve.MLN	9E-09	1E-08	2E-01	8E-01
MLP.BM	8E-09	1E-08	2E-01	8E-01
DC.pDC.8+.Sp	7E-09	9E-09	2E-01	8E-01
T.4Mem44h62l.Sp	7E-09	9E-09	2E-01	8E-01
proB.FrA.BM	8E-09	1E-08	2E-01	8E-01
preB.FrD.BM	7E-09	9E-09	2E-01	8E-01
Tgd.Th	7E-09	9E-09	2E-01	8E-01
B.T1.Sp	7E-09	9E-09	2E-01	8E-01
Tgd.vg3+24ahi.e17.Th	7E-09	1E-08	2E-01	8E-01
FRC.MLN	6E-09	8E-09	2E-01	8E-01
CD4Control	6E-09	9E-09	2E-01	8E-01
T.4SP24int.Th	7E-09	1E-08	2E-01	8E-01
Tgd.vg2+24ahi.e17.Th	6E-09	9E-09	2E-01	8E-01
FRC.Cad11.WT.v2	6E-09	9E-09	2E-01	8E-01
NK.DAP10-.Sp	6E-09	9E-09	3E-01	8E-01
NK.49CI+.Sp	6E-09	9E-09	3E-01	8E-01
MF.11cloSer.SI	6E-09	1E-08	3E-01	8E-01
T.4.PLN.BDC	7E-09	1E-08	3E-01	8E-01

MF.480hi.LV.Naive	5E-09	9E-09	3E-01	8E-01
T.4Mem49d+11a+.Sp.d30.LCMV	5E-09	9E-09	3E-01	8E-01
T.DP69+.Th.v2	5E-09	9E-09	3E-01	8E-01
NK.H+.MCMV1.Sp	6E-09	1E-08	3E-01	8E-01
BEC.MLN	5E-09	9E-09	3E-01	8E-01
CD4.5h.LN	6E-09	1E-08	3E-01	8E-01
B.FrE.BM	5E-09	9E-09	3E-01	8E-01
CD8.96h.LN	5E-09	9E-09	3E-01	8E-01
MF.Sbcaps.SLN	4E-09	8E-09	3E-01	8E-01
MF.11c-11b+.Lu	5E-09	1E-08	3E-01	8E-01
NKT.4+.Sp	5E-09	1E-08	3E-01	8E-01
T.4SP24-.Th	5E-09	1E-08	3E-01	8E-01
T.8Mem.LN	5E-09	1E-08	3E-01	8E-01
T.8Mem.Sp.OT1.d100.LisOva	5E-09	1E-08	3E-01	8E-01
MC.PC	4E-09	8E-09	3E-01	8E-01
NKT.44-NK1.1-.Th	4E-09	9E-09	3E-01	8E-01
T.4.LN.BDC	5E-09	1E-08	3E-01	8E-01
CD8.1h.LN	5E-09	1E-08	3E-01	8E-01
MF.11cloSer.Salm3.SI	4E-09	9E-09	3E-01	8E-01
SC.STSL.BM	4E-09	8E-09	3E-01	8E-01
Tgd.vg2+.Sp	4E-09	1E-08	3E-01	8E-01
B.T3.Sp	5E-09	1E-08	3E-01	8E-01

T.8Nve.Sp.OT1	4E-09	9E-09	3E-01	8E-01
DC.pDC.8+.SLN	3E-09	8E-09	3E-01	8E-01
T.8Eff.Sp.OT1.d8.LisOva	4E-09	9E-09	3E-01	8E-01
LEC.SLN.CFA.d6.v2	3E-09	8E-09	3E-01	8E-01
T.4SP69+.Th	4E-09	1E-08	3E-01	8E-01
Mo.Lu	4E-09	9E-09	3E-01	8E-01
proB.FrBC.BM	4E-09	9E-09	3E-01	8E-01
T.4+8int.Th	4E-09	9E-09	3E-01	8E-01
preB.FrC.BM	4E-09	1E-08	3E-01	8E-01
T.8Mem.Sp.OT1.d45.LisOva	4E-09	1E-08	3E-01	8E-01
T.4Nve44-49d-11a-.Sp	4E-09	9E-09	3E-01	8E-01
T.4Nve.Sp	4E-09	9E-09	3E-01	8E-01
Mo.6+2+.SLN	4E-09	9E-09	4E-01	8E-01
T.8Eff.Sp.OT1.d10.LisOva	4E-09	1E-08	4E-01	8E-01
B1a.PC	3E-09	9E-09	4E-01	8E-01
proB.FrBC.FL	3E-09	1E-08	4E-01	8E-01
T.DP.69-.e17.Th.v2	3E-09	9E-09	4E-01	8E-01
Mo.6C-IIint.BI	3E-09	1E-08	4E-01	8E-01
MEChi.GFP+.Adult.KO	2E-09	7E-09	4E-01	8E-01
NKT.44+NK1.1+.Th	3E-09	9E-09	4E-01	8E-01
NKT.4-.Lv	3E-09	9E-09	4E-01	8E-01
Fi.MTS15+.Th	3E-09	9E-09	4E-01	8E-01

T.8SP24int.Th	2E-09	8E-09	4E-01	8E-01
B1a.Sp.v2	2E-09	8E-09	4E-01	8E-01
NKT.4-.Sp	2E-09	1E-08	4E-01	8E-01
MF.103-11b+.Salm3.SI	2E-09	8E-09	4E-01	8E-01
proB.CLP.FL	2E-09	1E-08	4E-01	8E-01
T.DP69+.Th	2E-09	1E-08	4E-01	8E-01
LEC.SLN	2E-09	9E-09	4E-01	8E-01
T.4FP3-.Sp	2E-09	1E-08	4E-01	8E-01
NK.DAP12-.Sp	2E-09	1E-08	4E-01	8E-01
DN.SLN.CFA.d6.v2	2E-09	8E-09	4E-01	8E-01
CD19Control	2E-09	1E-08	4E-01	8E-01
CD4.1h.LN	2E-09	9E-09	4E-01	8E-01
Tgd.vg4+24alo.e17.Th	2E-09	1E-08	4E-01	8E-01
Tgd.vg5+.act.IEL	2E-09	1E-08	4E-01	8E-01
DC.pDC.8-.Sp	1E-09	8E-09	4E-01	8E-01
Eo.BL.v2	1E-09	8E-09	4E-01	8E-01
T.8Nve.LN	2E-09	1E-08	4E-01	8E-01
T.DPbl.Th	1E-09	8E-09	4E-01	8E-01
Mo.6C-II-.BM	9E-10	1E-08	5E-01	8E-01
DC.Iihilang+103-11b+.SLN	7E-10	9E-09	5E-01	8E-01
proB.CLP.BM	8E-10	1E-08	5E-01	8E-01
Tgd.vg1+vd6-24ahi.Th	8E-10	9E-09	5E-01	8E-01

NK.CD127-.Sp	5E-10	9E-09	5E-01	8E-01
FRC.SLN.CFA.d6.v2	4E-10	8E-09	5E-01	8E-01
FRC.SLN.OT	4E-10	8E-09	5E-01	8E-01
LN.TR.14w.B6	4E-10	9E-09	5E-01	8E-01
Tgd.vg1+vd6+24alo.Th	4E-10	9E-09	5E-01	8E-01
Mo.6+2+.MLN	2E-10	9E-09	5E-01	8E-01
DC.8-4-11b+.Sp	4E-11	9E-09	5E-01	8E-01
preT.DN3A.Th	1E-11	9E-09	5E-01	8E-01
Tgd.vg1+vd6+24ahi.Th	3E-12	9E-09	5E-01	8E-01
LEC.MLN	-1E-10	9E-09	5E-01	8E-01
ILC1.CD127+.Sp	-2E-10	9E-09	5E-01	8E-01
T.4Nve.LN	-2E-10	1E-08	5E-01	8E-01
MF.AT.v2	-5E-10	9E-09	5E-01	8E-01
B.GC.Sp	-6E-10	1E-08	5E-01	8E-01
Ep.5wk.MEChi.Th	-4E-10	7E-09	5E-01	8E-01
Tgd.vg2-.Sp	-7E-10	9E-09	5E-01	8E-01
FRC.SLN.v2	-7E-10	8E-09	5E-01	8E-01
B1b.PC	-8E-10	1E-08	5E-01	8E-01
ILC1.CD49b-.Lv	-9E-10	1E-08	5E-01	8E-01
MLP.FL	-9E-10	1E-08	5E-01	8E-01
T.8Eff.Sp.OT1.d5.VSVOva	-9E-10	1E-08	5E-01	8E-01
preT.DN2A.Th	-9E-10	1E-08	5E-01	8E-01

T.4int8+.Th	-8E-10	9E-09	5E-01	8E-01
T.4Nve.PP	-9E-10	1E-08	5E-01	8E-01
LEC.SLN.v2	-9E-10	8E-09	5E-01	8E-01
DC.pDC.8+.MLN	-1E-09	8E-09	5E-01	8E-01
T.8Eff.Tbet+.Sp.OT1.d6LisOVA	-1E-09	1E-08	6E-01	8E-01
T.8EffKLRG1+CD127-.Sp.d8.LisOVA	-1E-09	9E-09	6E-01	8E-01
CD8.48h.LN	-1E-09	1E-08	6E-01	8E-01
MC.digest.PC	-1E-09	8E-09	6E-01	8E-01
MF.F480hi.ctrl.PC	-1E-09	9E-09	6E-01	8E-01
MC.Tr	-1E-09	8E-09	6E-01	8E-01
Tgd.vg5+24ahi.Th	-2E-09	1E-08	6E-01	8E-01
B1a.Sp	-2E-09	1E-08	6E-01	8E-01
NK.49H+.Sp	-2E-09	1E-08	6E-01	8E-01
CD4.CTR.LN	-2E-09	9E-09	6E-01	8E-01
ILC3.NKp46+.Rorgthi.SI	-2E-09	8E-09	6E-01	8E-01
T.8Mem.Sp	-2E-09	9E-09	6E-01	8E-01
SC.CMP.BM.DR	-2E-09	1E-08	6E-01	8E-01
MC.To	-2E-09	8E-09	6E-01	8E-01
proB.FrA.FL	-2E-09	1E-08	6E-01	8E-01
Mo.6C+II-.BM	-3E-09	1E-08	6E-01	8E-01
B.Mem.Sp.v2	-2E-09	9E-09	6E-01	8E-01
MEChi.GFP+.Adult	-2E-09	7E-09	6E-01	8E-01

MF.Thio5.II+480lo.PC	-3E-09	1E-08	6E-01	8E-01
DN.SLN.v2	-2E-09	8E-09	6E-01	8E-01
Mo.6+2+.BL	-3E-09	9E-09	6E-01	8E-01
NK.49Cl-.Sp	-2E-09	9E-09	6E-01	8E-01
Tgd.vg2+24alo.Th	-3E-09	9E-09	6E-01	8E-01
DC.LC.Sk	-2E-09	9E-09	6E-01	8E-01
B.Fo.MLN	-3E-09	1E-08	6E-01	8E-01
Mo.6C+II-.Bl	-3E-09	9E-09	6E-01	8E-01
MF.II+480lo.PC	-3E-09	1E-08	6E-01	8E-01
CD4.96h.LN	-3E-09	1E-08	6E-01	8E-01
NK.MCMV1.Sp	-3E-09	9E-09	6E-01	8E-01
T.8SP69+.Th	-4E-09	1E-08	6E-01	8E-01
B.FrE.FL	-3E-09	8E-09	7E-01	8E-01
Tgd.vg1+vd6-24alo.Th	-3E-09	8E-09	7E-01	8E-01
MF.Lu	-4E-09	9E-09	7E-01	8E-01
DC.8-4-11b+.SLN	-4E-09	9E-09	7E-01	8E-01
DC.11b+.AT.v2	-4E-09	9E-09	7E-01	9E-01
DC.4+.SLN	-5E-09	9E-09	7E-01	9E-01
Ep.8wk.MEChi.Th	-4E-09	7E-09	7E-01	9E-01
CD8.5h.LN	-6E-09	1E-08	7E-01	9E-01
T.8SP24-.Th	-6E-09	1E-08	7E-01	9E-01
MC.Sk	-5E-09	8E-09	7E-01	9E-01

GN.BI.v2	-4E-09	8E-09	7E-01	9E-01
T.8Eff.Tbet-.Sp.OT1.d6LisOVA	-6E-09	1E-08	7E-01	9E-01
T.8Eff.Sp.OT1.24hr.LisOva	-5E-09	9E-09	7E-01	9E-01
NK.CD49b+.Lv	-6E-09	1E-08	7E-01	9E-01
preT.DN3-4.Th	-6E-09	1E-08	7E-01	9E-01
MC.Es	-5E-09	8E-09	7E-01	9E-01
Ep.MEChi.Th	-4E-09	7E-09	7E-01	9E-01
Tgd.vg3+24alo.e17.Th	-6E-09	9E-09	7E-01	9E-01
DC.4+.MLN	-5E-09	8E-09	7E-01	9E-01
Mo.6C+II+.Bl	-6E-09	9E-09	7E-01	9E-01
Ep.5wk.MEC.Sca1+.Th	-5E-09	7E-09	7E-01	9E-01
FRC.SLN	-6E-09	8E-09	8E-01	9E-01
CD8.CTR.LN	-7E-09	1E-08	8E-01	9E-01
Fi.Sk	-6E-09	8E-09	8E-01	9E-01
MF.II-480hi.PC	-6E-09	8E-09	8E-01	9E-01
Mo.6C+II-.LN	-7E-09	1E-08	8E-01	9E-01
preT.DN2.Th	-7E-09	1E-08	8E-01	9E-01
DC.Iihilang-103-11blo.SLN	-6E-09	8E-09	8E-01	9E-01
MF.Thio5.II+480int.PC	-6E-09	9E-09	8E-01	9E-01
MF.F480hi.Gata6ko.PC	-6E-09	8E-09	8E-01	9E-01
NK.CD127-.SI	-8E-09	1E-08	8E-01	9E-01
Ep.5wk.MEClo.Th	-5E-09	6E-09	8E-01	9E-01

preT.DN2-3.Th	-7E-09	9E-09	8E-01	9E-01
MF.103-11b+.Lu	-6E-09	8E-09	8E-01	9E-01
T.8Eff.Sp.OT1.48hr.LisOva	-8E-09	1E-08	8E-01	9E-01
MF.Medl.SLN	-8E-09	9E-09	8E-01	9E-01
MF.RP.Sp	-7E-09	8E-09	8E-01	9E-01
MF.Alv.Lu	-7E-09	8E-09	8E-01	9E-01
SC.MPP34F.BM	-9E-09	1E-08	8E-01	9E-01
SC.ST34F.BM	-9E-09	9E-09	8E-01	9E-01
B.Fo.PC	-8E-09	9E-09	8E-01	9E-01
T.8Eff.Sp.OT1.12hr.LisOva	-1E-08	1E-08	8E-01	9E-01
preT.DN2B.Th	-8E-09	8E-09	8E-01	9E-01
ILC1.CD127+.SI	-9E-09	9E-09	8E-01	9E-01
ILC3.NKp46-.4+.SI	-9E-09	8E-09	9E-01	9E-01
MF.Thio5.II-480int.PC	-9E-09	8E-09	9E-01	9E-01
DC.103+11b-.Lu	-1E-08	9E-09	9E-01	9E-01
MF.BM	-1E-08	1E-08	9E-01	9E-01
Mo.6C-II+.Bl	-8E-09	8E-09	9E-01	9E-01
MEChi.GFP-.Adult	-7E-09	7E-09	9E-01	9E-01
preT.DN3B.Th	-1E-08	1E-08	9E-01	9E-01
DC.8-4-11b-.MLN	-9E-09	8E-09	9E-01	9E-01
T.8MemKLRG1-CD127+.Sp.d8.LisOVA	-1E-08	9E-09	9E-01	9E-01
ILC3.NKp46-.4-.SI	-9E-09	8E-09	9E-01	9E-01

DC.8-.Th	-1E-08	8E-09	9E-01	9E-01
MF.103-11b+.SI	-1E-08	9E-09	9E-01	9E-01
SC.CDP.BM	-1E-08	9E-09	9E-01	9E-01
DC.103+11b-.Lv	-1E-08	8E-09	9E-01	9E-01
Ep.8wk.MEClo.Th	-8E-09	6E-09	9E-01	9E-01
DC.Ilhilang-103-11b+.SLN	-1E-08	8E-09	9E-01	9E-01
MF.PPAR-.Lu	-1E-08	8E-09	9E-01	9E-01
Ep.8wk.CEC.Sca1+.Th	-1E-08	7E-09	9E-01	9E-01
SC.MDP.BM	-1E-08	1E-08	9E-01	9E-01
T.ISP.Th	-1E-08	1E-08	9E-01	9E-01
CD4.48h.LN	-1E-08	9E-09	9E-01	9E-01
T.DN4.Th	-1E-08	1E-08	9E-01	9E-01
MF.Thio5.II-480hi.PC	-1E-08	8E-09	9E-01	9E-01
DC.8+.Th	-1E-08	8E-09	9E-01	9E-01
Ep.8wk.CEChi.Th	-1E-08	7E-09	9E-01	9E-01
DC.103-11b+F4_80lo.Kd	-1E-08	9E-09	9E-01	9E-01
CD4.24h.LN	-2E-08	1E-08	9E-01	9E-01
DC.11b-.AT.v2	-1E-08	9E-09	9E-01	9E-01
DC.4+.Sp.ST	-1E-08	8E-09	9E-01	9E-01
SC.GMP.BM	-2E-08	1E-08	1E+00	9E-01
DC.8-4-11b-.SLN	-1E-08	8E-09	1E+00	9E-01
DC.Ilhilang+103+11blo.SLN	-1E-08	8E-09	1E+00	9E-01

B.MZ.Sp	-2E-08	9E-09	1E+00	9E-01
DC.103-11b+24+.Lu	-1E-08	8E-09	1E+00	9E-01
DC.8+.SLN	-2E-08	9E-09	1E+00	9E-01
SC.MEP.BM	-2E-08	1E-08	1E+00	9E-01
MF.169+11chi.SLN	-2E-08	9E-09	1E+00	9E-01
CD8.24h.LN	-2E-08	1E-08	1E+00	9E-01
DC.8-4-11b-.Sp	-2E-08	8E-09	1E+00	9E-01
DC.8-4-11b+.MLN	-2E-08	8E-09	1E+00	9E-01
DC.8+.Sp.ST	-2E-08	8E-09	1E+00	9E-01
DC.8+.MLN	-2E-08	8E-09	1E+00	9E-01

초록

노화에 대한 관심의 증가는, 노화를 정의하는 다양한 방법을 산출했다.

최근 기술의 발전으로 뇌 연령 추정이라는 새로운 노화의 추정 방법이 등장했다. 뇌 연령은 뇌영상에서 얻어진 자료를 기반으로 추정되는 것이 일반적으로, T1 강조 뇌 자기공명영상이 대표적인 뇌영상 자료로써 추정에 활용되고 있다. 지난 10년 간, 뇌연령이 사람들의 개인적인 뇌 노화를 측정하는데 유용하고, 임상적인 지표로도 활용될 수 있음이 증명되었다. 하지만, 뇌 연령에 추정에 대한 방법은 여전히 수렴되지 않았고, 뇌 연령이라는 뇌 노화의 대리지표의 생물학적 타당도 역시 명확히 규명되지 않았다. 따라서 뇌 연령이 뇌 노화를 반영하기 위한 강건한 지표가 되기 위해서 추정방법의 개선 및 비교와 이에 해당하는 생물학적 타당도를 확보할 필요성이 있다.

이 논문은 뇌연령에 대한 2개의 연구로 구성이 되어있다. 첫 번째 논문은 T1-강조 영상과 확산 강조 영상을 활용한 다중 모달리티 기반 뇌 영상 추정 방법을 제공하고, 7개의 뇌 연령 추정방법에 대한 성능을 비교한 연구를 수행하였다. 연구참여자는 UK Biobank의 34,430명의 T1-강조 영상 및 확산 강조 영상 모두 있는 사람들을 대상으로, 4,560명의 질병이 없는 건강한 사람들을 대상으로 뇌연령이 산출된 후, 나머지 29,870명의 참가자들에게도 적용되었다. 154개의 T1-강조 영상과 225개의 확산 강조

영상이 뇌영상 을 추정하는데 사용되었다. 분석 결과, XGBoost가 가장 좋은 성능을 나타냈다(MAE = 3.50). XGBoost로 추정된 뇌연령은 다양한 건강지표들과 관련이 있는 것으로 나타났다.

두 번째 연구는 XGBoost로 추정된 뇌연령에 대한 유전학적 결과를 제공한다. 뇌 연령이 추정된 UK Biobank 34,430명 중, 유전형 데이터가 확보된 29,909명의 European ancestry를 대상으로 분석이 수행되었다. 먼저 전장유전체분석이 수행되었고, 이후에 발견된 유전변이에 대한 후-전장유전체 분석이 수행되었다. 뇌연령과 관련 있는 유전변이를 탐색하기 위하여 BOLT-LMM¹⁰이 수행되었고, $P < 5 \times 10^{-8}$ 수준에서 7개의 독립적인 변이가 확보되었다. 7개 중 2개의 변이가 뇌연령과 관련이 있는 잠재적인과 변이로 간주되었다: rs35771878 및 rs2316768. 해당 변이들은 각각 TLR1 유전자와 MAPT-AS1¹¹ 연결되었는데, 이는 뇌 노화와 관련이 있는 유전자들로 나타났다. 이 후 LDSC 분석을 통해 단일염기다형성 기반 21% 유전력을 규명하였고, 전장유전체에서 분석된 변이들은 중추신경계 조직에서 발현되는 것을 확인하였다. 마지막으로 유전상관분석 결과 뇌 연령은 제 2형 당뇨와 유전적으로 상관이 있는 것을 확인하였다.

감사의 글

영원할 것 같았던 박사학위 과정이 끝나가고 있습니다. 사실, 학위논문을 쓰는 것보다 이 감사의 글을 어떻게 써야할 지에 대해서 더 오래 고민했던 것 같습니다. 아직도 어떻게 말을 전해야 할지 잘 모르겠지만, 지면관계상 제가 박사 과정을 시작하고, 지내고, 마치는데 있어서 도움을 주신 분들께 주로 감사의 말을 전달하게 되었습니다.

이동영 교수님은 제가 박사과정을 시작하고 마무리하는데 가장 큰 울림을 주셨습니다. 교수님께 치매와 알츠하이머병을 배웠던 2년은 제 인생에서 가장 영광스러웠던 시간이었습니다. AAIC 2016 구연발표를 준비하면서 오피스에서 해주셨던 말씀과 네트워크 라운지에 앉아서 자신 있게 발표하는 Jagust 연구실 소속의 어느 연구원의 모습을 보며 해주신 격려 말씀은 아직까지 제 마음 속 깊이 남아있습니다. 교수님의 말씀 덕분에 자신 있게 박사학위를 시작할 수 있었고, 이렇게 잘 마무리하게 된 것 같습니다. 많이 촌스러웠던 제가, 교수님 덕분에 해외학회도 가보고 해외여행도 가게 되었네요. 그 후엔 잘 다니고 있습니다. AAIC도 2번은 더 다녀왔답니다. 아마 그 때 그 경험이 없었던라면 도전하지 않고 계속 위축된 채로 지내고 있었을지도 모르겠습니다. 제가 더 큰 꿈을 꾸기 시작한 것, 자신감을 가질 수 있었던 것, 치매연구를 사랑하게 된 것 모두 교수님께 배운 덕분이라고 생각하고, 항상 교수님께 감사하고 있습니다. 졸업 후 좋은 연구를 통해서 교수님께 보답할 수 있길 진심으로 소원합니다.

명우재 교수님과 원홍희 교수님, 그리고 김소연 선생님 덕분에 제가 감히 유전체 연구를 수행할 수 있었습니다. 세 분께 깊은 감사를 전합니다. 명우재 교수님, 벌써 교수님과 인연을 맺은 지도 많은 시간이 흘렀네요. 유전학에 대해서 일자무식이었던 저에게 큰 기회를 주셔서 감사합니다. 중간에 저를 포기할 법한 시간들도 있었을 텐데 포기하지 않고 함께해주셔서 감사합니다. 덕분에 제가 용기내서 더 배우고 전진하려고 노력했던 것 같습니다. 그리고 그 노력이 좋은 연구 결과로 이어져서 아주 행복했습니다. 앞으로도 계속 좋은 연구를 함께 할 수 있었으면 좋겠습니다. 원홍희 교수님, 방탈출게임에서 저를 유일하게 구해 주신

그날부터 교수님을 전적으로 신뢰하고 있습니다. 농담을 빌려 표현했지만 제 마음은 진심인 거 아시죠? 엄밀히 말하면 제게 유전체 분석을 공부시키고 논문을 쓰게 하는 것이 교수님께는 큰 부담이었을 텐데, 저를 처음부터 지금까지 계속 신뢰하고 이끌어 주셔서 항상 감사하면서 죄송스럽습니다. 앞으로도 꾸준히 공부해서 제 뜻은 할 수 있는 사람이 되도록 노력하겠습니다. 일원동에서 많이 배우겠습니다! 제가 표현은 잘 하지 않지만 두 분을 많이 좋아하고 존경합니다. 단순히 좋은 연구가 결과물로 나와서 하는 소리가 아닙니다. 연구를 진행하는 과정 속에서 교수님들께 많은 것들을 보고 배우고 생각하는 시간들이 저에게 정말 소중한 시간입니다. 앞으로도 잘 부탁드리겠습니다! 김소연 선생님, 제 실질적인 유전체 사수이신 선생님 덕분에 무식하지만 용감하게 유전체 분석으로 박사 학위논문 연구를 시도할 수 있었습니다. 선생님은 항상 저를 부끄럽게 만드시는 것 같습니다. 세밀함이 부족한 제가 선생님을 보면서 얼마나 부러움과 부끄러움을 느끼는지, 하지만 역설적으로 제가 세밀하지 않아서 오히려 선생님과 협력연구가 더 재미있는 것 같습니다. 물론 선생님께서는 답답한 순간이 더 많으셨을 수도 있겠네요. 죄송하고 항상 감사합니다! 앞으로도 많은 가르침 부탁드리겠습니다. 그리고 원っぱ 식구들께, 제가 눈치 없이 컴퓨터 자원을 많이 사용했습니다. 양해해 주셔서 감사하고 죄송했습니다!

곽세열 교수님은 좋은 학위논문의 주제를 떠올리게 해주신 분입니다. 뇌의 노화와 연령이라는 이야기를 교수님과 하고 난 뒤, 제가 이 개념에 사로잡혔던 것 같습니다. 덕분에 즐거운 논문을 재밌게 쓸 수 있었습니다. 물론 아직까지 뇌연령이라는 개념이 과연 타당한지에 대해서는 자신 있게 설명하긴 어려울 것 같습니다. AAIC 2022 포스터 세션에서 뇌 연령이 예년에 비해 많이 등장했던 것 같습니다. 특히 바르셀로나 학자들이 이 분야에 요즘 관심을 갖고 있던 것 같은데, 질문을 해보면 그 사람들도 역시 현상학적인 설명만을 할 뿐, 그 개념의 의미와 타당도에 대해서는 아직까지 유효한 답을 찾진 못한 것 같습니다. 그래서 더 재밌는 것 같습니다. 앞으로 같이 찾아갈 수 있었으면 좋겠습니다. 교수님과 함께 했던 시간, 저는 참 즐거웠습니다. 교수님도 그러셨으면 좋겠네요. 참으로 존경하고 좋아합니다! 관심 분야는 유사할 수 있어도 보는 시야와 깊이가 참 다른 것 같아서 더 재미있습니다. 물론 제가 깊이가 많이 없죠. 교수님의 깊이가 너무

부립습니다! 교수님 덕분에 제 박사과정의 여정이 더 즐거울 수 있었습니다. 앞으로도 좋은 인연을 계속 함께하길 소망하며, 좋은 연구 같아해요!

이준영 교수님은 제가 다양한 연구에 도전할 수 있도록 많은 가르침과 기회를 주셨습니다. 생물학적 노화에 대해서 교수님과 이야기 나눴던 것이 결국 이 논문으로 이어질 수 있지 않았을까 생각합니다. ‘디지털’이라는 키워드는 분명 매력적이고 혁신적인 것 분야인 것 같습니다. 그러한 내용들을 직접 보고 배우고 공부할 수 있게 해주셔서 늘 감사합니다. 디지털 표현형에 대한 연구를 준비하고 생각하면서 저의 연구 폭이 굉장히 넓어진 것 같습니다. 연구 뿐만 아니라 다양한 장면에서 교수님 덕분에 많은 경험을 쌓게 되었던 것 같습니다. 많은 사람들도 알게 되었구요. 덕분에 정말 즐거웠습니다. 생각을 거듭할수록 제게 많은 권한과 기회를 주셨음에 감사할 따름입니다. 저의 장점과 단점도 교수님과 있으면서 가장 많이 깨달었던 것 같습니다. 부족한 제가 창업이라는 큰 과업에도 전할 수 있는 것도 교수님 덕분입니다. 아마 교수님과 함께 하지 않았더라면 그저 생각에 머물지 않았을까 생각합니다. 앞으로 많은 일들을 교수님과 함께 할 수 있었으면 좋겠습니다. 앞으로도 많은 가르침 부탁드리겠습니다.

이혜원 교수님과 정지윤 박사님, 함께 대기오염 연구를 할 수 있어서 즐겁습니다. 비록 제가 대기오염에 대해서도 잘 모르고 통계도 약하지만 앞으로도 잘 부탁드릴게요. 치매와 대기오염 간의 관계도 좋고, 다양한 역학연구를 통해 좋은 연구성과를 같이 내었으면 좋겠습니다. 제가 많이 노력하겠습니다!

독일에 계신 양승희 교수님, 교수님이라고 부르니까 많이 어색하네요. 아마 박사과정 동료들 중에서 저를 가장 잘 인정해주고 높게 평가해주신 분이 아마 교수님이 아니었을까 싶네요. 덕분에 많이 의지가 되었습니다. 음성인식도 교수님 덕분에 알게나마 공부를 했었고, 관심을 갖게 되었던 것 같아요. 즐거운 추억도 많이 만들었구요. 앞으로도 즐겁게 같이 연구해요. 한-독 연구 과제 수주를 기원합니다.

김홍기 교수님, 박사학위 면접 때부터 BIKE에 머물 때 많은 가르침을 주셔서 감사했습니다. 무엇보다 질문이 별로 없었던 제가 질문이 많이 생기게 되었습니다. 류현모 교수님, 일면식이 없던 제 학위논문을 심사에 기꺼이 응해주셔서 감사했습니다. 교수님의 가르침을 통해서 노화에 대해 더욱 다양한 이해를

가질 수 있게 되었습니다. 교수님과 후성유전체 연구까지 함께 할 날이 있었으면 좋겠습니다.

지도교수님, 제가 자유롭고 편하게 박사과정 생활을 해줄 수 있게 도와 주셔서 감사했습니다. 가끔 보다 자주 교수님을 난처하게 했던 것 같습니다. 그럼에도 항상 저를 믿고 아껴 주셔서 감사합니다. 앞으로는 독립된 한 명의 연구자가 되어 교수님을 많이 도울 수 있도록 하겠습니다. 앞으로도 함께 할 날이 많으니 깊게만 감사함을 남기겠습니다!

저의 기괴함과 자만함을 어여쁘게 봐주던 인지과학 동료들께 진심으로 감사합니다. 특히 학위 과정 전반부는 인지과학 동기들 - 김태형 박사님, 황유진 박사님, 그리고 조성재, 임재서, 정지수- 여러분의 관심과 지지 덕분에 제가 낯선 환경에 잘 정착할 수 있었습니다. 특히 태형이 형에게는 많은 신세를 진 것 같습니다. 보스턴에 있을 박세호 형, 항상 보고 싶습니다. 그리고 저를 끊임없이 아끼고 지지해주던 BIKE의 하경식 박사님, 박준호, 조현환, 손지원, 김혜연, 장수은, 이용주, 신준혁, 최원석, 여러분 덕분에 생각보다 많은 추억을 만들었던 것 같습니다. 같이 일본에 다시 가면 더 재밌게 놀텐데!

그리고 잊지 않고 감사함을 전합니다. 서울대 의료빅데이터연구센터 및 가천대 지능형뇌과학연구센터의 ITRC사업의 수혜를 입었습니다. 두 사업의 아낌없는 지원 덕분에 많은 연구를 할 수 있었습니다. 감사합니다.

최근 부쩍 가까워진 권순용 원장님, 원장님의 지지 덕분에 앞으로 대단한 일을 많이 할 수 있을 것 같습니다. 그리고 원장님 말씀 한마디 한마디에 제가 많은 생각을 하게 됩니다. 더욱 큰 꿈을 꾸게 되었습니다. 감사합니다!

저의 가장 가까운 멘토 권석봉 박사님 덕분에 큰일에 도전하고 있습니다. 학위 과정이 잘 마무리될 수 있게 물심양면으로 도와 주셔서 감사합니다. 함께 꿈꾸는 좋은 세상은 아마 저만 잘 하면 잘 되지 않을까 싶습니다. 인생과 사회생활 선배님으로서 항상 제게 많은 가르침을 주셔서 얼마나 좋은지 모르겠습니다.
Hola Mago!

고생했던 제 자신에게도 감사함, 서운함, 아쉬움을 전합니다. 조금 더 사람들에게 잘 했으면 좋았을텐데, 조금 더 치열하게 연구하면 좋았을텐데, 하지

만 그렇지 못해서 많이 아쉽고 서운합니다. 그렇지만 몇번의 고비 속에서도 모두 잘 해쳐내고 끝까지 완주해낸 점, 그리고 생각보다 놀라운 성과를 냈던 점은 참 자랑스럽게 느껴집니다. 앞으로도 꿈을 향해 지치지 않고 나아가길 제 자신에게 희망합니다.

그리고 마지막으로 진정한 유러피안 MD에게도 짧지만 진심으로 감사함을 전합니다. 항상 고맙습니다.

한 명의 박사학위가 탄생하기까지 많은 사람들의 노고가 있었던 것 같습니다. 무엇보다 아무것도 아닌 제 자신의 가치를 알아 봐주고 이끌어주신 많은 분들이 고현웅 박사를 탄생시켰다고 생각합니다. 진심으로 감사합니다. 저 역시 누군가의 학위과정 속에서 도움이 될 수 있기를 바라며 감사의 글을 마치겠습니다.